Dynamical origin of the Cosmic Web

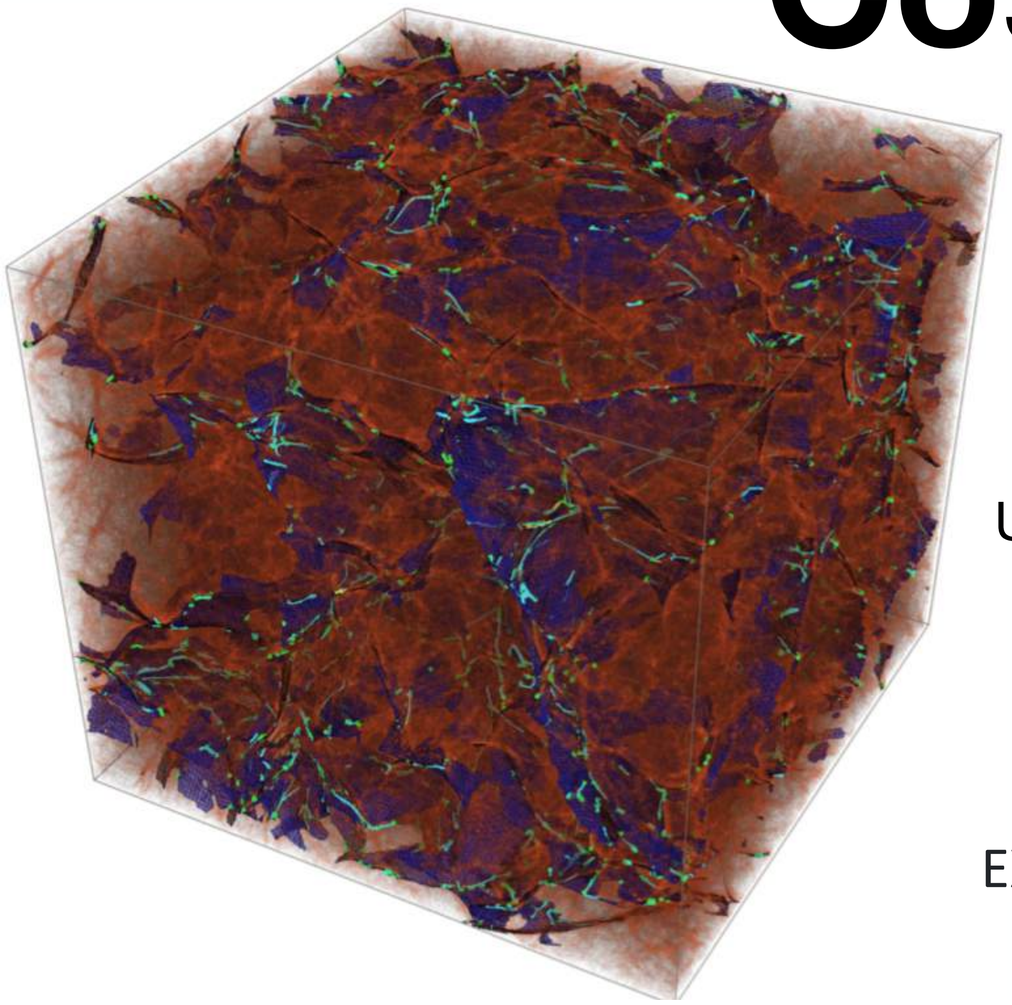

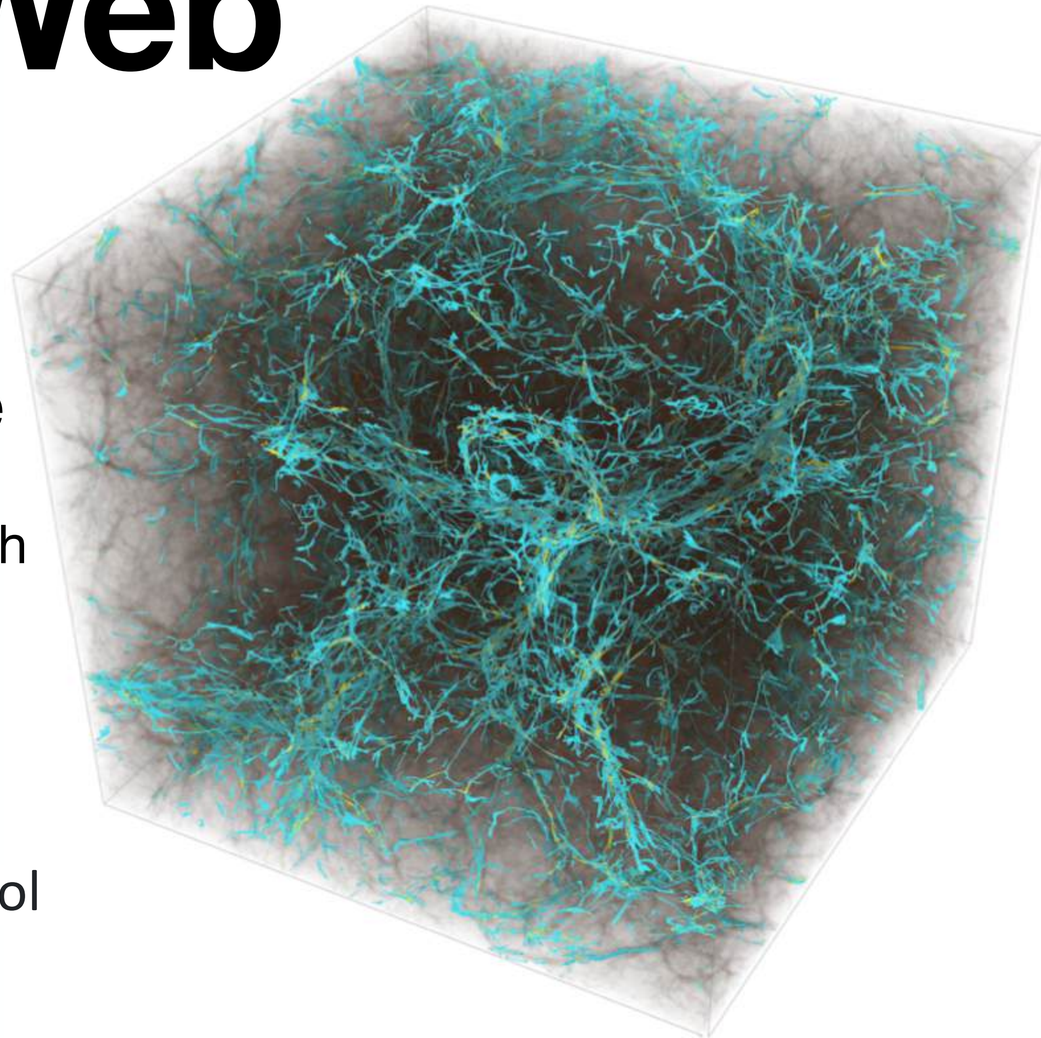

Job Feldbrugge
Higgs Fellow
University of Edinburgh

7th of July 2025
EXCOSM summer school

The cosmic web

The simple initial fluctuations are close to Gaussian.

This collapses into an intricate cosmic web with **voids**, **walls**, **filaments**, and **clusters**, inheriting this information

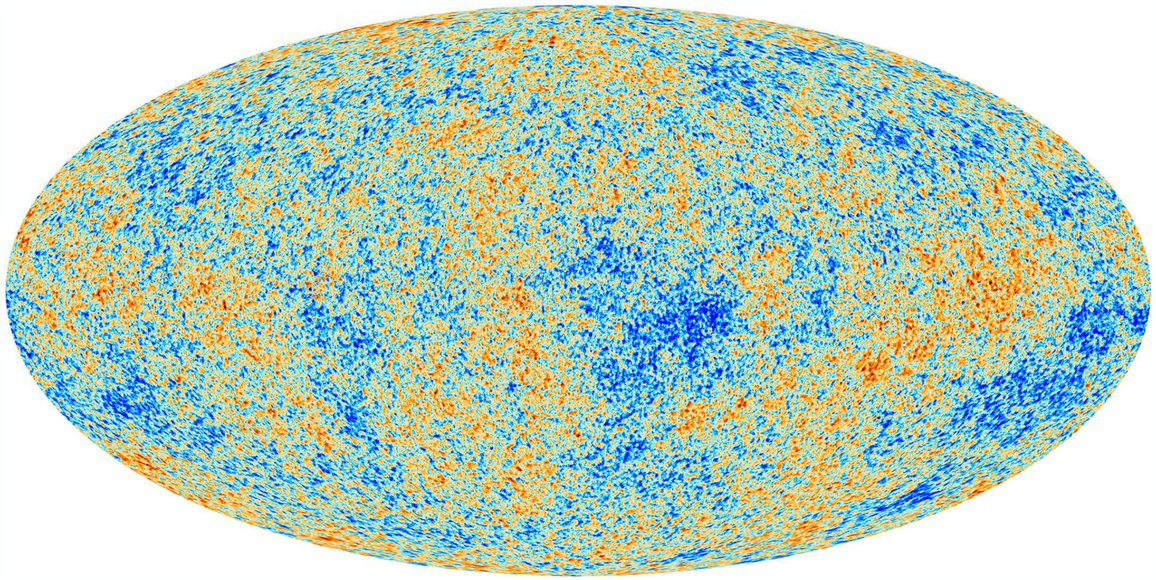

Planck Satellite

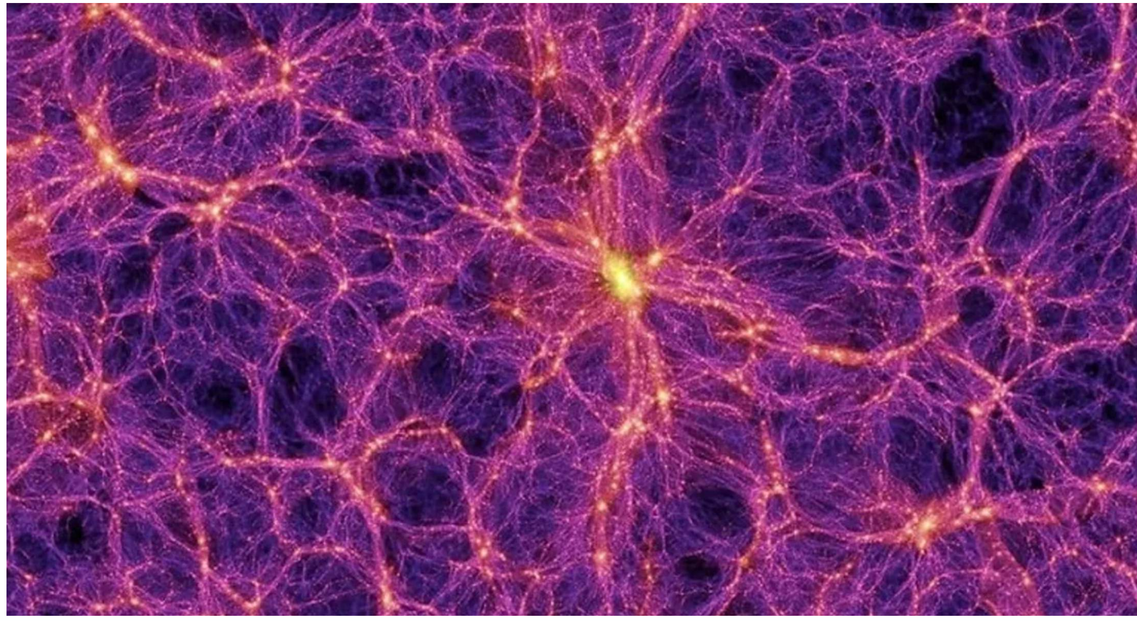

Millenium simulation

This paradigm has now been verified with a vast range of N-body simulations including the Millennium, TNG, Eagle, and Quijote simulations

Springel et al. (2005)

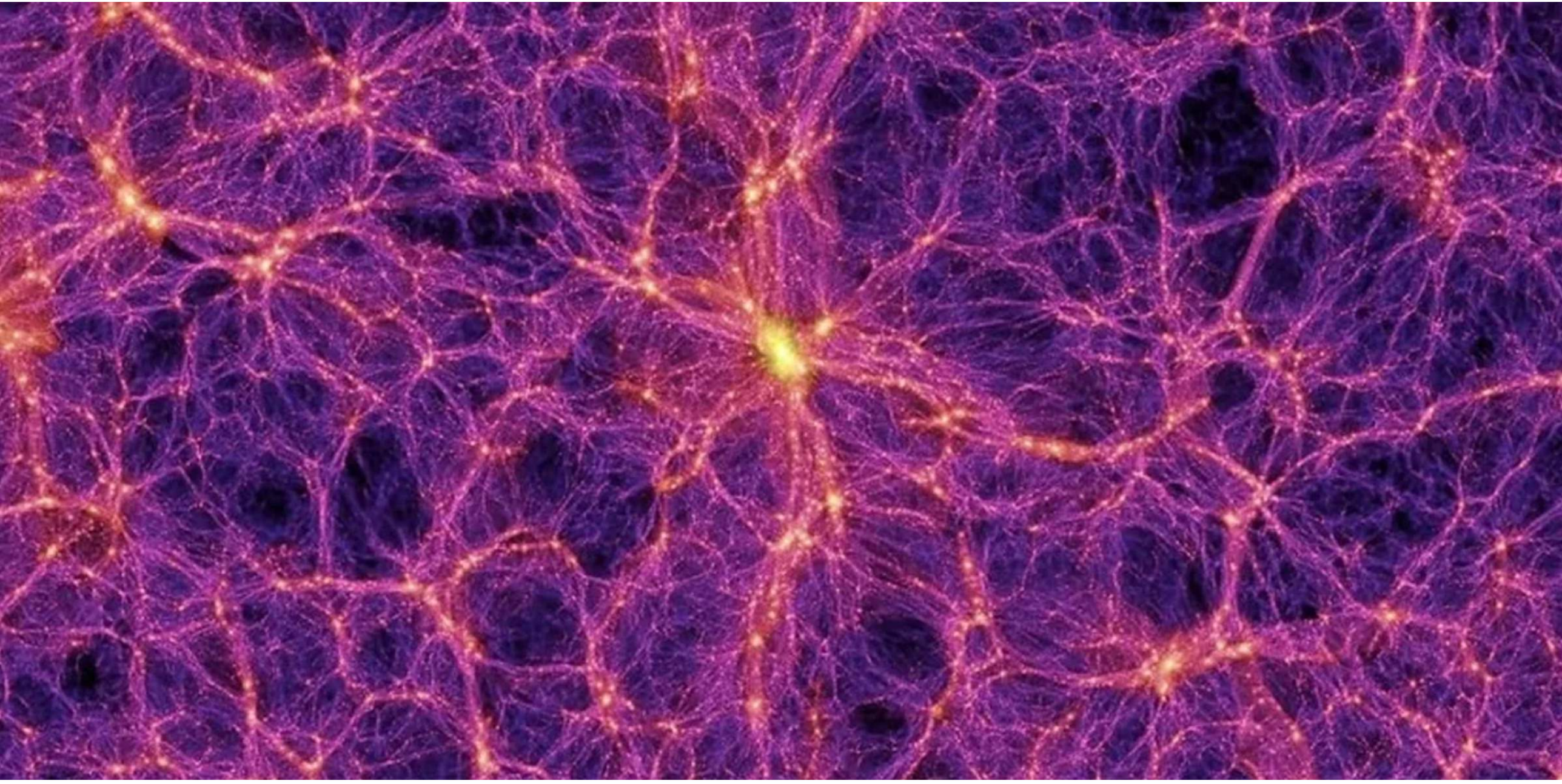

The cosmic web

The predicted distribution of galaxies is in qualitative agreement with the cosmological redshift surveys.

Given the details of the upcoming redshift surveys and the link between the cosmic web and the embedded galaxies, it is important to develop new analytic methods.

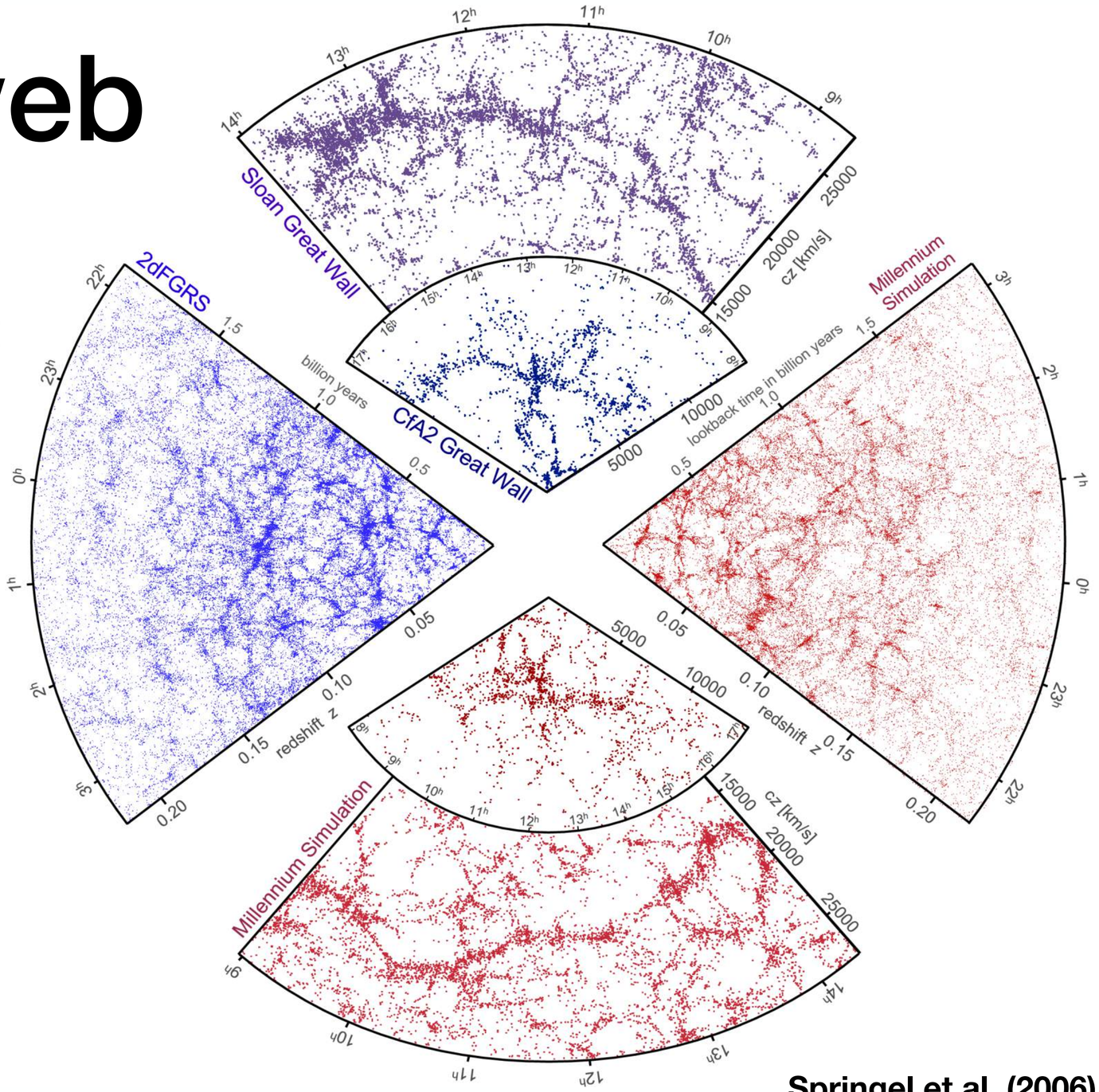

Springel et al. (2006)

The multi-stream nature of the cosmic web

Cosmology

Expanding universe: From Einstein's GR to the Friedmann equations

$$R_{\mu\nu} - \frac{1}{2}Rg_{\mu\nu} + \Lambda g_{\mu\nu} = \frac{8\pi G}{c^4}T_{\mu\nu}$$

$$\frac{\dot{a}^2}{a^2} = \frac{8\pi G}{3}\rho - \frac{kc^2}{a^2} + \frac{\Lambda c^2}{3}$$

$$\frac{\ddot{a}}{a} = -\frac{4\pi G}{3}\left(\rho + \frac{3p}{c^2}\right) + \frac{\Lambda c^2}{3}$$

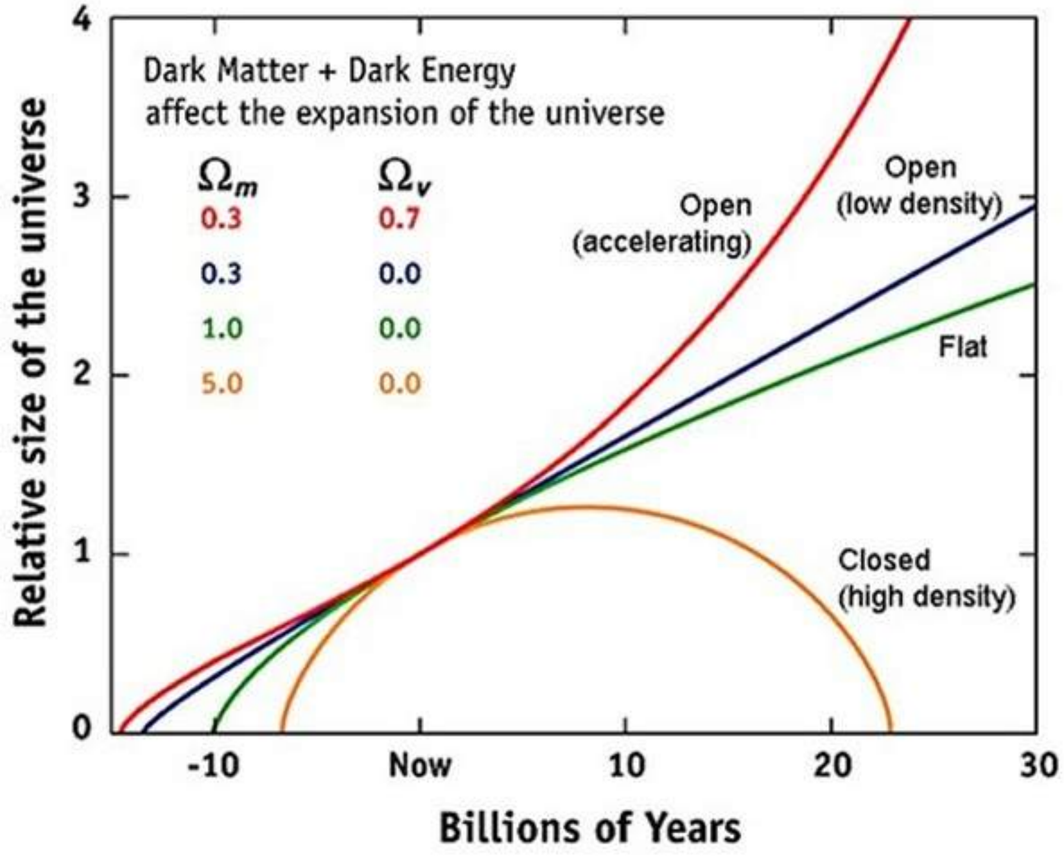

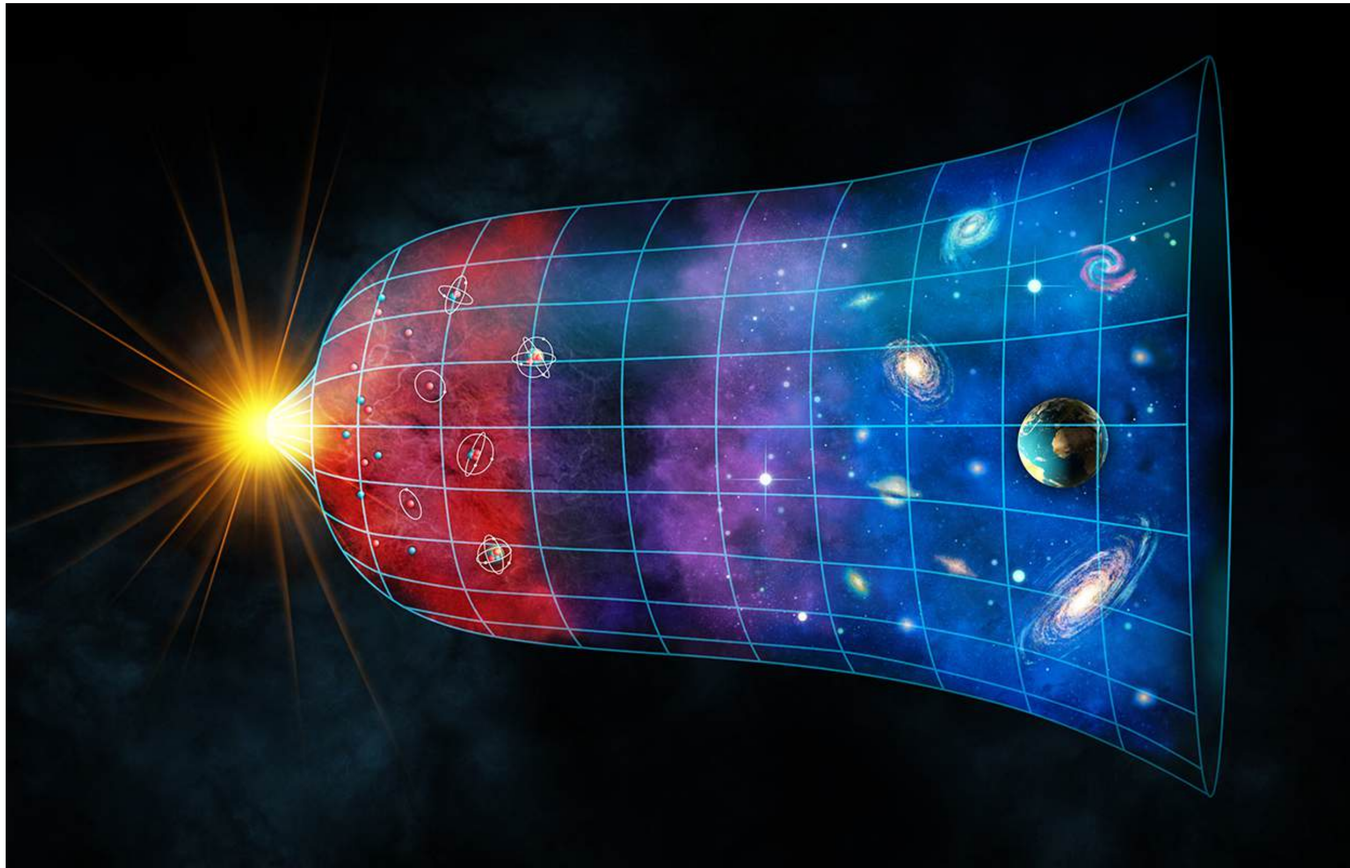

Cosmology

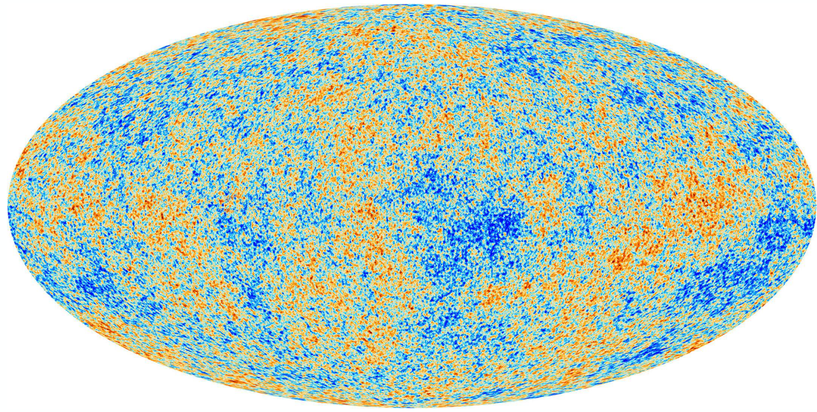

At the time of recombination, the density perturbations were Gaussian

$$P[f \in \mathcal{S}] = \mathcal{N} \int \mathbf{1}_{\mathcal{S}}(f) e^{-S[f]} \mathcal{D}f$$

with the ‘action’

$$S[f] \equiv \frac{1}{2} \iint [f(\boldsymbol{q}_1) - \bar{f}(\boldsymbol{q}_1)] K(\boldsymbol{q}_1, \boldsymbol{q}_2) [f(\boldsymbol{q}_2) - \bar{f}(\boldsymbol{q}_2)] \mathrm{d}\boldsymbol{q}_1 \mathrm{d}\boldsymbol{q}_2,$$

where the kernel is the inverse of the two-point correlation function

$$\int K(\boldsymbol{q}_1, \boldsymbol{q}) \xi(\boldsymbol{q}, \boldsymbol{q}_2) \mathrm{d}\boldsymbol{q} = \delta_D^{(2)}(\boldsymbol{q}_1 - \boldsymbol{q}_2)$$

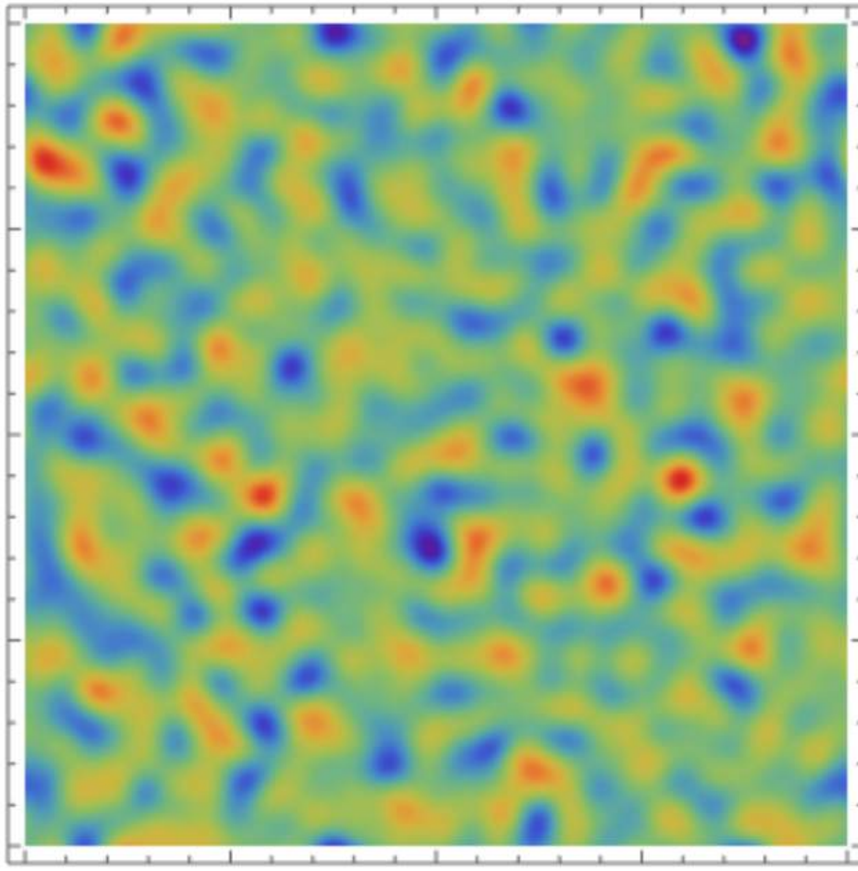

Cosmology

The gravitational collapse in cosmology is governed by the

- **Conservation of mass:** $$\frac{\partial \delta}{\partial t} + \frac{1}{a}\nabla \cdot (1+\delta)\mathbf{v} = 0$$
- **Euler equation:** $$\frac{\partial \mathbf{v}}{\partial t} + \frac{1}{a}(\mathbf{v}\cdot\nabla)\,\mathbf{v} + \frac{\dot{a}}{a}\mathbf{v} = -\frac{1}{a}\nabla\phi$$
- **Poisson equation:** $$\nabla^2\phi = 4\pi G a^2 \rho_u \delta$$

How do these equations lead to the large-scale structure we see today?

How does the **geometry** of voids, walls, filaments and clusters emerge?

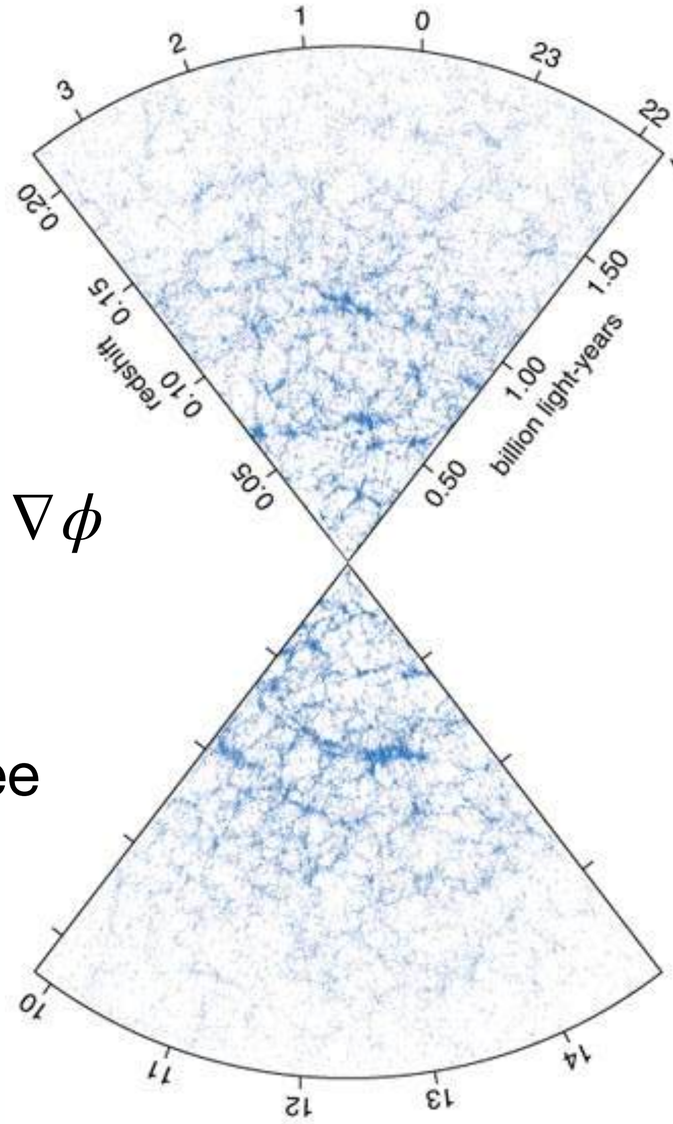

Lagrangian fluid dynamics

Flowing with the dark matter fluid

- Conservation of mass
- Euler equation and
- Poisson equation

This is how N-body simulations work

$$\mathbf{x}_t(\mathbf{q}) = \mathbf{q} + \mathbf{s}_t(\mathbf{q})$$

$$1 + \delta = \frac{\rho}{\rho_u} = \sum_{\mathbf{q} \in \mathbf{x}_t^{-1}(\mathbf{x})} \frac{\rho_u}{\|\nabla \mathbf{x}_t(\mathbf{q})\|}$$

$$\frac{\mathrm{d}\mathbf{v}}{\mathrm{d}t} + \frac{\dot{a}}{a}\mathbf{v} = -\frac{1}{a}\nabla\phi$$

$$\nabla^2\phi = 4\pi G a^2 \rho_u \delta$$

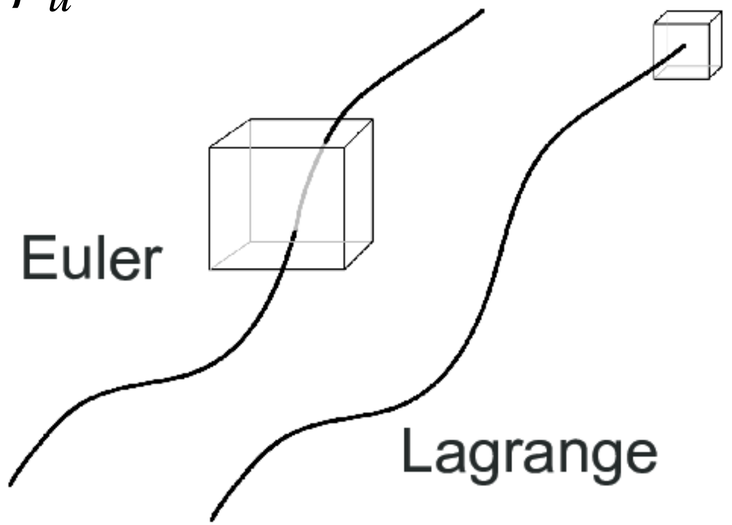

Lagrangian fluid dynamics

To first order, these equations are solved by the **Zel'dovich approximation**

$$\mathbf{x}_t(\mathbf{q}) = \mathbf{q} + \mathbf{s}_t(\mathbf{q}) \qquad \mathbf{s}_t(\mathbf{q}) = -\, b_+(t)\, \nabla \Psi(\mathbf{q})$$

with the primordial displacement potential and growing mode

$$\Psi(\mathbf{q}) = \frac{2\phi_0(\mathbf{q})}{3\Omega_0 H_0^2} \qquad \frac{\mathrm{d}^2 b_+(t)}{\mathrm{d}t^2} + 2\frac{\dot{a}}{a}\frac{\mathrm{d}b_+(t)}{\mathrm{d}t} = 4\pi G \rho_u b_+(t)$$

capturing the spatial and temporal dependencies.

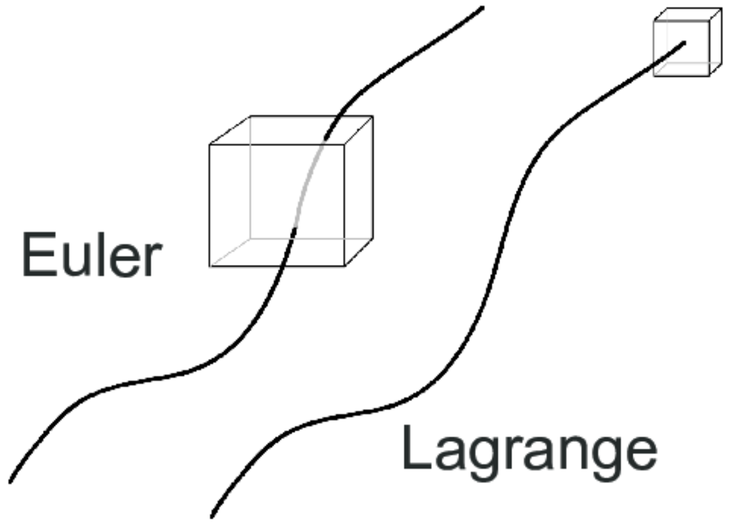

Lagrangian fluid dynamics

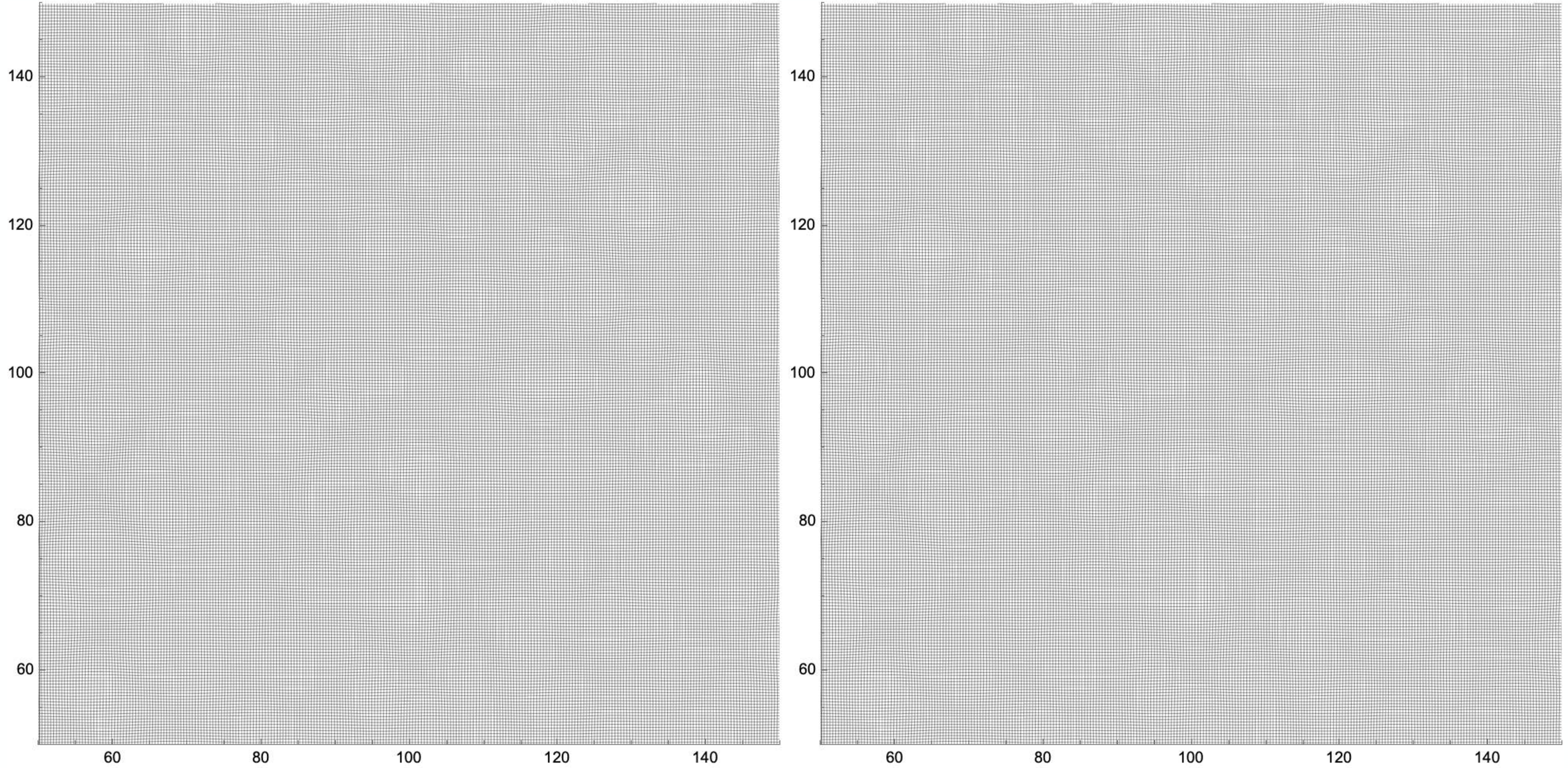

The density field

During shell-crossing, the density field spikes to infinity

$$\mathbf{x}_t(\mathbf{q}) = \mathbf{q} + \mathbf{s}_t(\mathbf{q})$$
$$\nabla \mathbf{s}_t(\mathbf{q}) \mathbf{v}_i(\mathbf{q}) = \mu_i(\mathbf{q}) \mathbf{v}_i(\mathbf{q})$$

$$\rho_t(\mathbf{x}') = \sum_{\mathbf{q} \in \mathbf{x}_t^{-1}(\mathbf{x}')} \frac{\bar{\rho}}{|\det \nabla \mathbf{x}_t(\mathbf{q})|} = \sum_{\mathbf{q} \in \mathbf{x}_t^{-1}(\mathbf{x}')} \frac{\bar{\rho}}{|1+\mu_1(\mathbf{q})||1+\mu_2(\mathbf{q})||1+\mu_3(\mathbf{q})|}$$

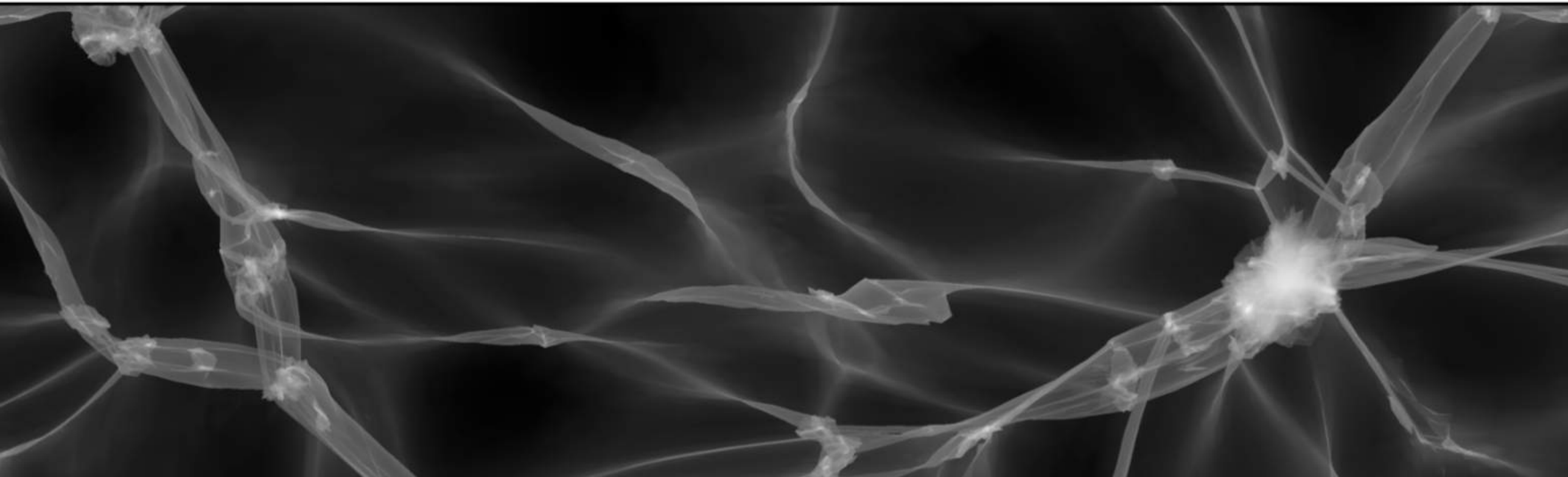

The density field

$$\mathbf{x}_t(\mathbf{q}) = \mathbf{q} - b_+(t)\,\nabla\Psi(\mathbf{q})$$

$$1 + \mu_i(\mathbf{q}) = 1 - b_+(t)\lambda_i(\mathbf{q})$$

During shell-crossing, the density field spikes to infinity

$$\rho_t(\mathbf{x}') = \sum_{\mathbf{q}\in\mathbf{x}_t^{-1}(\mathbf{x}')} \frac{\bar{\rho}}{|\det \nabla\mathbf{x}_t(\mathbf{q})|} = \sum_{\mathbf{q}\in\mathbf{x}_t^{-1}(\mathbf{x}')} \frac{\bar{\rho}}{|1+\mu_1(\mathbf{q})||1+\mu_2(\mathbf{q})||1+\mu_3(\mathbf{q})|}$$

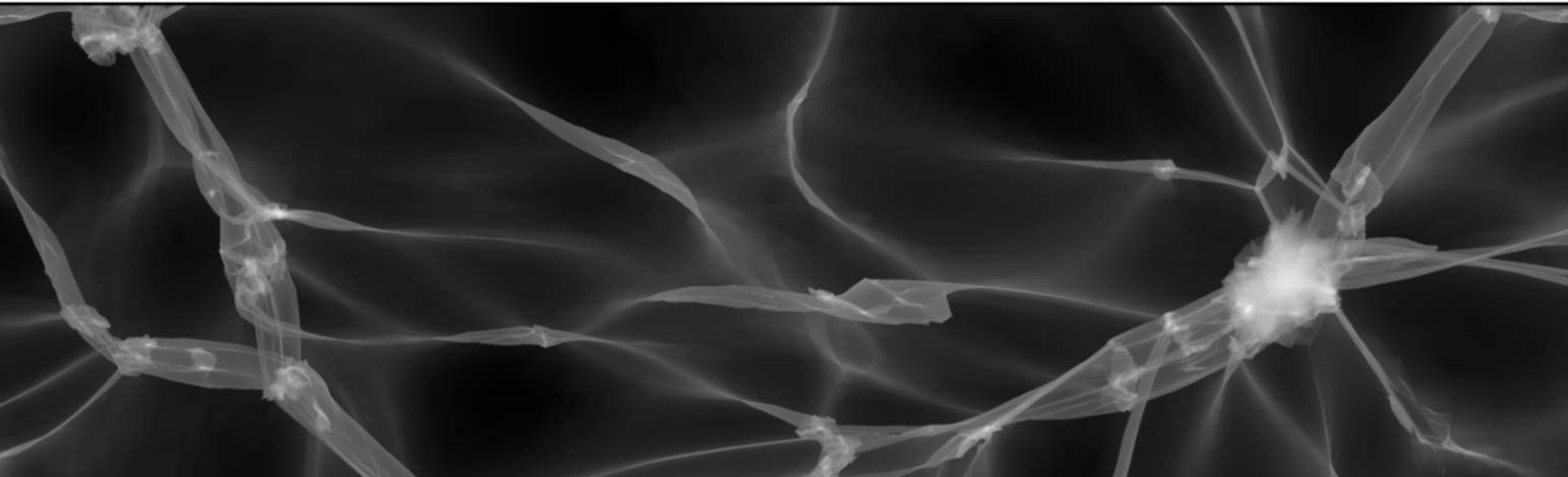

Zel’dovich Pancake

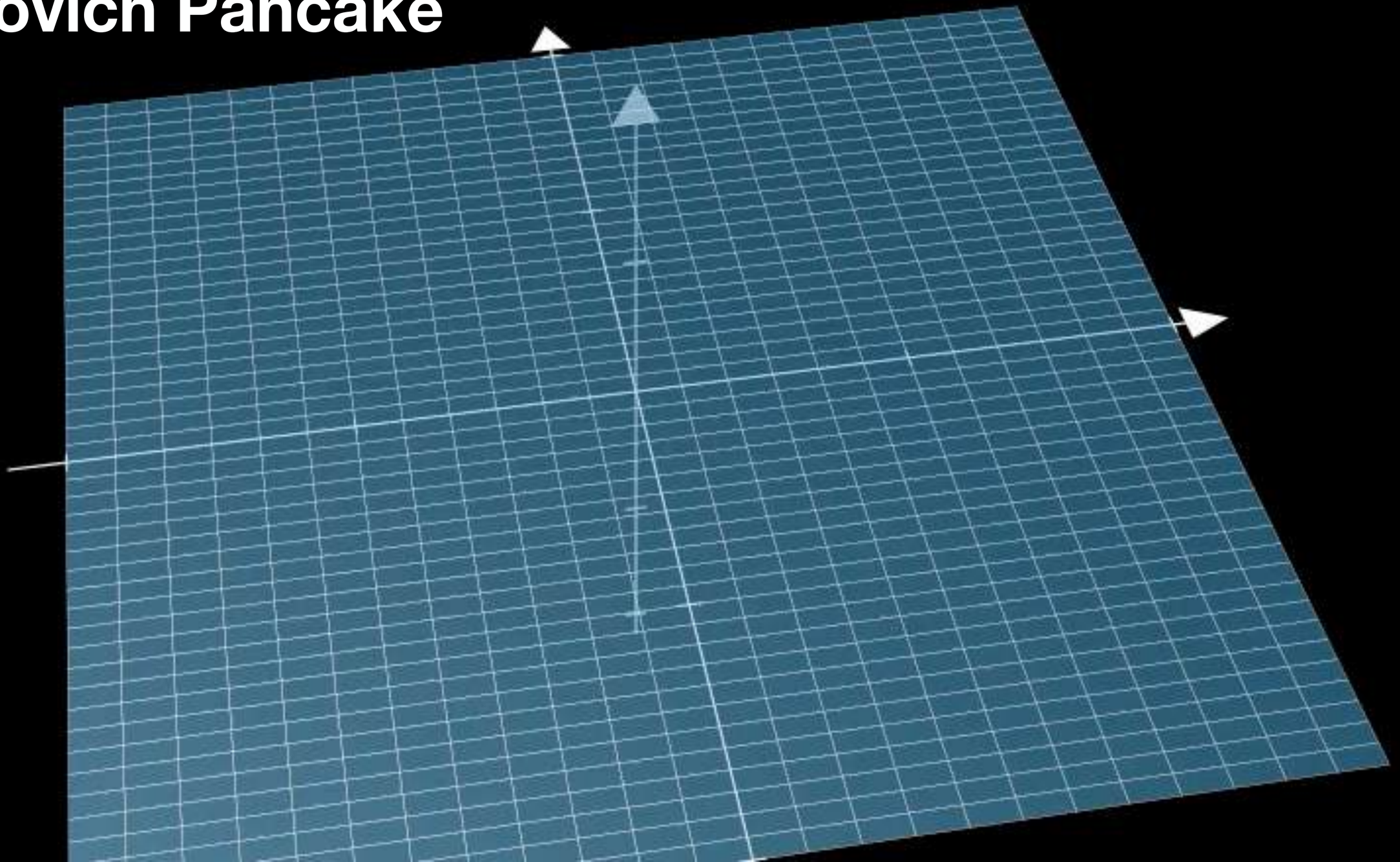

Catastrophe theory

Catastrophe theory

Catastrophe theory is a beautiful field in mathematics, with universal applications in physics and astronomy

- Studied by **Da Vinci, Newton, Huygens, Laplace,** and **Poincaré**

- Formally developed by René Thom (1960s), Christopher Zeeman, Vladimir Arnol'd, and Micheal Berry (1970s)

- **Large changes** as a result of **infinitesimal variations of the control parameters**

- Applications in **geometry, differential equations, soap films, dynamical systems, optics, chemistry, quantum physics,** and even **population and social science**

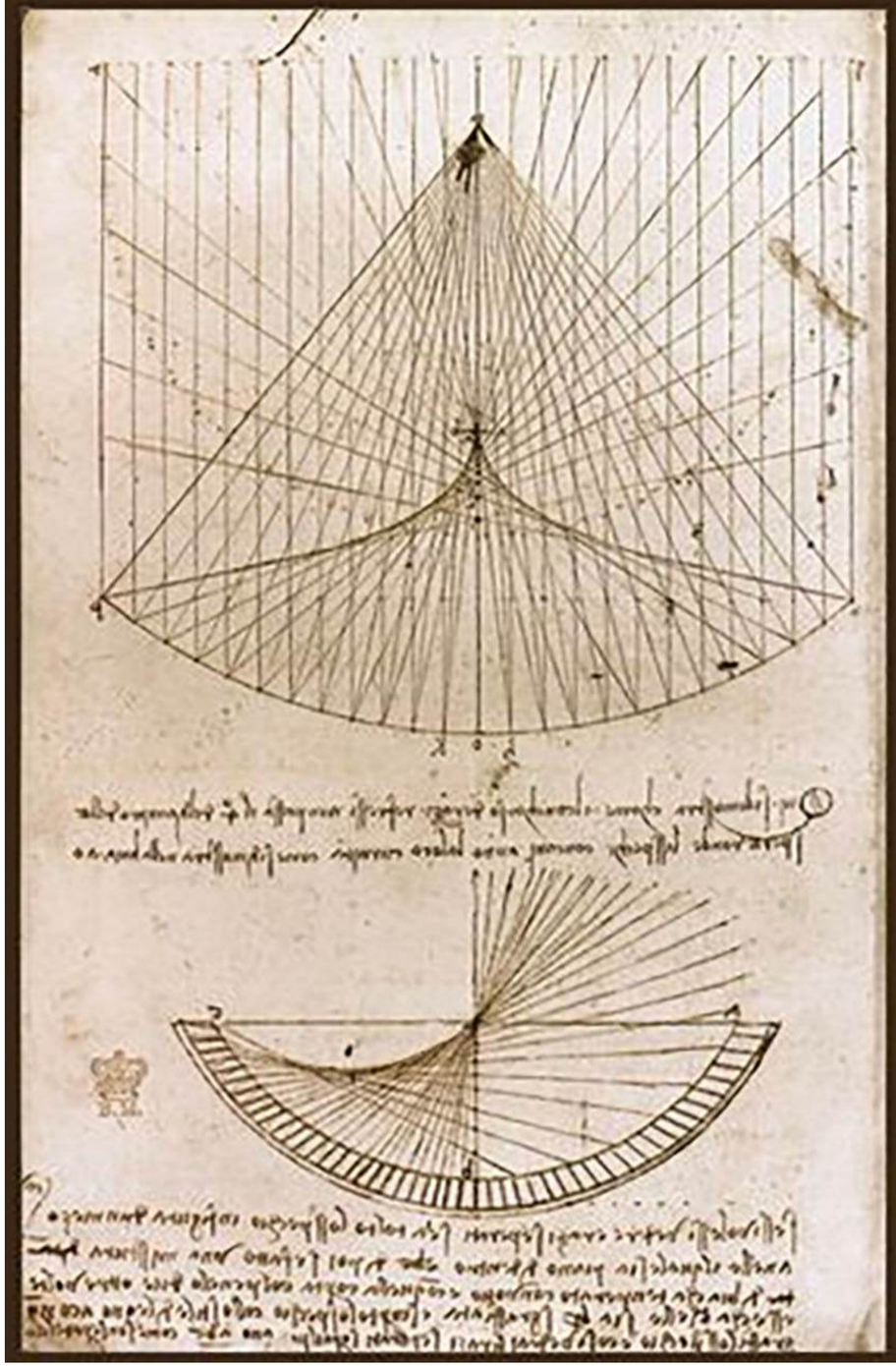

[Leonardo Da Vinci, ~1508, codex Arundel 263, folio 87v]

Catastrophe theory

Catastrophe theory is a beautiful field in mathematics, with universal applications in physics and astronomy

- Studied by **Da Vinci, Newton, Huygens, Laplace,** and **Poincaré**
- Formally developed by René Thom (1960s), Christopher Zeeman, Vladimir Arnol'd, and Micheal Berry (1970s)
- **Large changes** as a result of **infinitesimal variations of the control parameters**
- Applications in **geometry, differential equations, soap films, dynamical systems, optics, chemistry, quantum physics,** and even **population and social science**

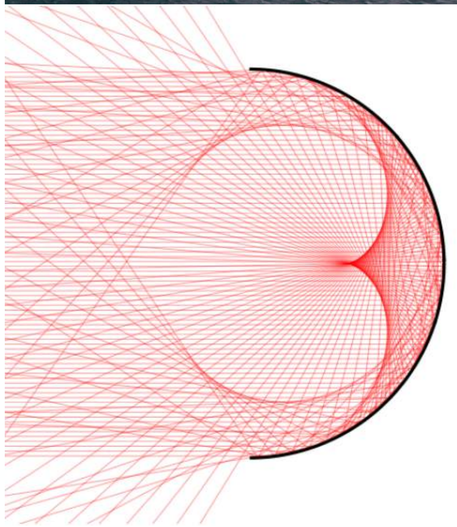

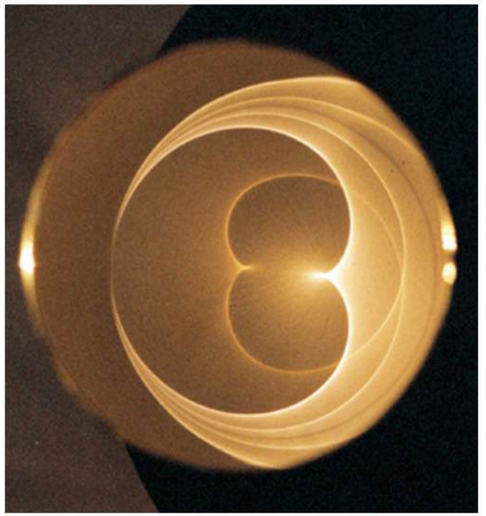

Catastrophe theory

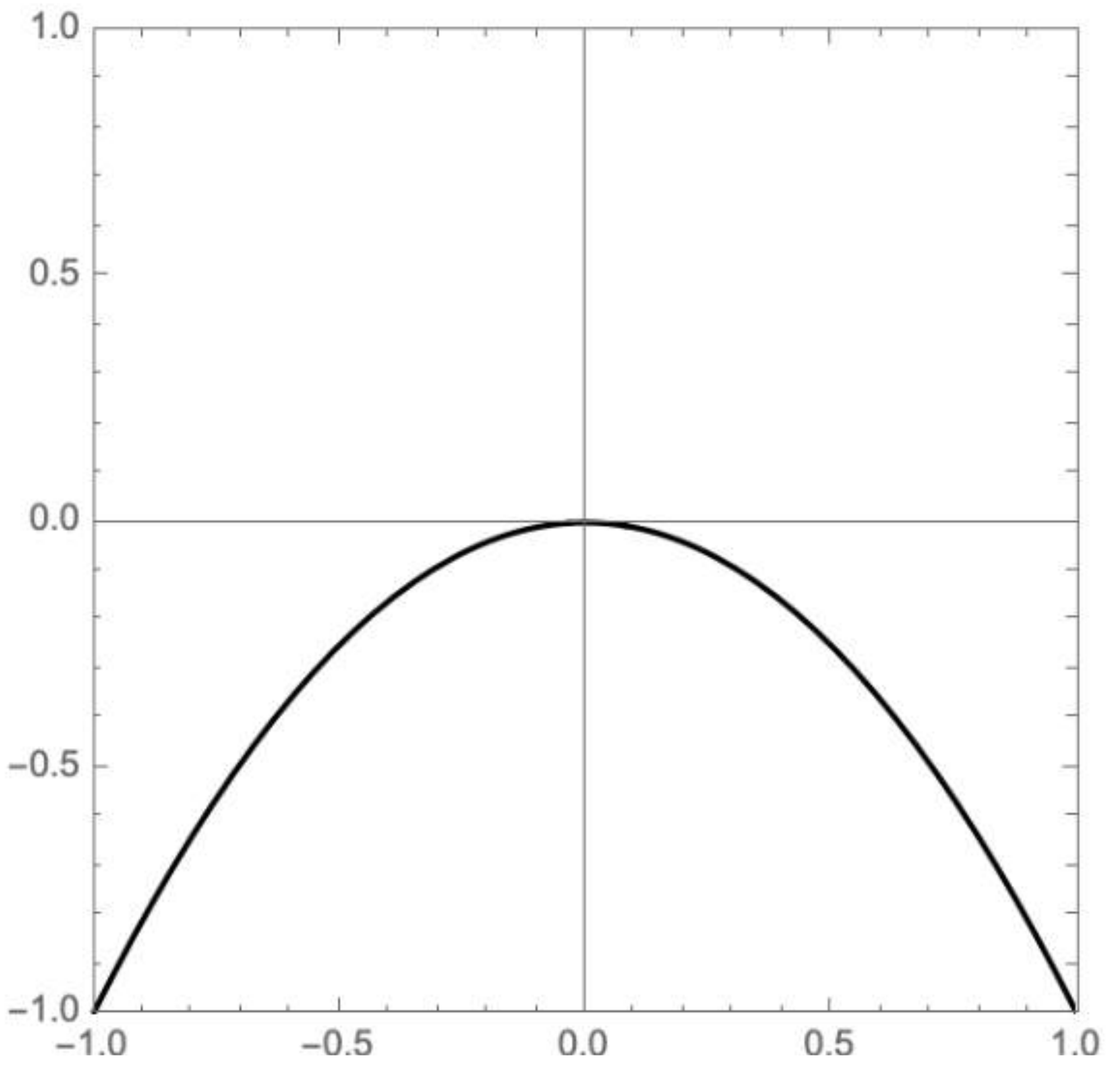

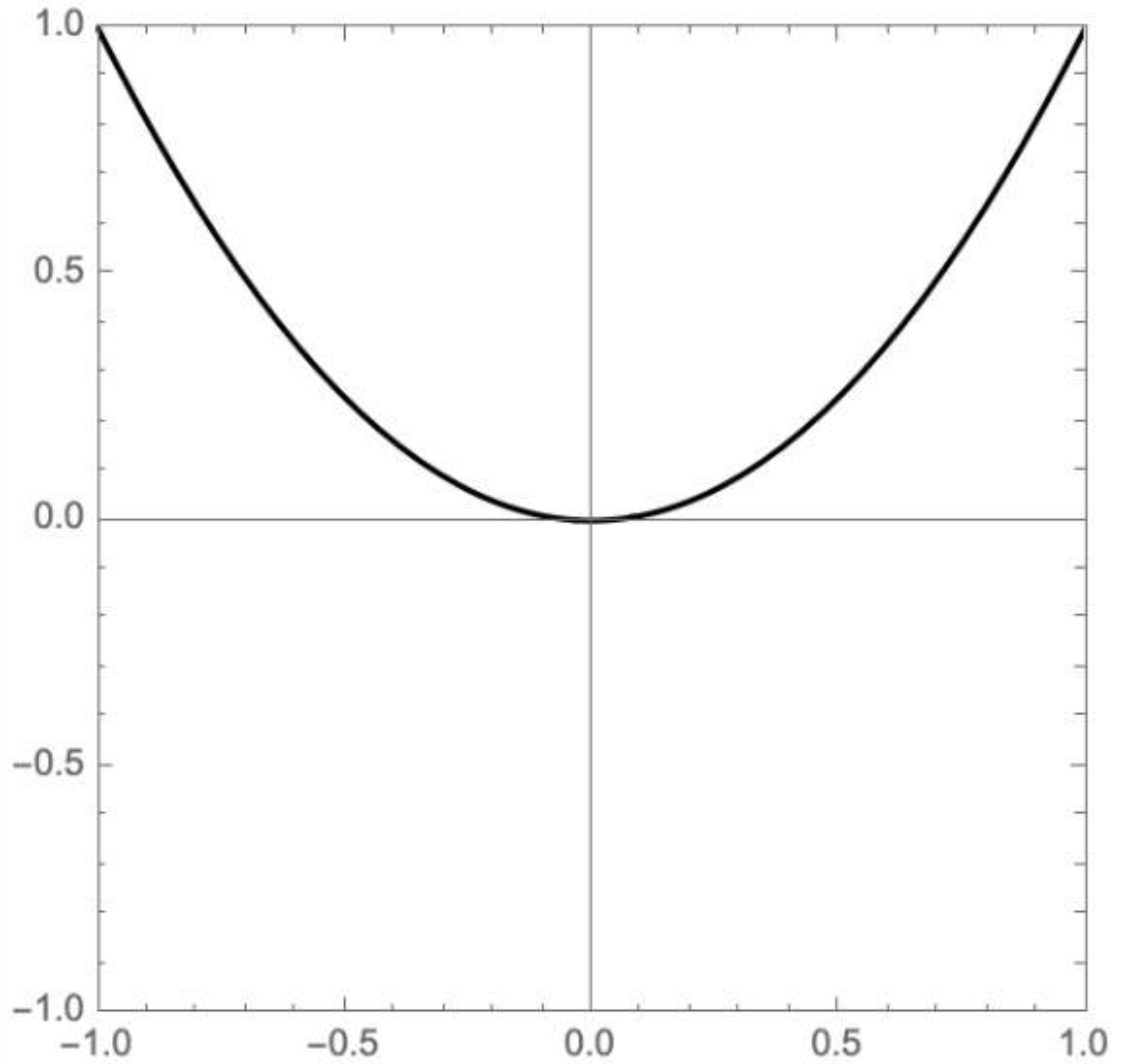

Classification of non-degenerate critical points

$$\nabla f = 0 \quad \det \mathscr{H} f \neq 0$$

Morse lemma: a stable critical point is classified by its index s

$$f(\psi(x)) = f(0) - x_1^2 - \ldots - x_s^2 + x_{s+1}^2 + \ldots + x_n^2$$

Stable with respect to perturbations $f(x) = x^3 + \alpha x$

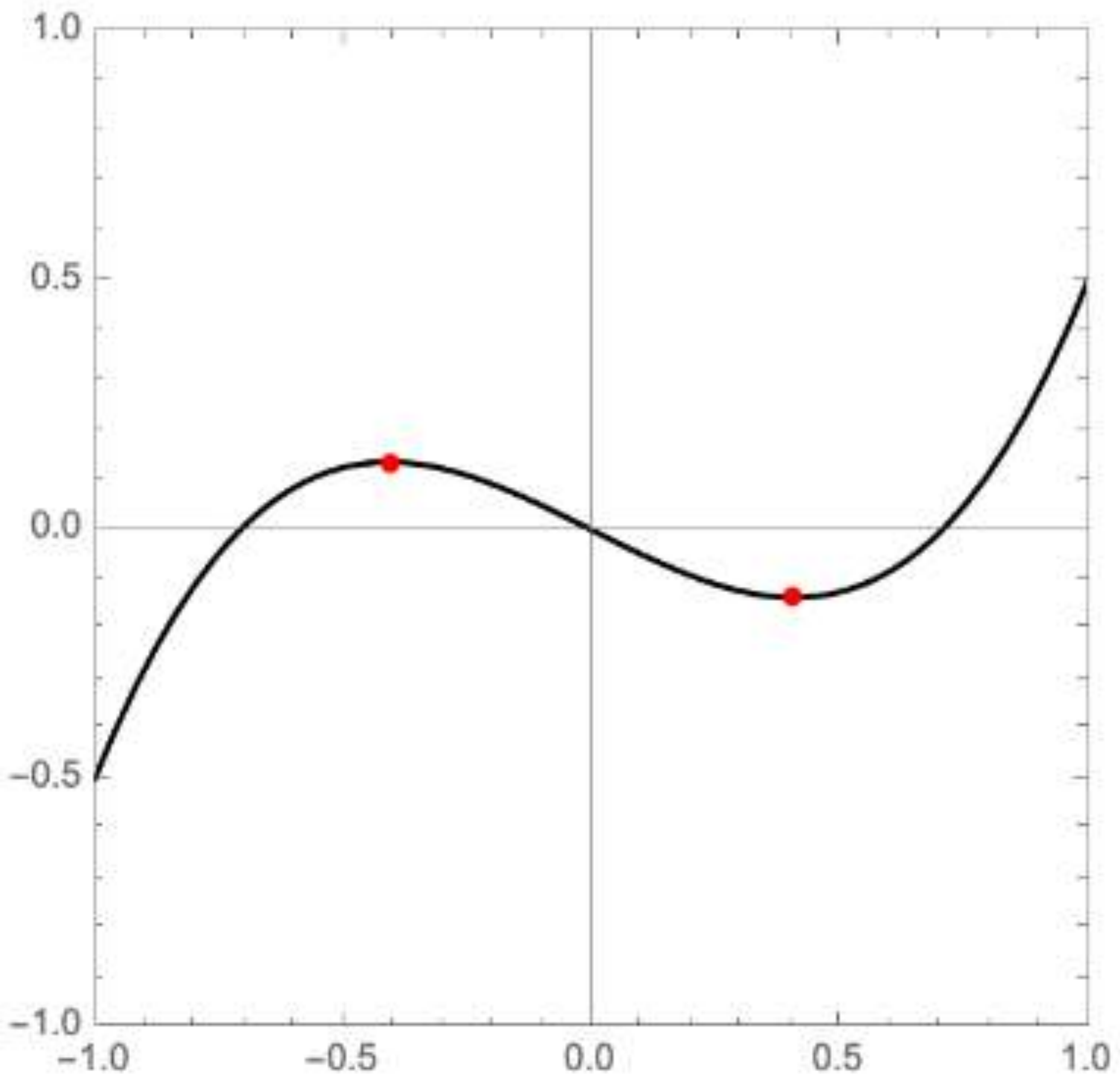

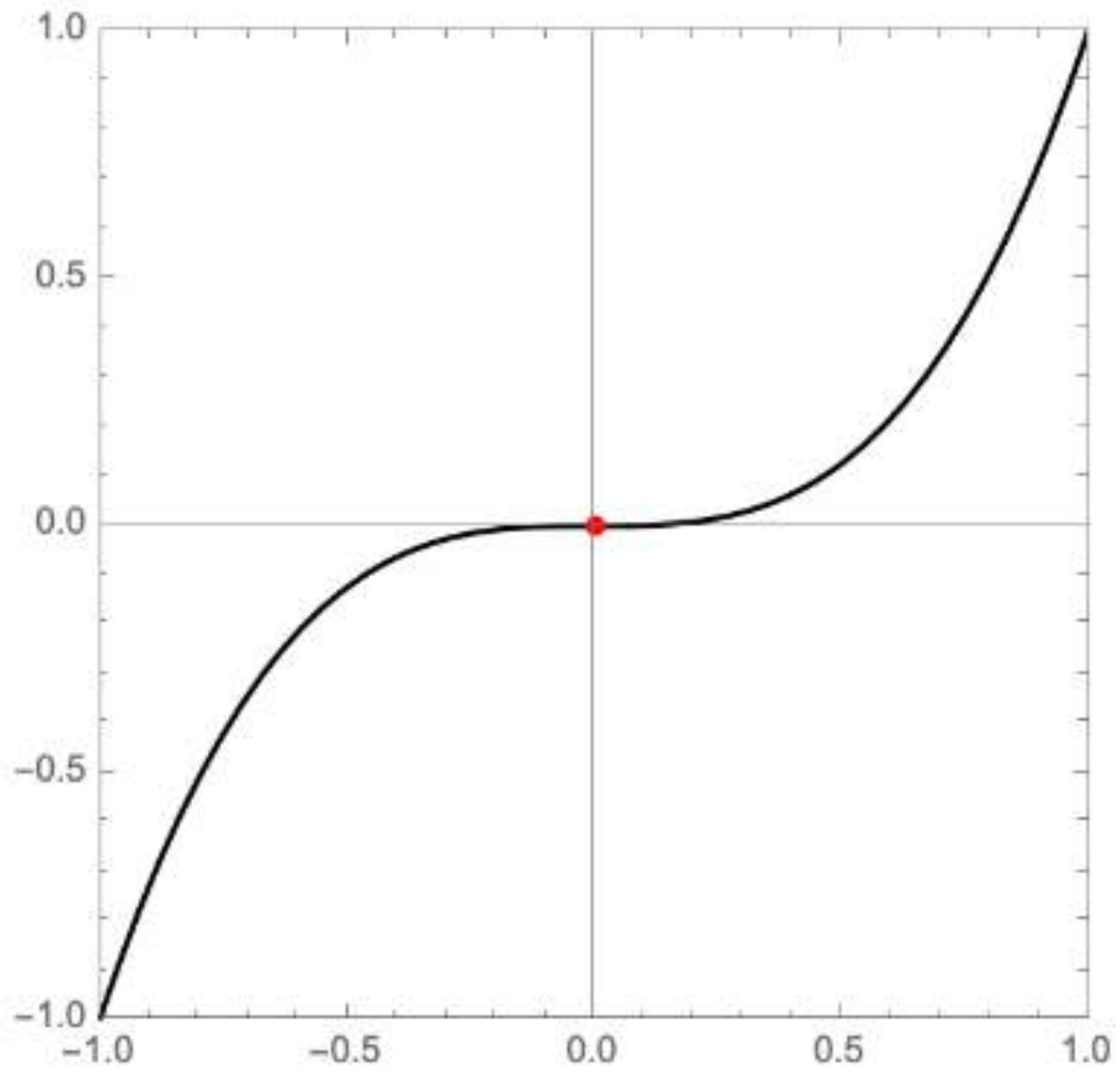

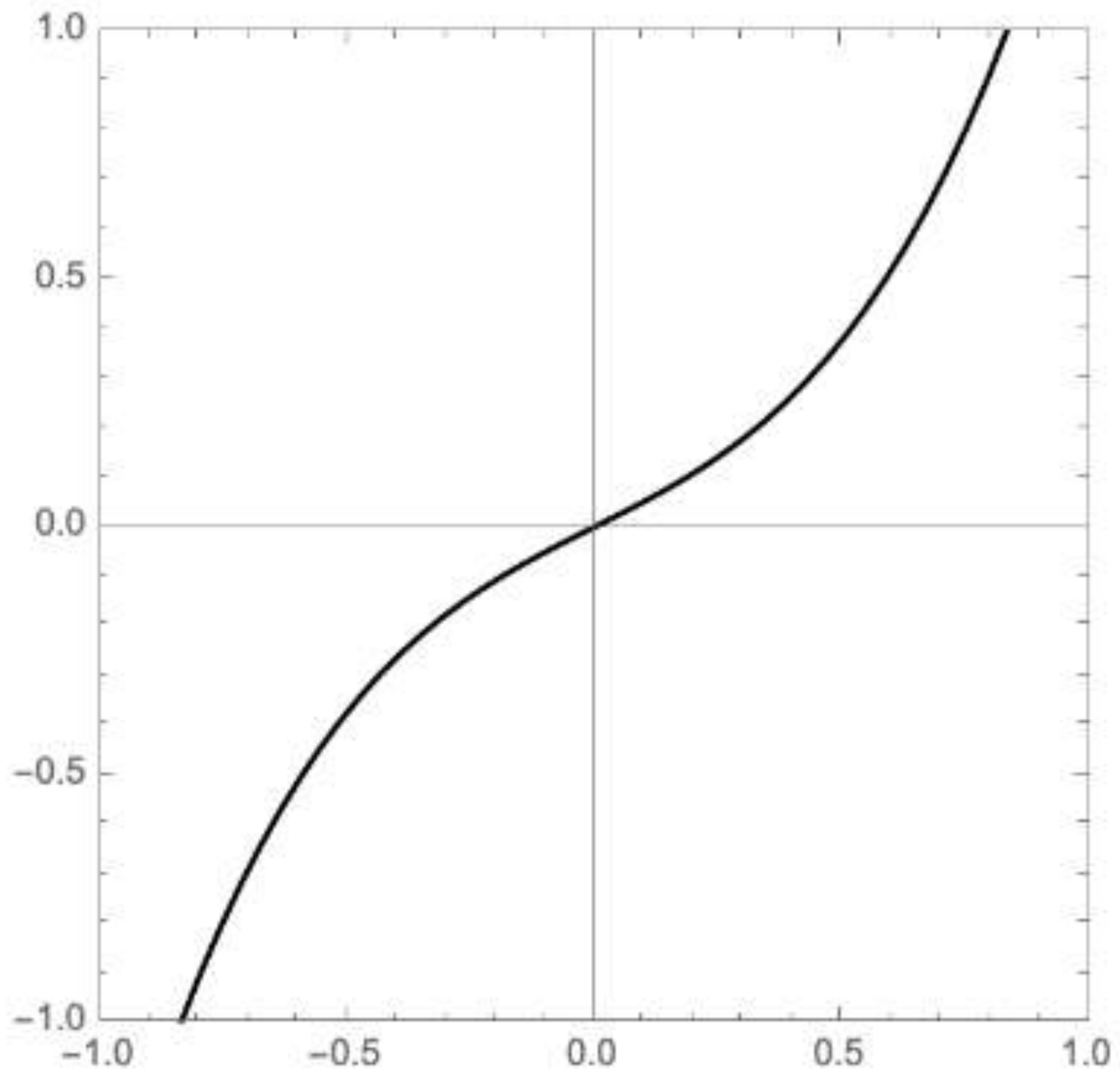

Catastrophe theory

However, many physical systems can display degenerate critical points when varying control parameters

$$\nabla_x f(x,\lambda) = 0 \qquad \det \mathscr{H}_x f(x,\lambda) = 0$$

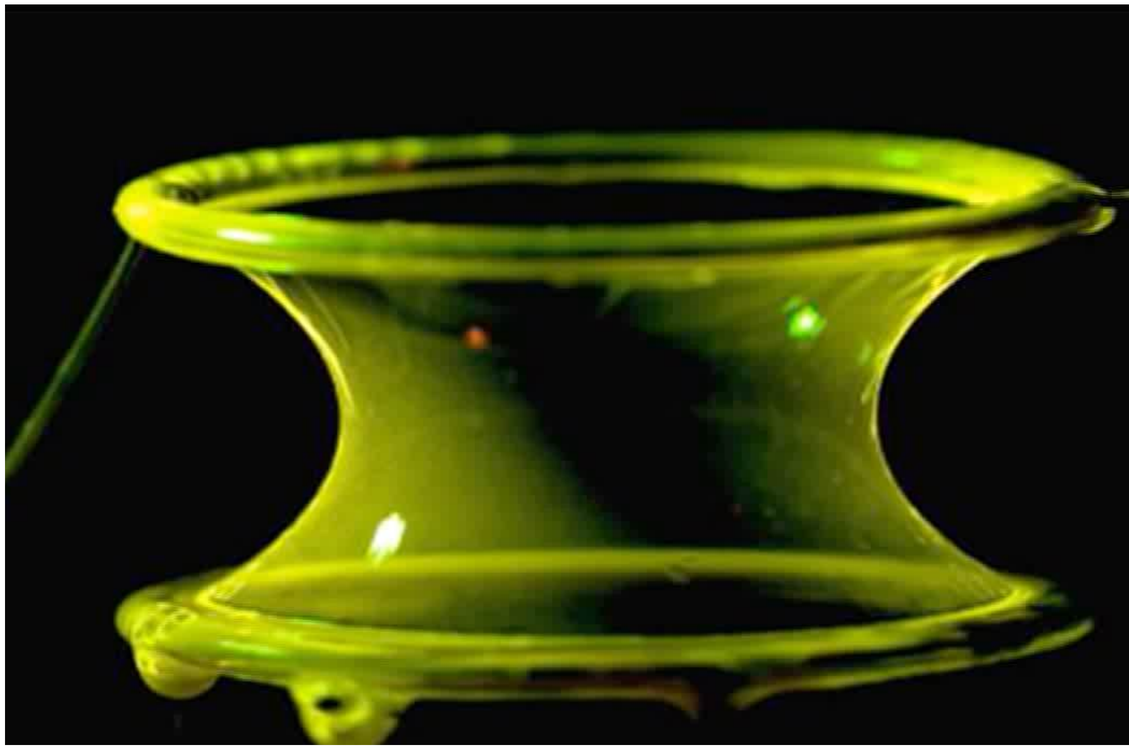

How does the classification of non-degenerate critical points extend to degenerate critical points?

How are these critical points characterized?

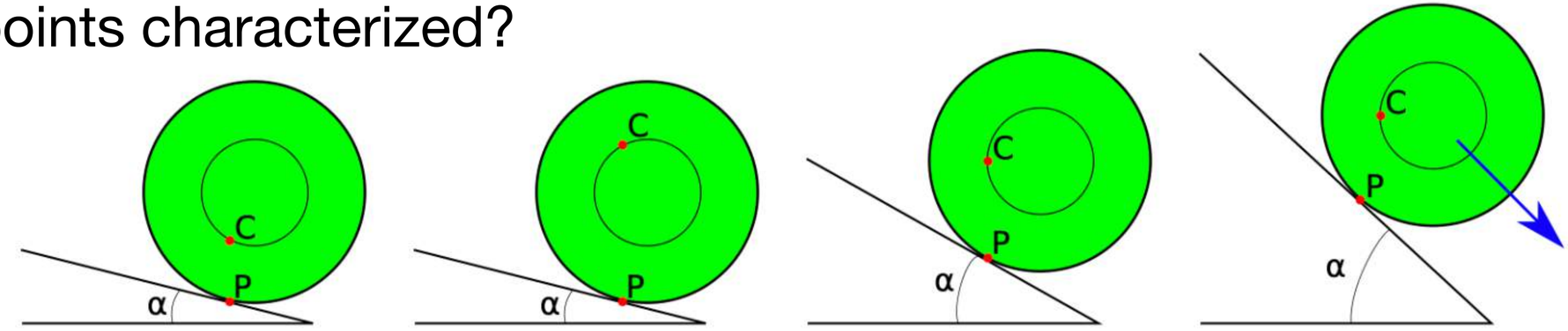

Catastrophe theory

Zeeman catastrophe machine

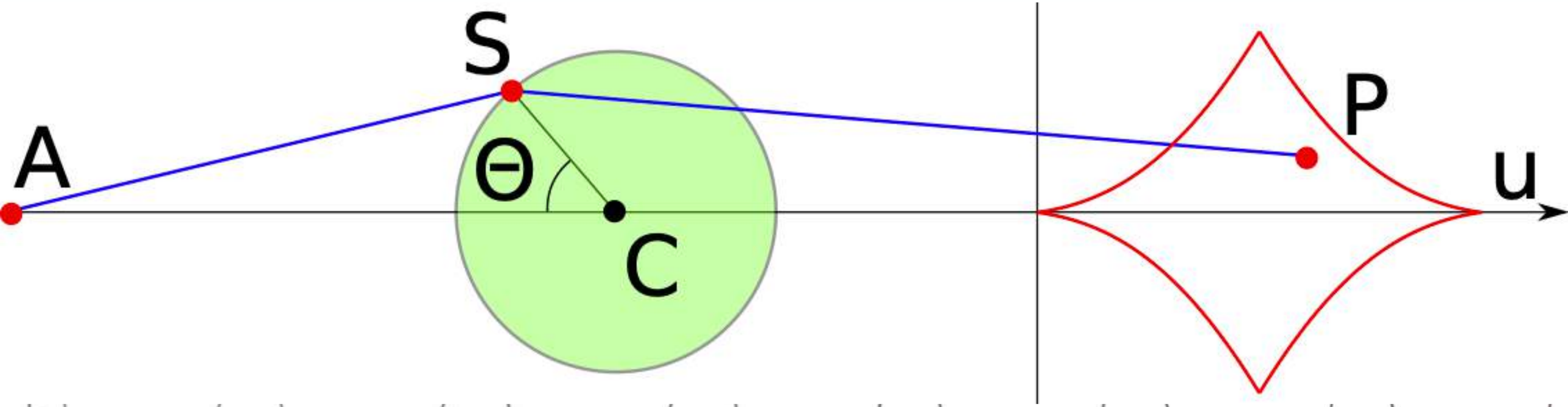

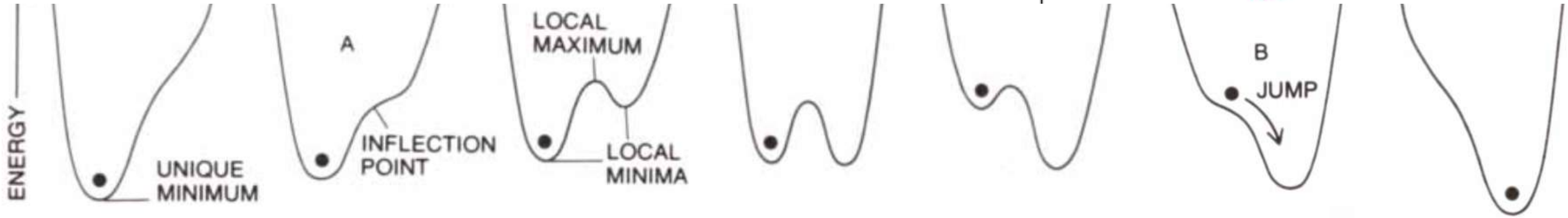

[https://www.geneva.edu/dept/chemistry-math-physics/physics-research/catastrophe-machine/index]

Catastrophe theory

In optics, catastrophes lead to caustics, where classical rays merge. The intensity spikes!

In quantum physics, the Feynman path integral spikes when classical paths of the boundary value problem merge. The quantum amplitude spikes!

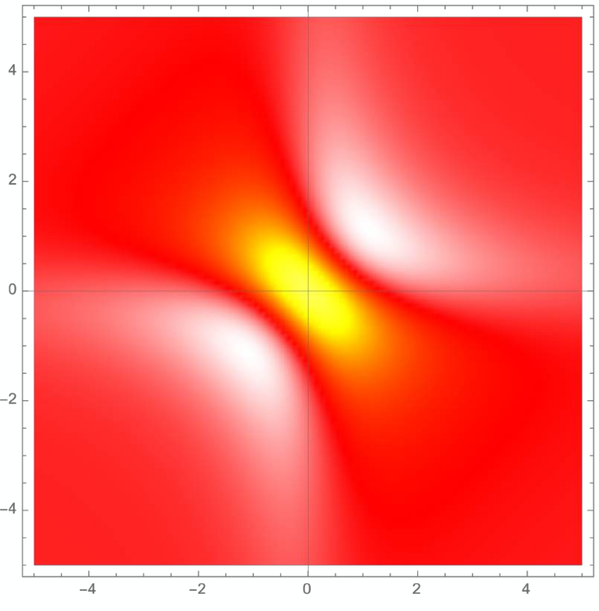

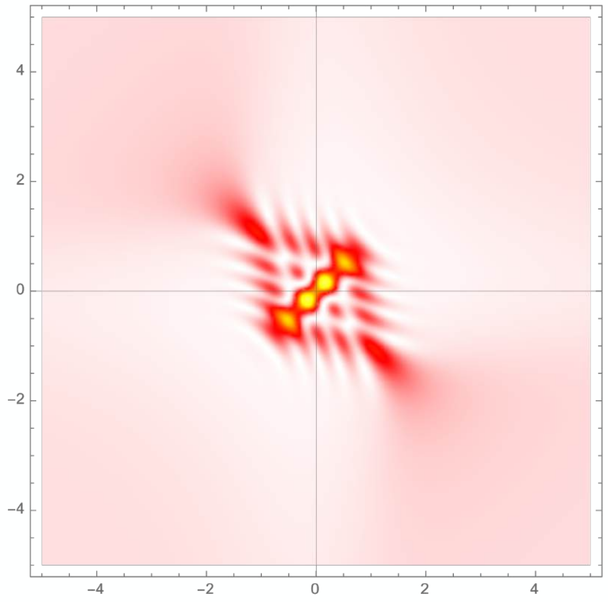

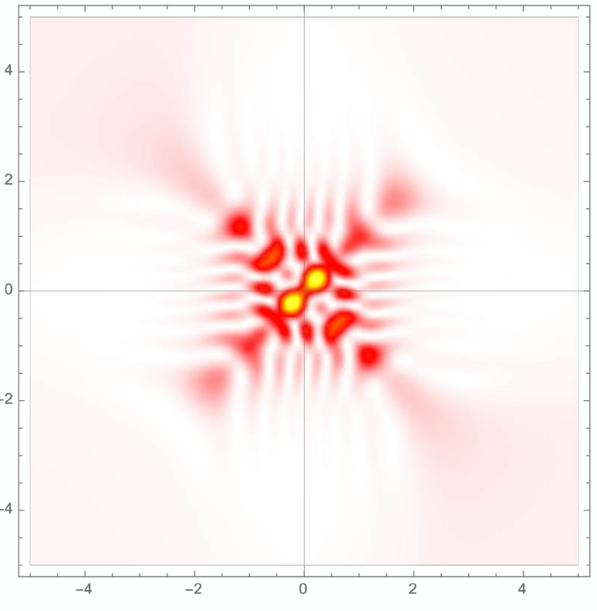

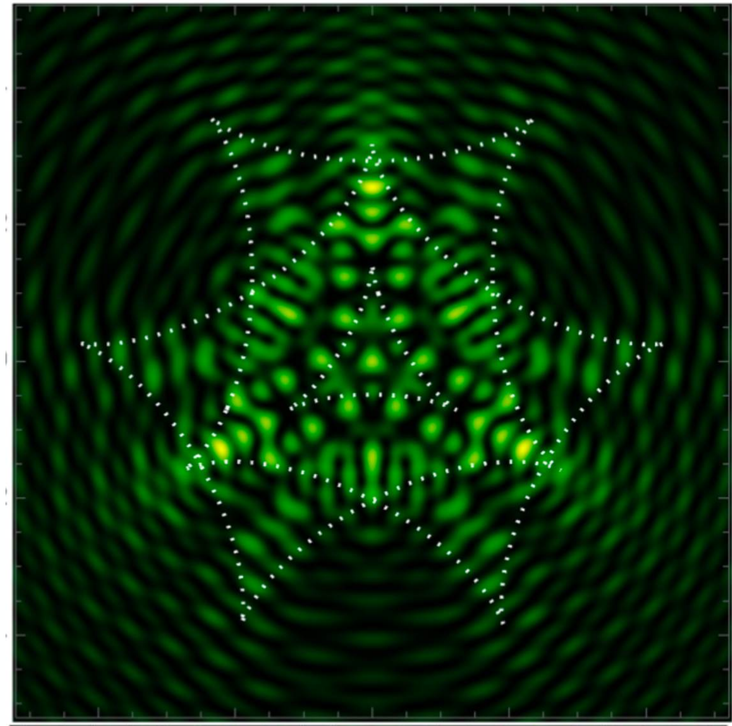

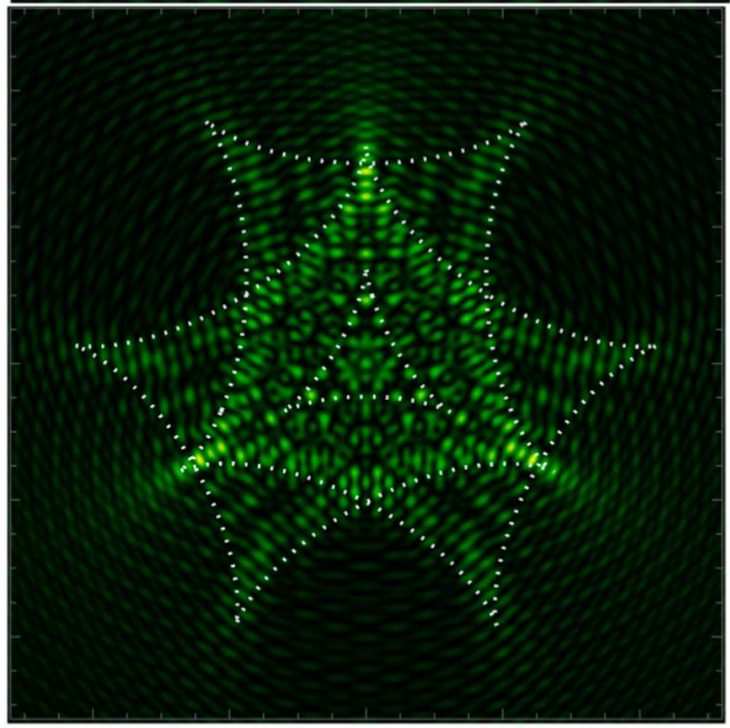

Catastrophe theory

Teller potential Barrier caustics

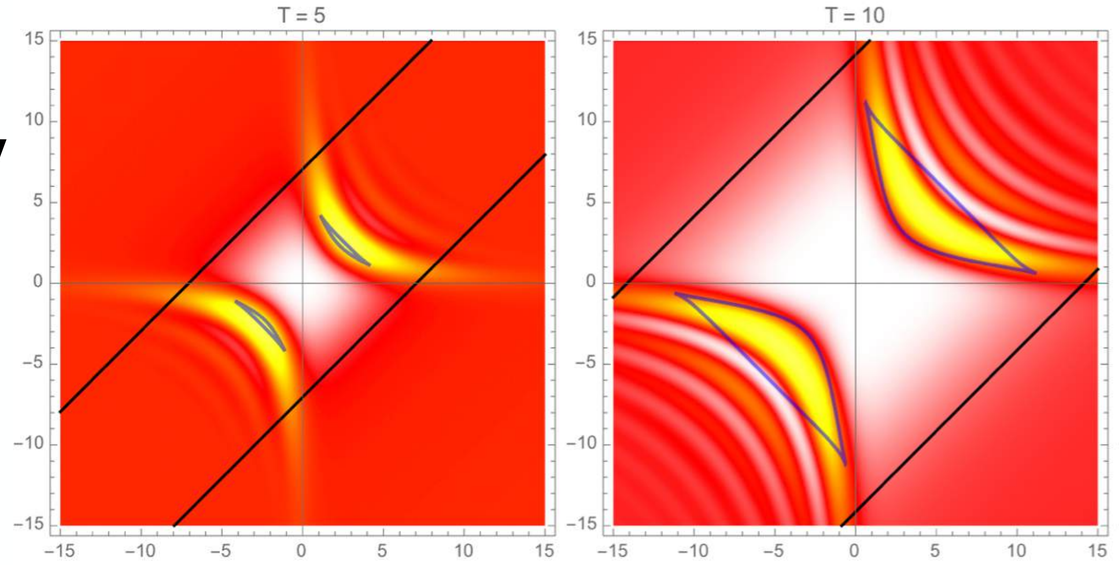

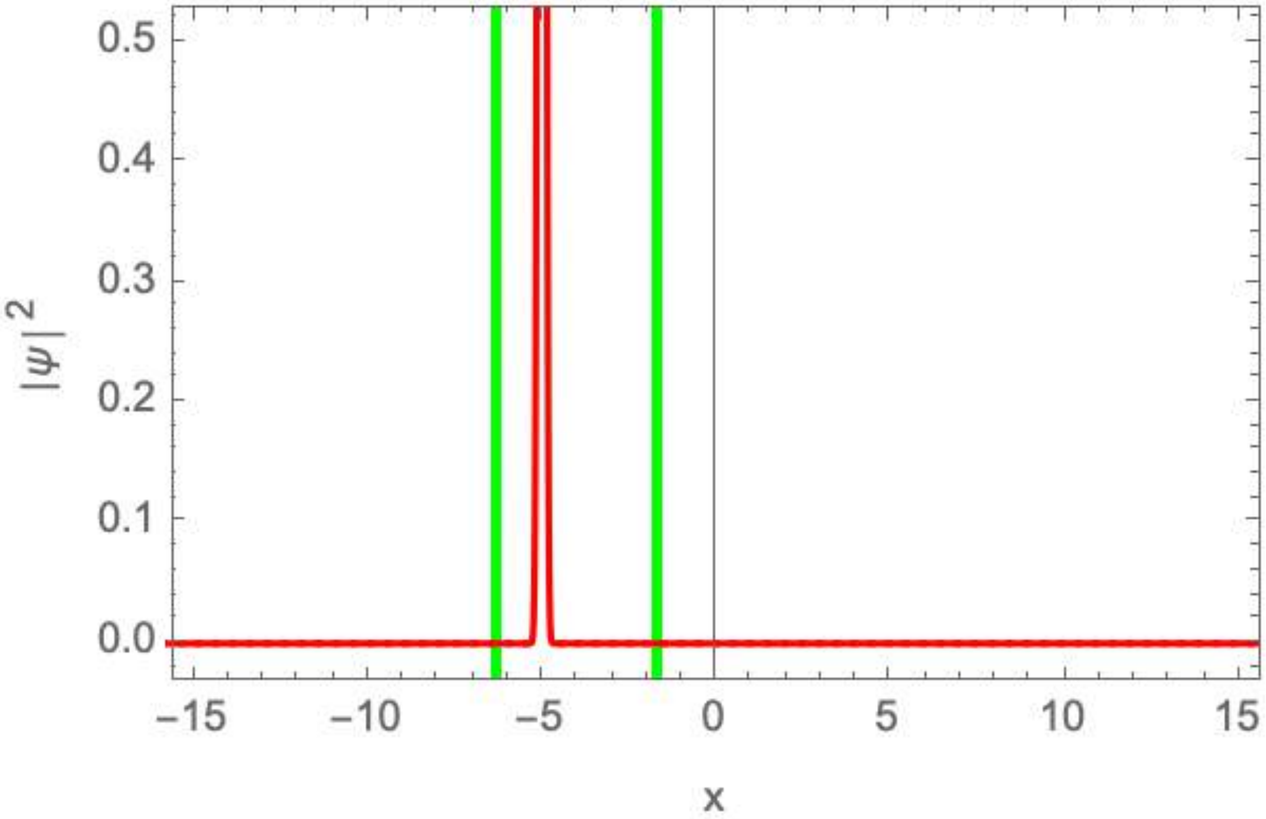

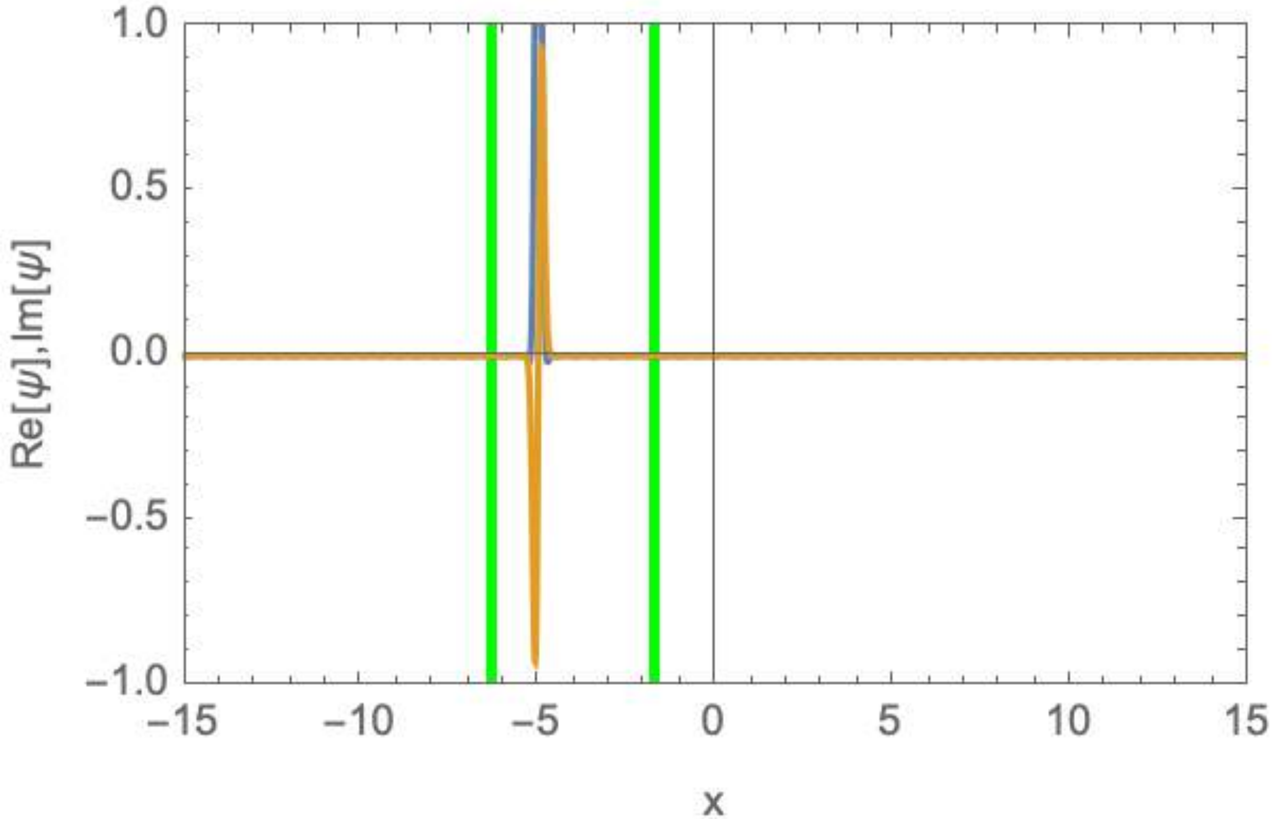

Catastrophe theory

Classification of degenerate critical points, extending Morse Lemma

$$\nabla_x f(x, \lambda) = 0 \qquad \det \mathscr{H}_x f(x, \lambda) = 0$$

Elementary catastrophes

	CATASTROPHE	CONTROL DIMENSIONS	BEHAVIOR DIMENSIONS	FUNCTION
CUSPOIDS	FOLD	1	1	$\frac{1}{3}x^3 - ax$
	CUSP	2	1	$\frac{1}{4}x^4 - ax - \frac{1}{2}bx^2$
	SWALLOWTAIL	3	1	$\frac{1}{5}x^5 - ax - \frac{1}{2}bx^2 - \frac{1}{3}cx^3$
	BUTTERFLY	4	1	$\frac{1}{6}x^6 - ax - \frac{1}{2}bx^2 - \frac{1}{3}cx^3 - \frac{1}{4}dx^4$
UMBILICS	HYPERBOLIC	3	2	$x^3 + y^3 + ax + by + cxy$
	ELLIPTIC	3	2	$x^3 - xy^2 + ax + by + cx^2 + cy^2$
	PARABOLIC	4	2	$x^2y + y^4 + ax + by + cx^2 + dy^2$

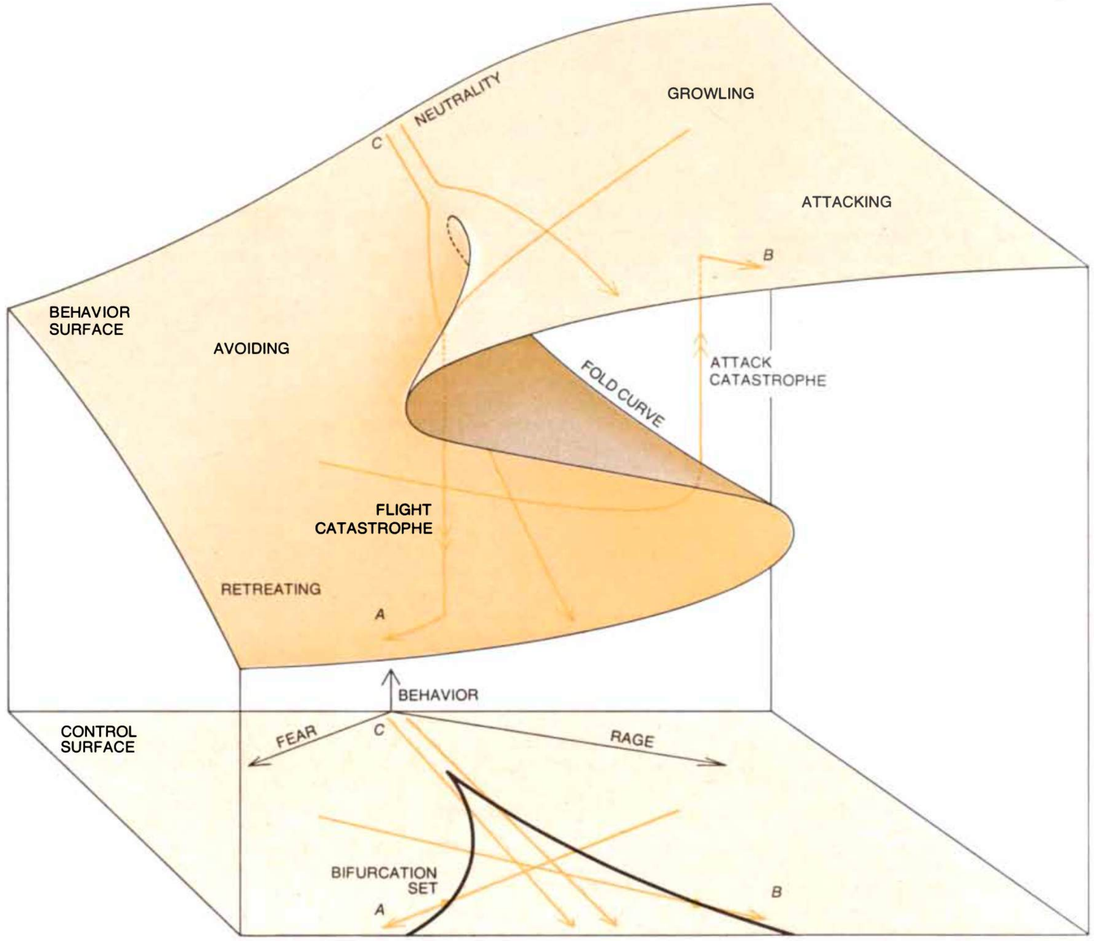

Caustics in the sky

Caustics

In **non-linear gravitational collapse** the geometric structure follows the geometry of the **multi-stream regions**

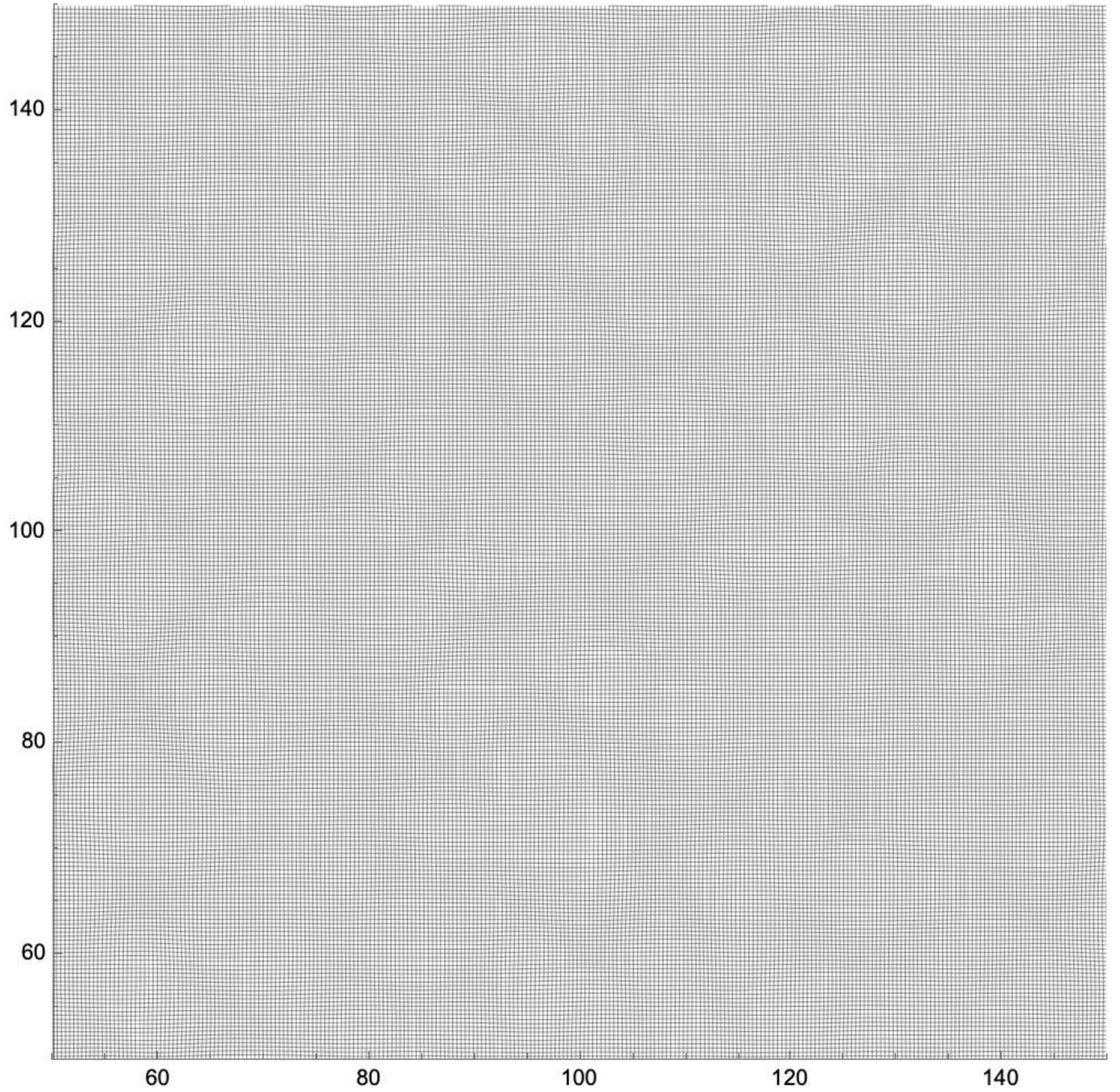

Caustics

- Dark matter forms the geometric structure of the cosmic web through formation of multi-stream regions

- The caustics bound the multi-stream regions

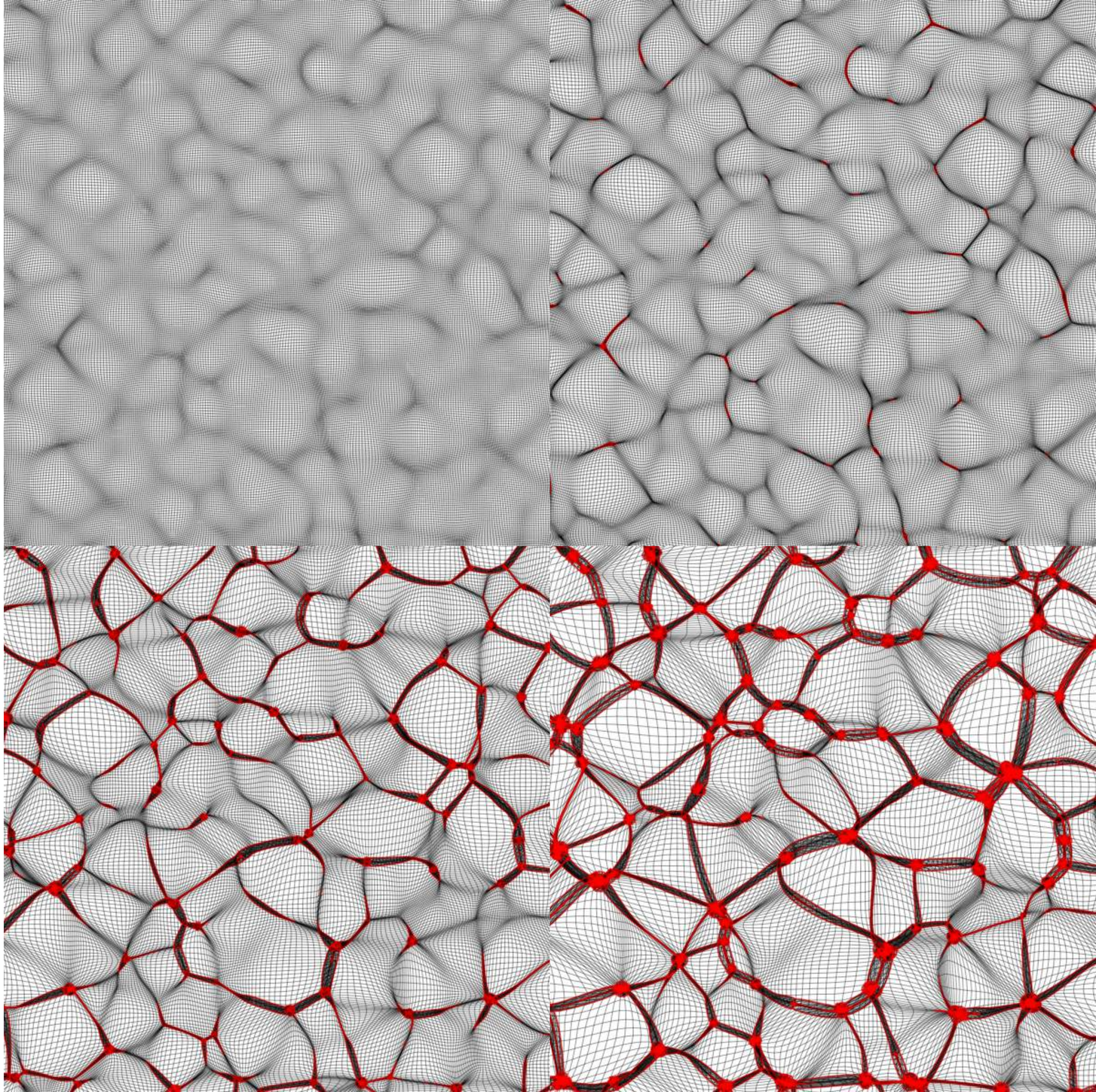

Caustics

- *Vladimir Arnol'd* extended *René Thom's* classification of stable degenerate critical points to **Lagrangian catastrophe theory**
- The **classification of caustics** was applied to *large-scale structure formation* to predict the geometric structure of the *cosmic web*

1972 NORMAL FORMS FOR FUNCTIONS NEAR DEGENERATE CRITICAL POINTS, THE WEYL GROUPS OF A_k, D_k, E_k AND LAGRANGIAN SINGULARITIES

V. I. Arnol'd

1980 EVOLUTION OF SINGULARITIES OF POTENTIAL FLOWS IN COLLISION-FREE MEDIA AND THE METAMORPHOSIS OF CAUSTICS IN THREE-DIMENSIONAL SPACE

V. I. Arnol'd

1982 The Large Scale Structure of the Universe I. General Properties. One- and Two-Dimensional Models

V. I. ARNOLD
Moscow State University, U.S.S.R.

and

S. F. SHANDARIN and YA. B. ZELDOVICH
Institute of Applied Mathematics, Moscow, U.S.S.R.

(*Received August* 11, 1981)

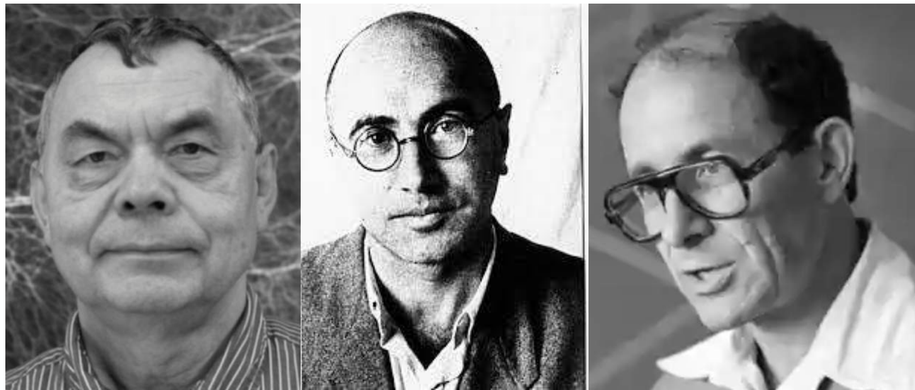

Caustics

Arnol'd, Shandarin, Zel'dovich (1982)

Lagrangian fluid dynamics

$$\mathbf{x}_t(\mathbf{q}) = \mathbf{q} + \mathbf{s}_t(\mathbf{q})$$

where the displacement map solves the Euler equation and the Poisson equation while implementing the conservation of mass. The density follows as the reciprocal of the Jacobian

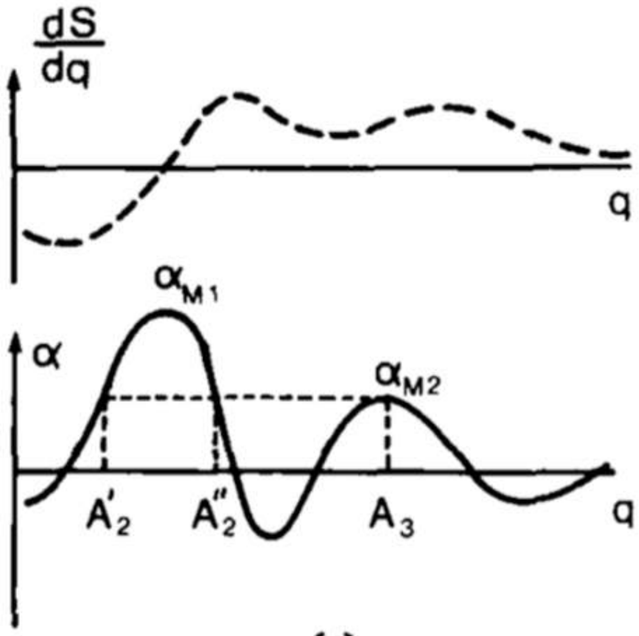

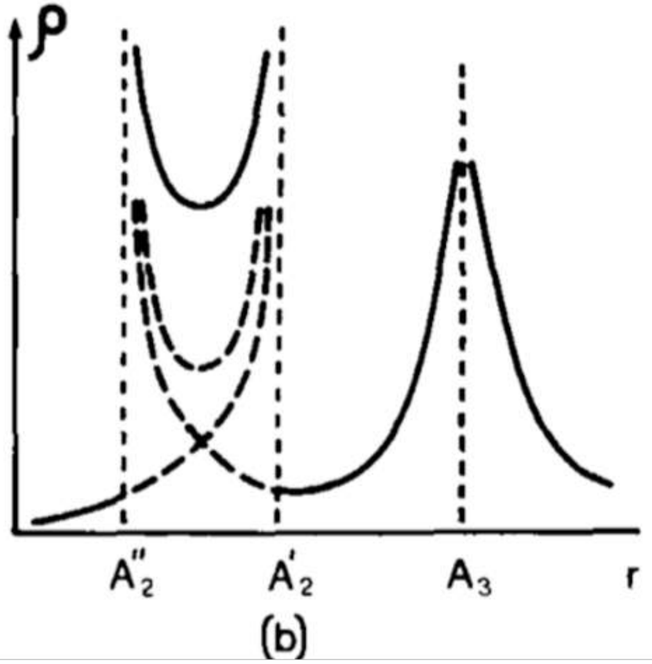

$$\rho_t(\mathbf{x}') = \sum_{\mathbf{q}\in\mathbf{x}_t^{-1}(\mathbf{x}')} \frac{\bar{\rho}}{|\det \nabla \mathbf{x}_t(\mathbf{q})|} = \sum_{\mathbf{q}\in\mathbf{x}_t^{-1}(\mathbf{x}')} \frac{\bar{\rho}}{|1+\mu_1(\mathbf{q})||1+\mu_2(\mathbf{q})||1+\mu_3(\mathbf{q})|}$$

with the eigenvalues of the deformation tensor $\nabla \mathbf{s}_t(\mathbf{q})\mathbf{v}_i(\mathbf{q}) = \mu_i(\mathbf{q})\mathbf{v}_i(\mathbf{q})$

Caustic conditions

Up to recently, we only knew how to evaluate the fold caustic in 2D. Now we can evaluate any caustic in any dimension

$$\frac{\Delta x}{|\Delta q|} = \frac{\|x_t(q') - x_t(q'')\|}{\|q' - q''\|} \to 0 \qquad q', q'' \to q_s$$

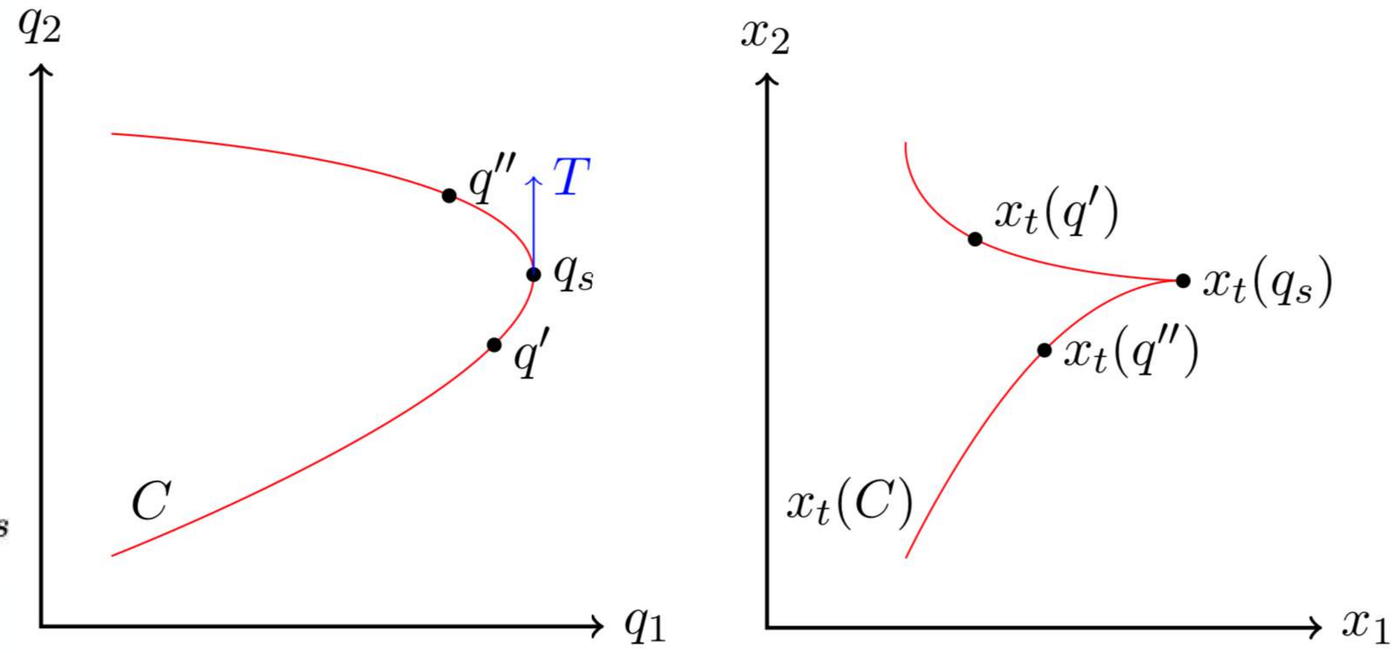

Theorem: *A manifold $M \subset L$ forms a singularity under the mapping x_t in the point $x_t(q_s) \in x_t(M) \subset E$ at time t, meaning that $x_t(M)$ is not smooth in $x_t(q_s)$, if and only if there exists at least one nonzero tangent vector $T \in T_{q_s}M$ satisfying*

$$(1 + \mu_{it}(q_s))v_{it}^*(q_s) \cdot T = 0$$

for all $i = 1, 2, \ldots, dim(L)$.

Feldbrugge et al (2019)

Caustic conditions

When applying the caustic condition to a Lagrangian space, we obtain the fold condition

$$A_2^i(t) = \{\mathbf{q} \in L \mid 1 + \mu_{it}(\mathbf{q}) = 0\}$$

Applying the caustic condition a second time, we obtain the cusp caustic in terms of both the eigenvalue and eigenvector fields

$$A_3^i(t) = \{\mathbf{q} \in L \mid \mathbf{q} \in A_2^i(t), \mathbf{v}_i \cdot \nabla \mu_{it} = 0\}$$

$$(1 + \mu_{it}(q_s))v_{it}^*(q_s) \cdot T = 0$$

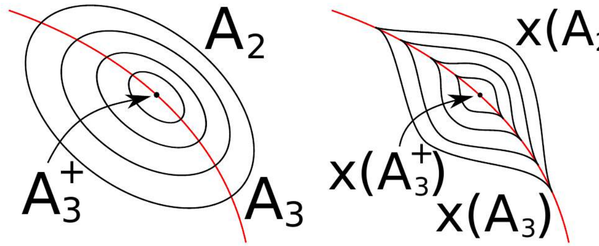

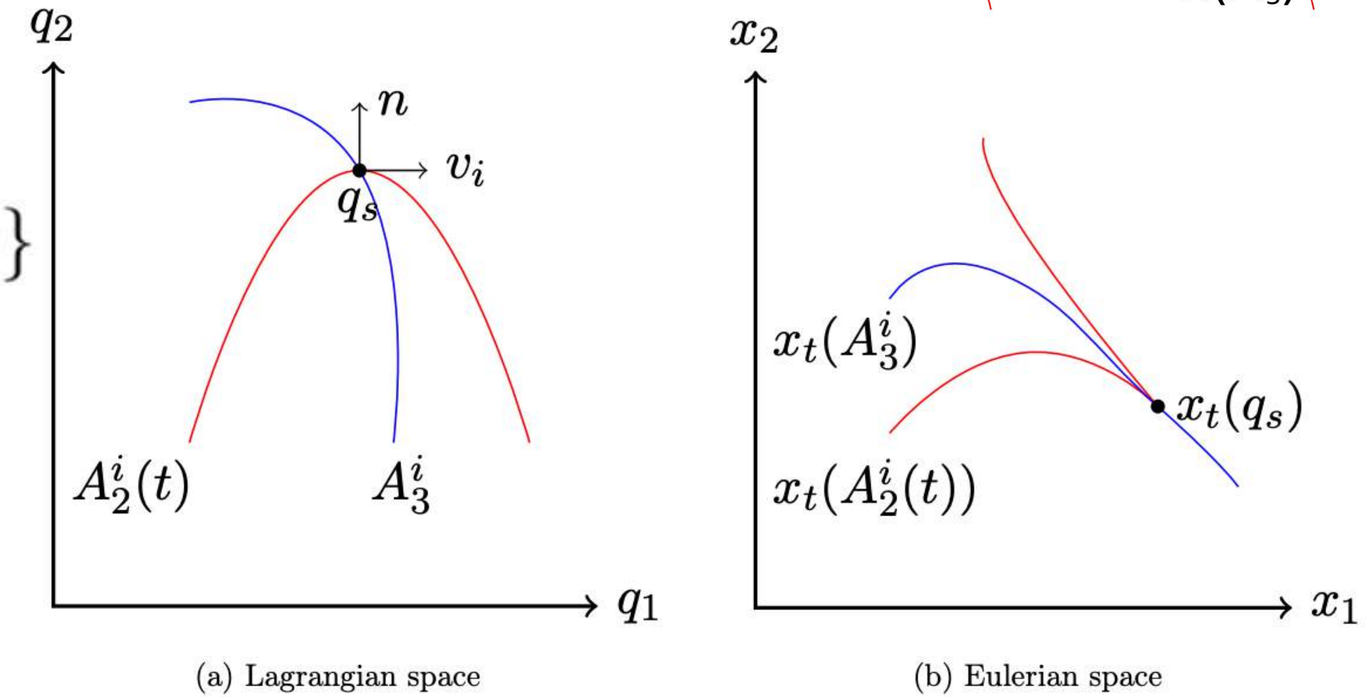

(a) Lagrangian space

(b) Eulerian space

Feldbrugge et al (2019)

Caustic conditions

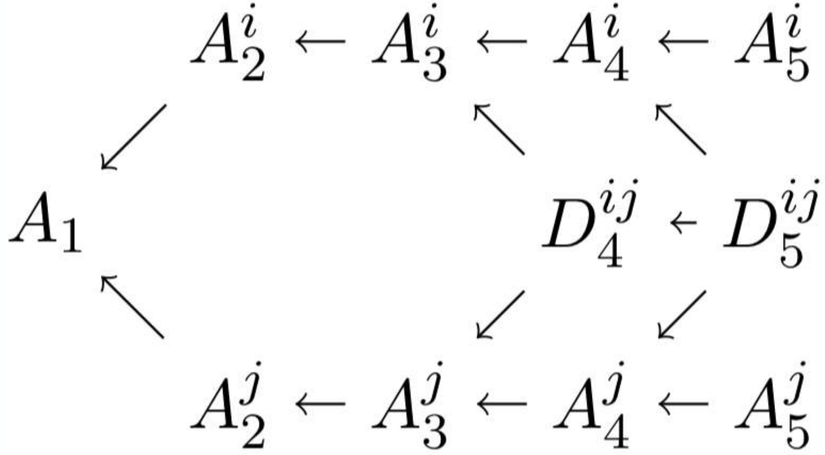

Iterative application of the shell-crossing condition

$$(1 + \mu_{it}(q_s))v_{it}^*(q_s) \cdot T = 0$$

leads to the caustic conditions on both the eigenvalue and eigenvector fields:

$$
\begin{aligned}
&\text{Fold:} && A_2^i(t) = \{\mathbf{q} \in L \mid 1 + \mu_{it}(\mathbf{q}) = 0\} \\
&\text{Cusp:} && A_3^i(t) = \{\mathbf{q} \in L \mid \mathbf{q} \in A_2^i(t), \mathbf{v}_i \cdot \nabla \mu_{it} = 0\} \\
&\text{Swallowtail:} && A_4^i(t) = \{\mathbf{q} \in L \mid \mathbf{q} \in A_3^i(t), \mathbf{v}_i \cdot \nabla (\mathbf{v}_i \cdot \nabla \mu_{it}) = 0\} \\
&\text{Butterfly:} && A_5^i(t) = \{\mathbf{q} \in L \mid \mathbf{q} \in A_4^i(t), \mathbf{v}_i \cdot \nabla (\mathbf{v}_i \cdot \nabla (\mathbf{v}_i \cdot \nabla \mu_{it})) = 0\} \\
&\text{Umbilic:} && D_4^{ij}(t) = \{\mathbf{q} \in L \mid 1 + \mu_{it}(\mathbf{q}) = 1 + \mu_{jt}(\mathbf{q}) = 0\} \\
&\text{Parabolic:} && D_5^{ij}(t) = \{\mathbf{q} \in L \mid q \in D_4^{ij}(t), \mathbf{v}_i \cdot \nabla \mu_i = \mathbf{v}_j \cdot \nabla \mu_j = 0\}
\end{aligned}
$$

Morse-Smale theory of full deformation tensor field. No free parameters!

Feldbrugge et al (2019)

Caustic conditions

Singularity class	Singularity name	Feature in the 2D cosmic web	Feature in the 3D cosmic web	Profile $\rho(r)$
A_2	fold	collapsed region	collapsed region	$\rho(r) \propto r^{-1/2}$
A_3	cusp	filament	wall or membrane	$\rho(r) \propto r^{-2/3}$
A_4	swallowtail	cluster or knot	filament	$\rho(r) \propto r^{-3/4}$
A_5	butterfly	not stable	cluster or knot	$\rho(r) \propto r^{-4/5}$
D_4	hyperbolic/elliptic	cluster or knot	filament	$\rho(r) \propto r^{-1}$
D_5	parabolic	not stable	cluster or knot	$\rho(r) \propto r^{-1} \log(1/r)$

The identification of the different caustics in the 2- and 3-dimensional cosmic web

Feldbrugge et al (2019)

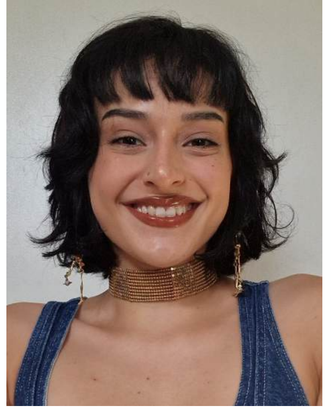

Maé Rodriguez **Benjamin Hertzsch**

The geometry of the cosmic web

Caustic conditions

Note that:

- The **eigenvalue and eigenvector** fields are **non-linear transformations of the density perturbations**
- The web-like nature is embedded in the distribution of the **eigenvalue** *and* **eigenvector fields**

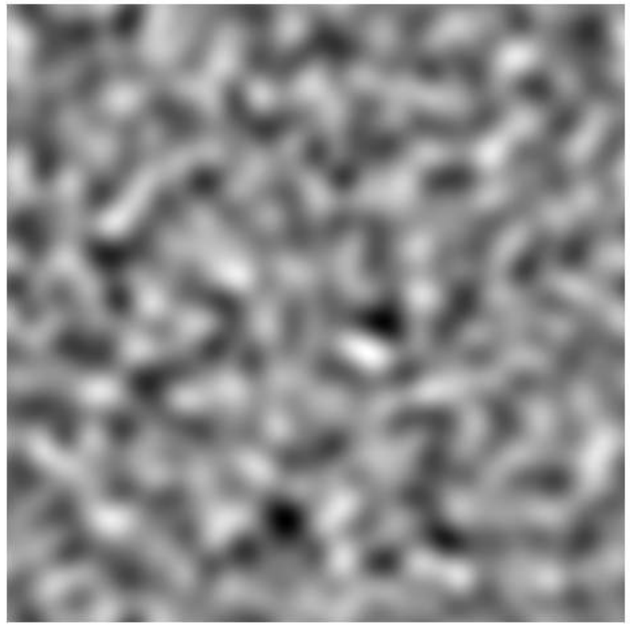

(a) The density perturbation δ

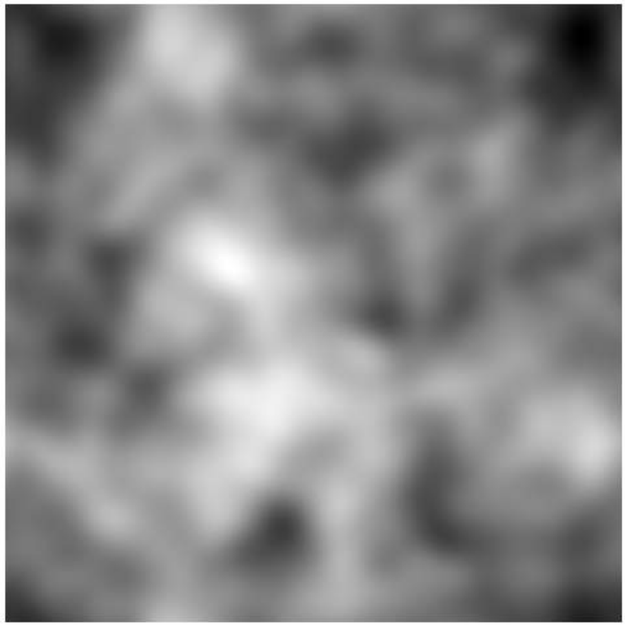

(b) The displacement potential Ψ

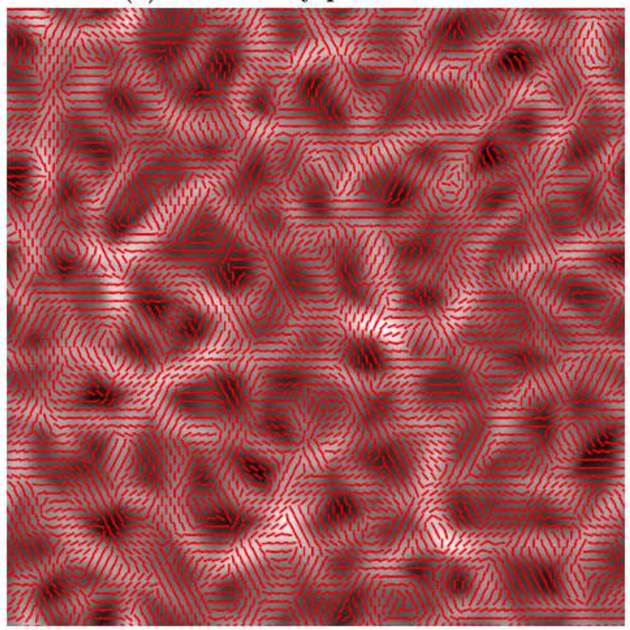

(c) The first eigenvalue and eigenvector fields λ_1, and $\boldsymbol{v}_1$

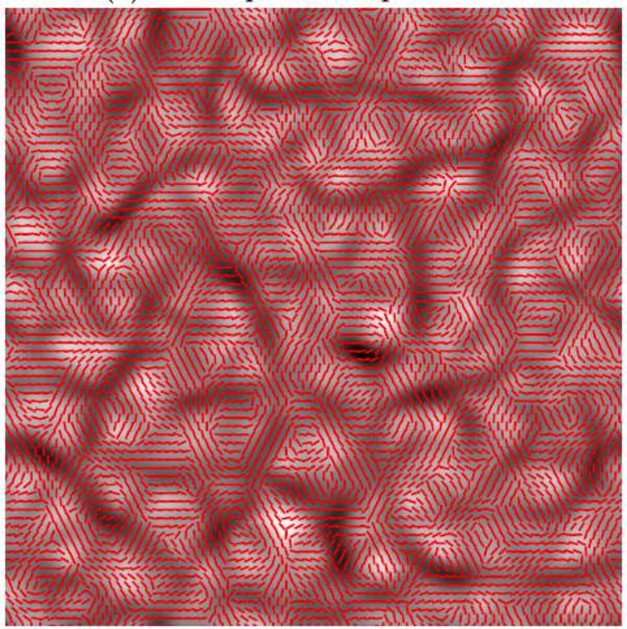

(d) The second eigenvalue and eigenvector fields λ_2, and $\boldsymbol{v}_2$

Caustic conditions

$\mathbf{x}_t(\mathbf{q}) = \mathbf{q} - b_+(t)\,\nabla\Psi(\mathbf{q})$

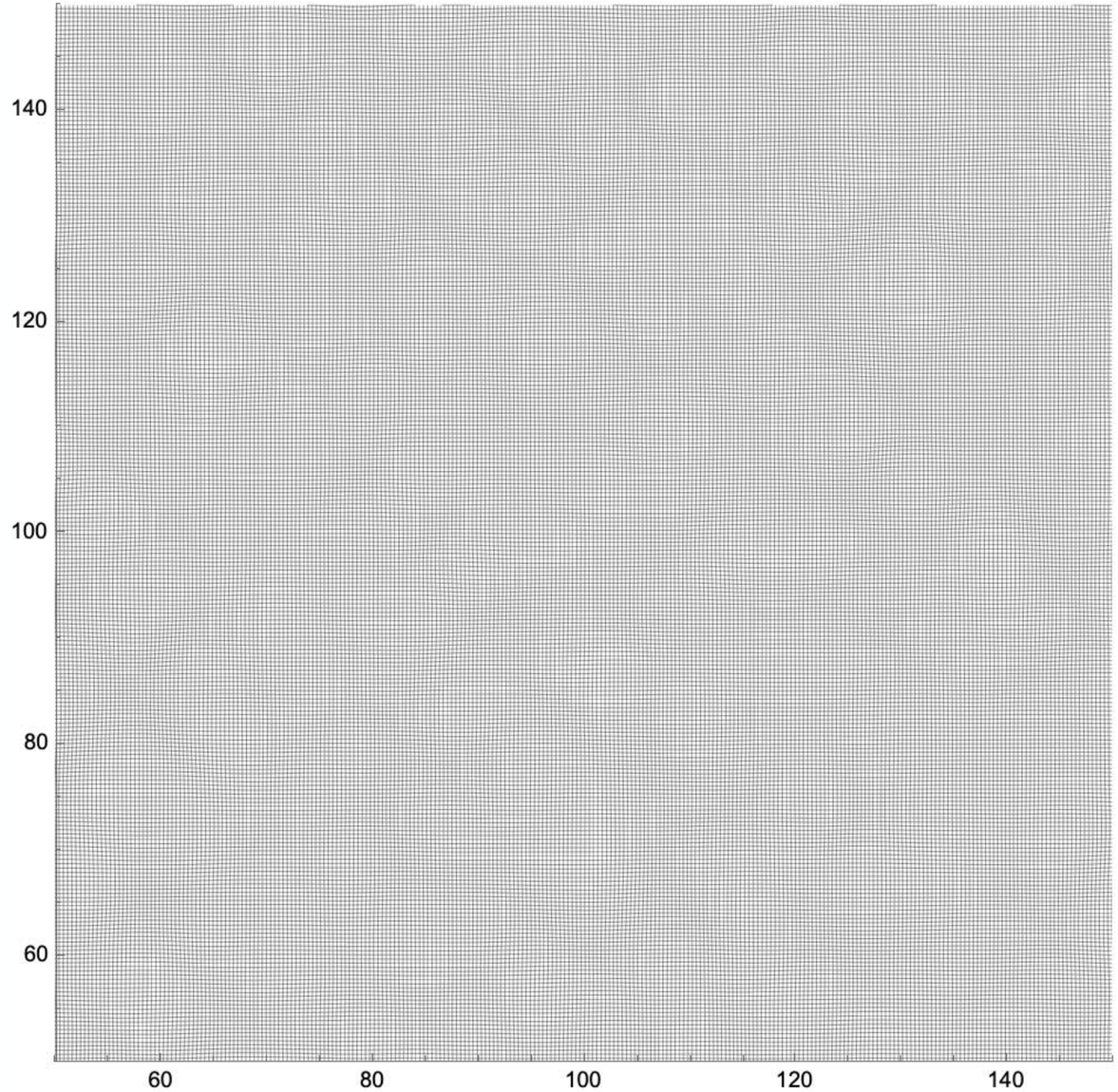

$\mathbf{x}_t(\mathbf{q}) = \mathbf{q} + \mathbf{s}_t(\mathbf{q})$

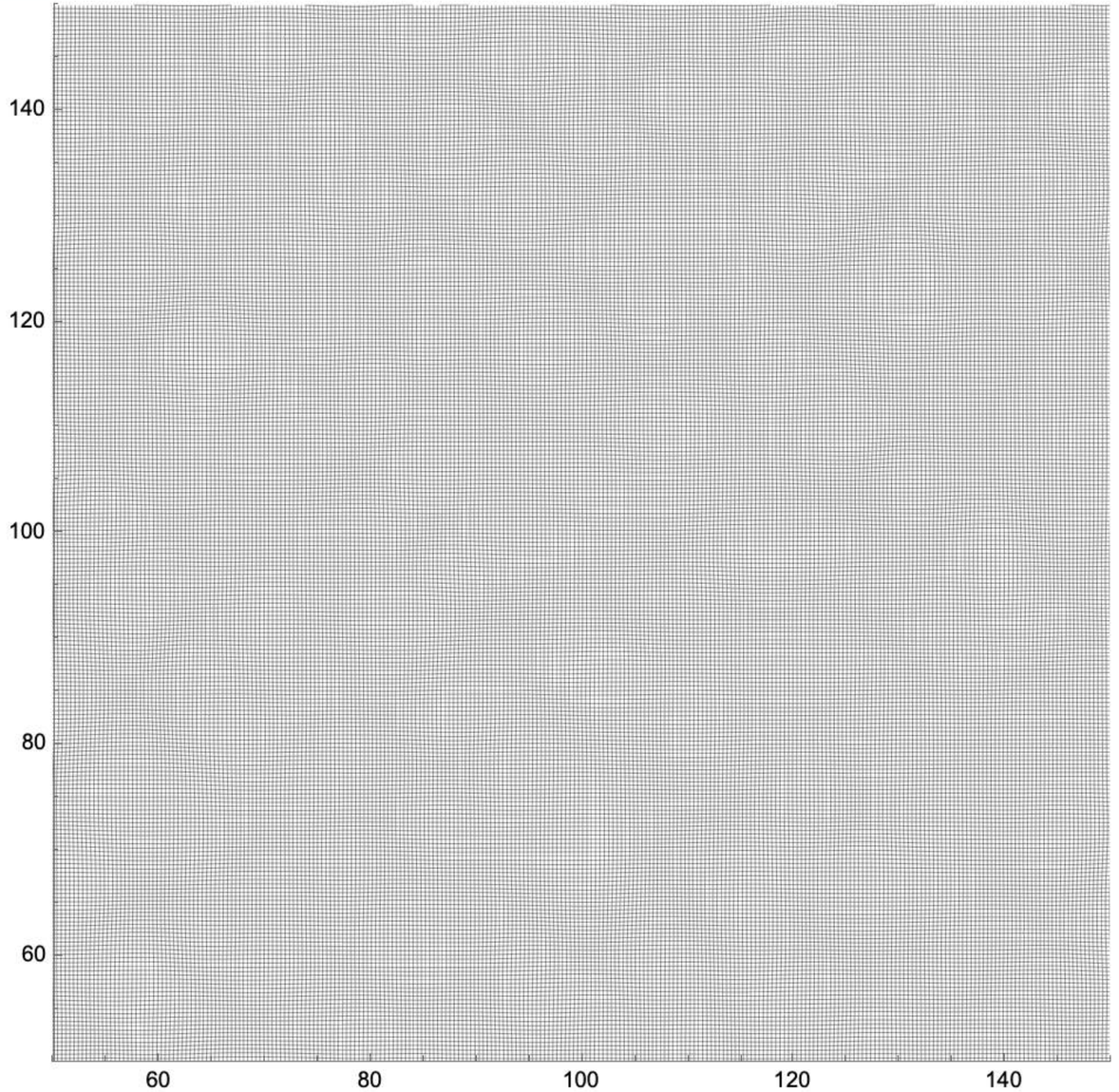

Caustic conditions

$$\mathbf{x}_t(\mathbf{q}) = \mathbf{q} - b_+(t)\,\nabla\Psi(\mathbf{q})$$

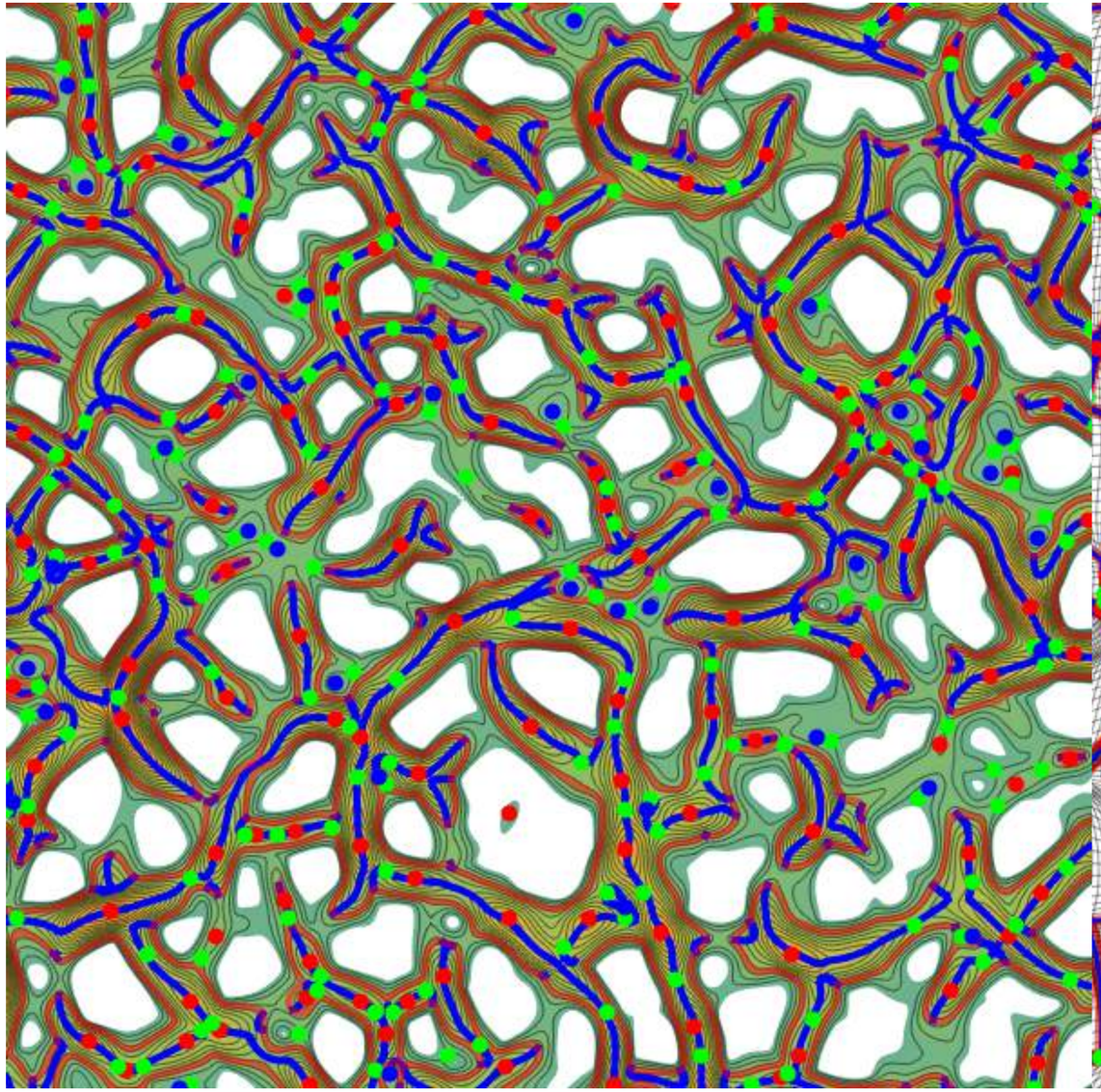

$$\mathbf{x}_t(\mathbf{q}) = \mathbf{q} + \mathbf{s}_t(\mathbf{q})$$

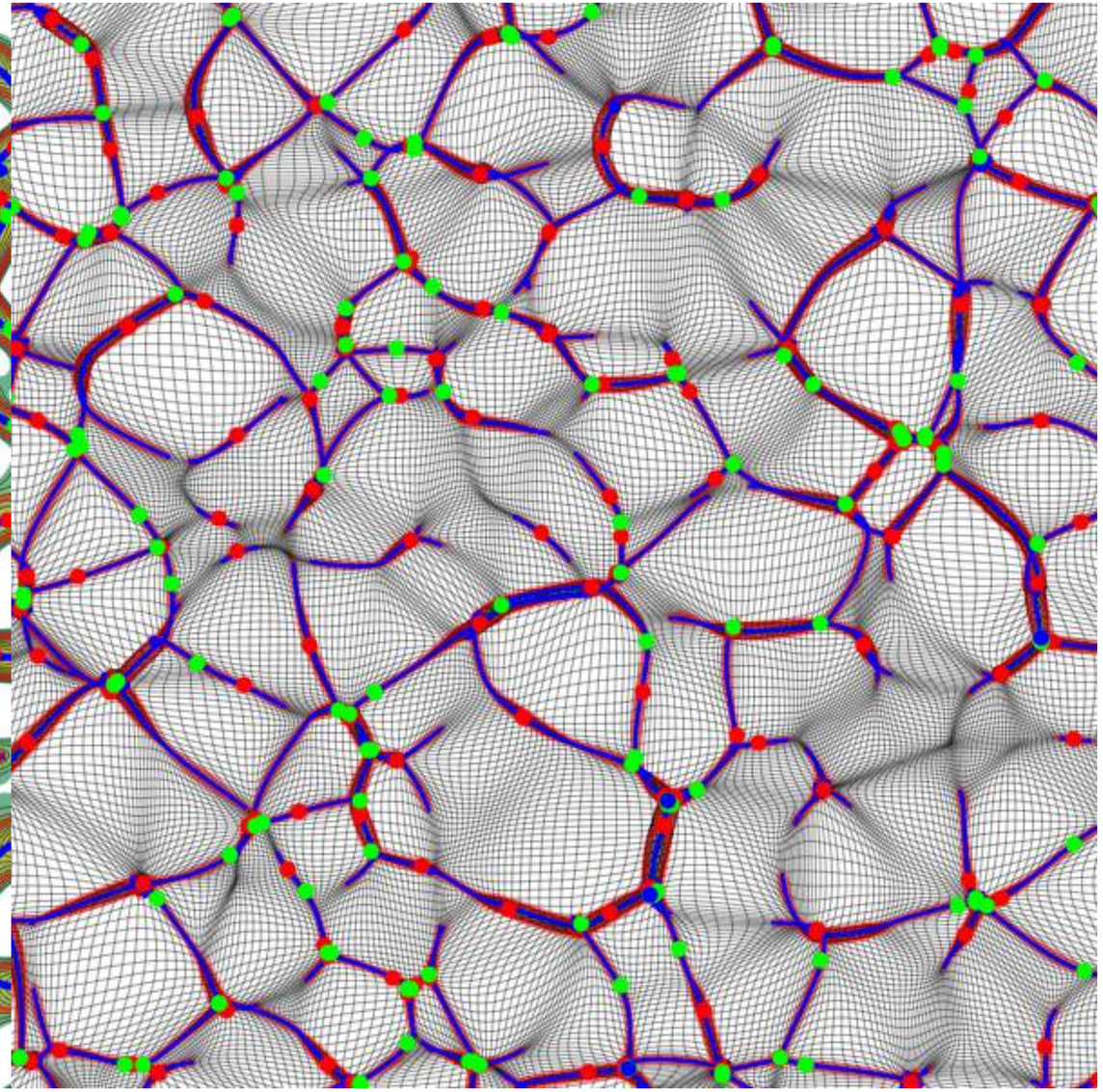

Zel’dovich Pancake

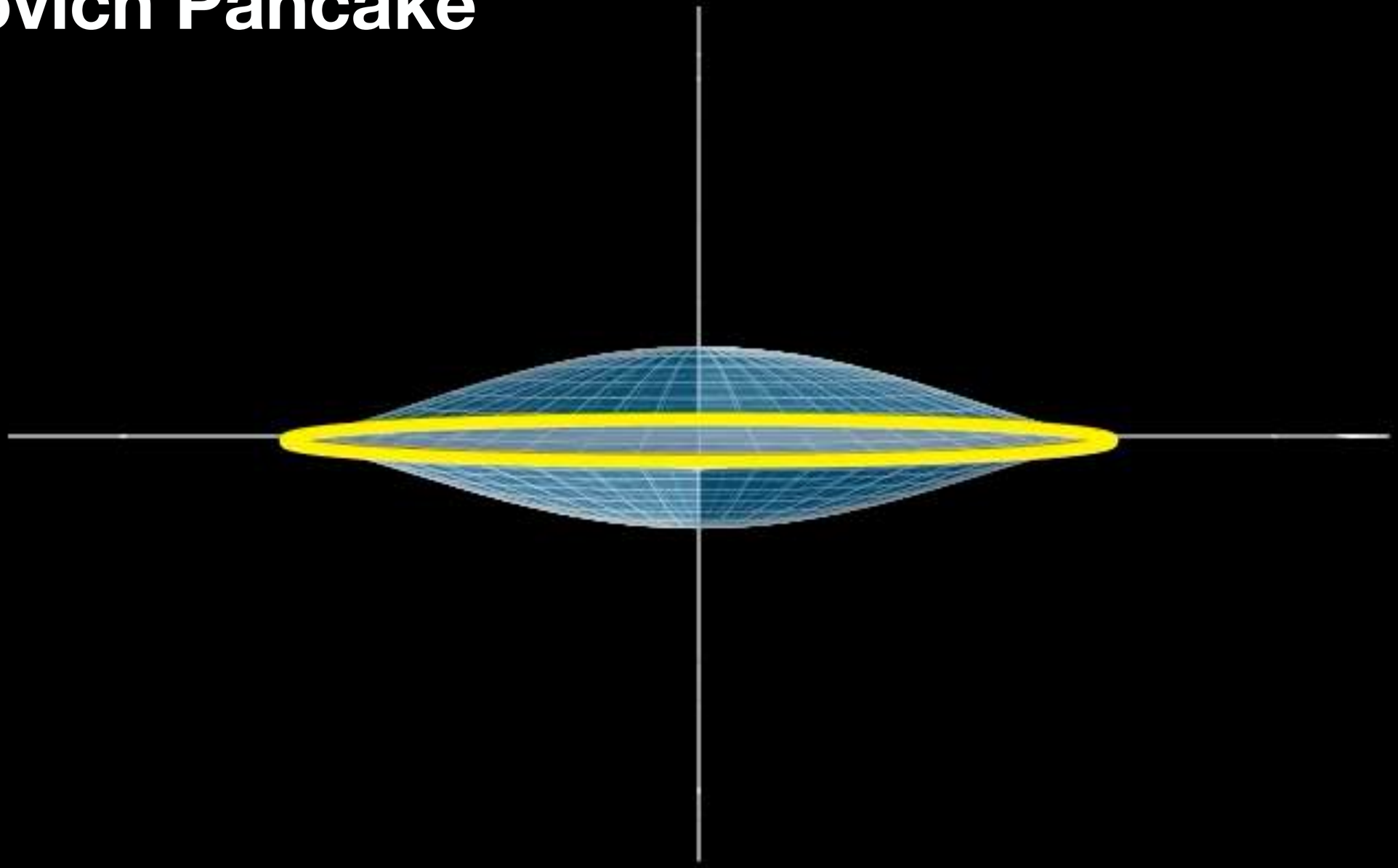

Caustic in 3D

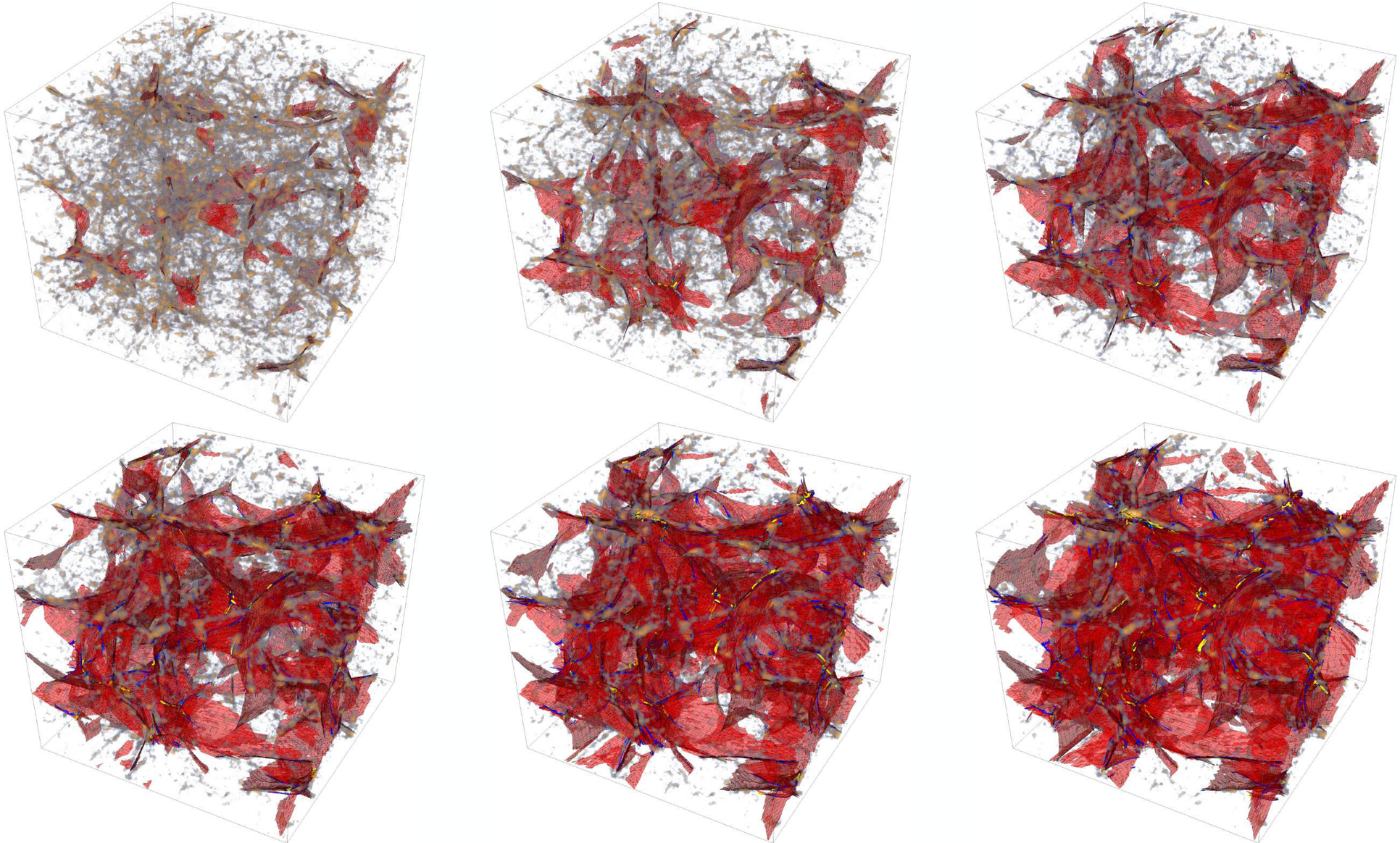

Caustic conditions

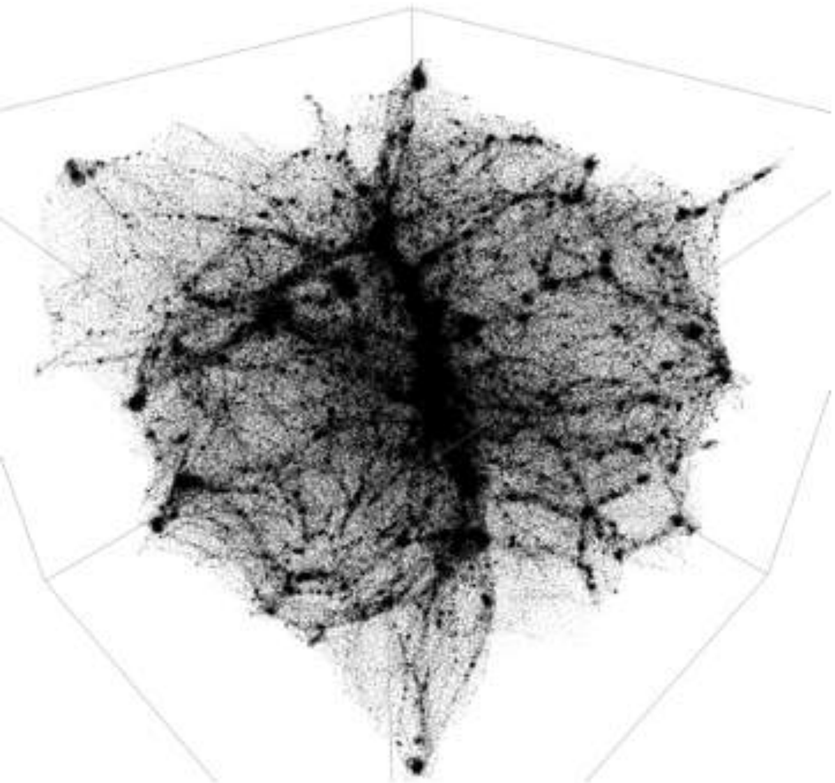

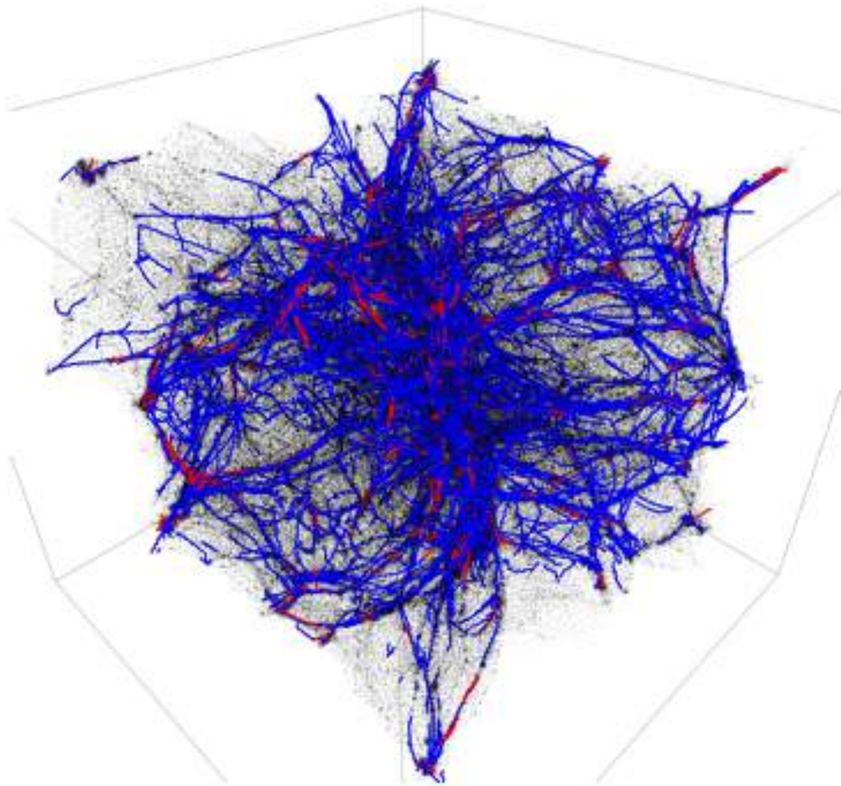

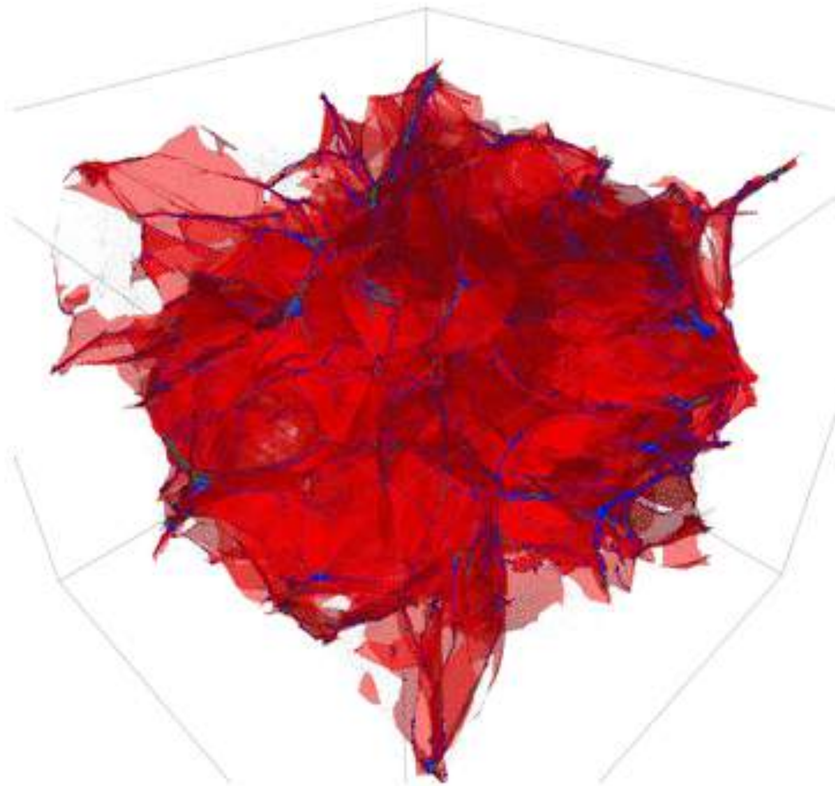

Caustic in 3D

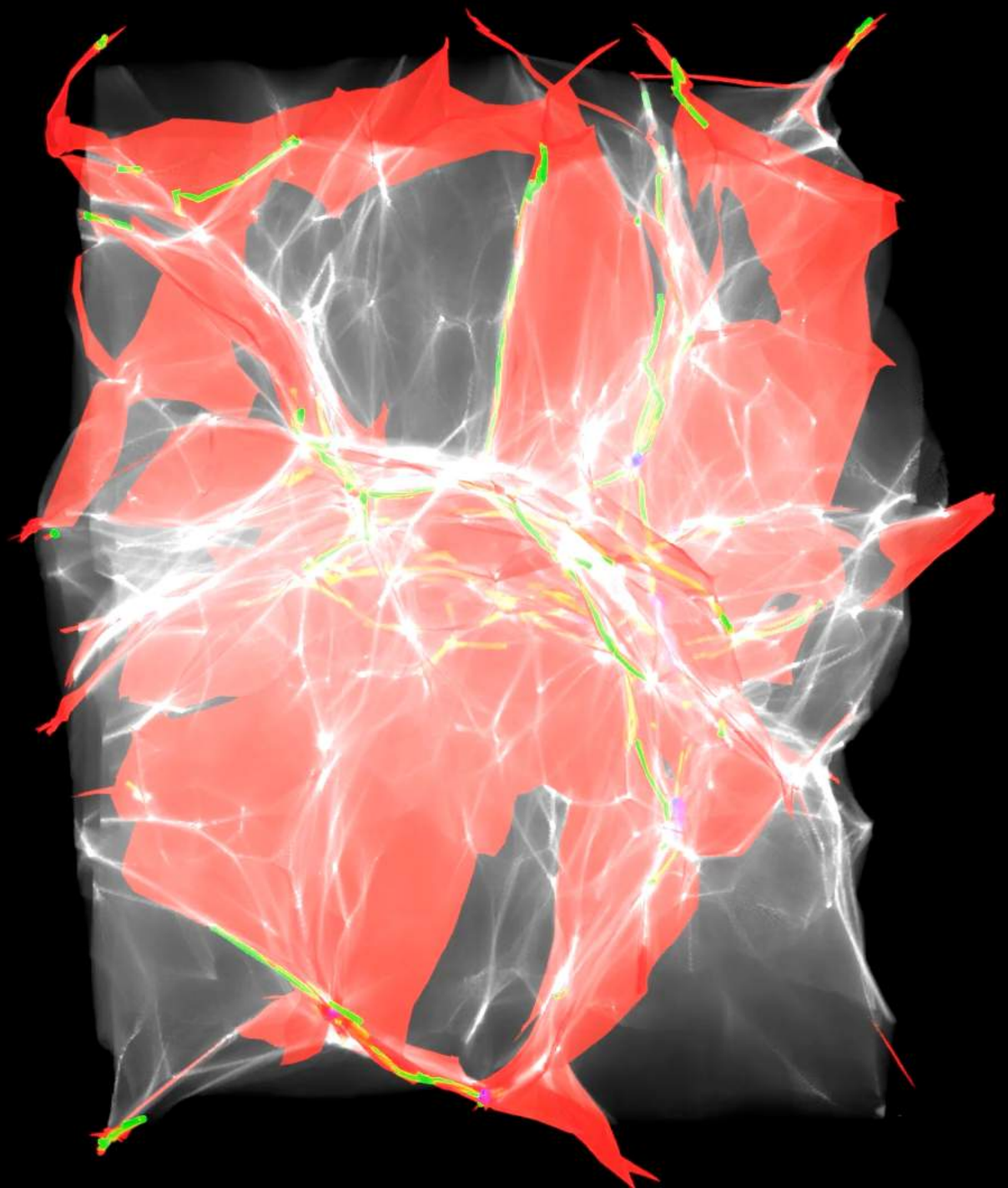

Caustic in 3D

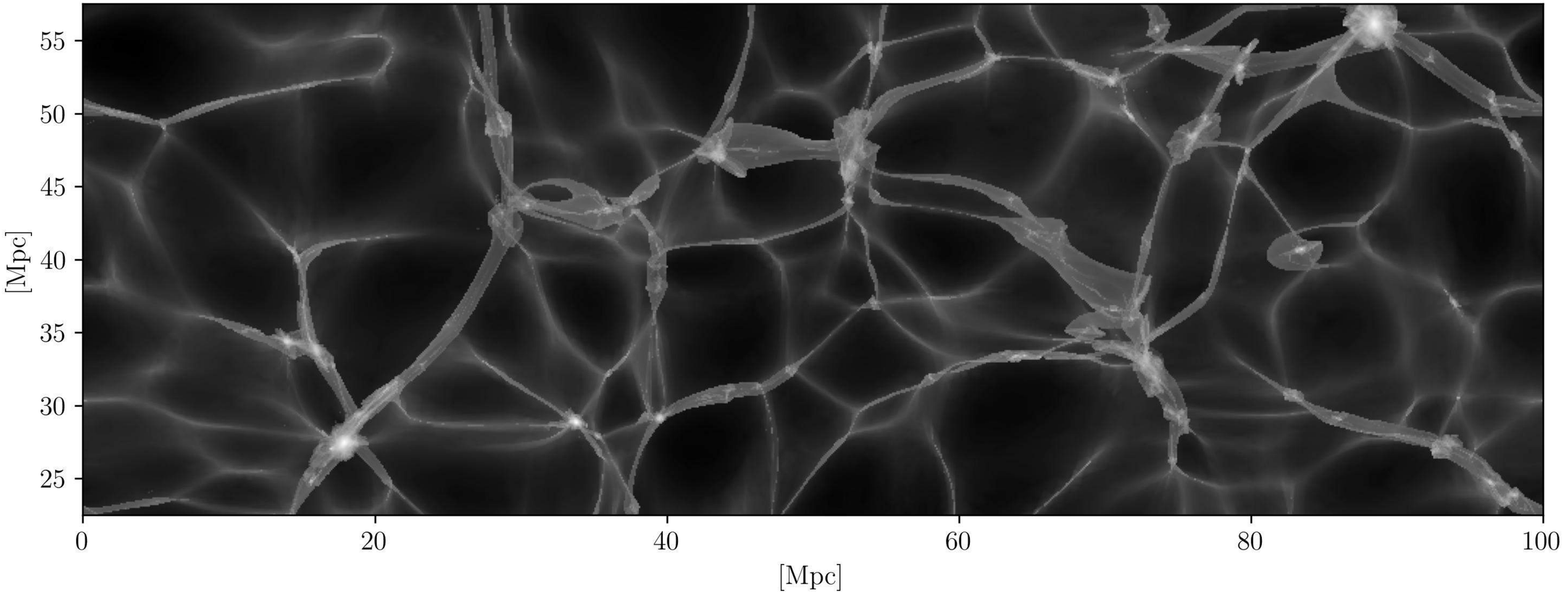

Caustic in 3D

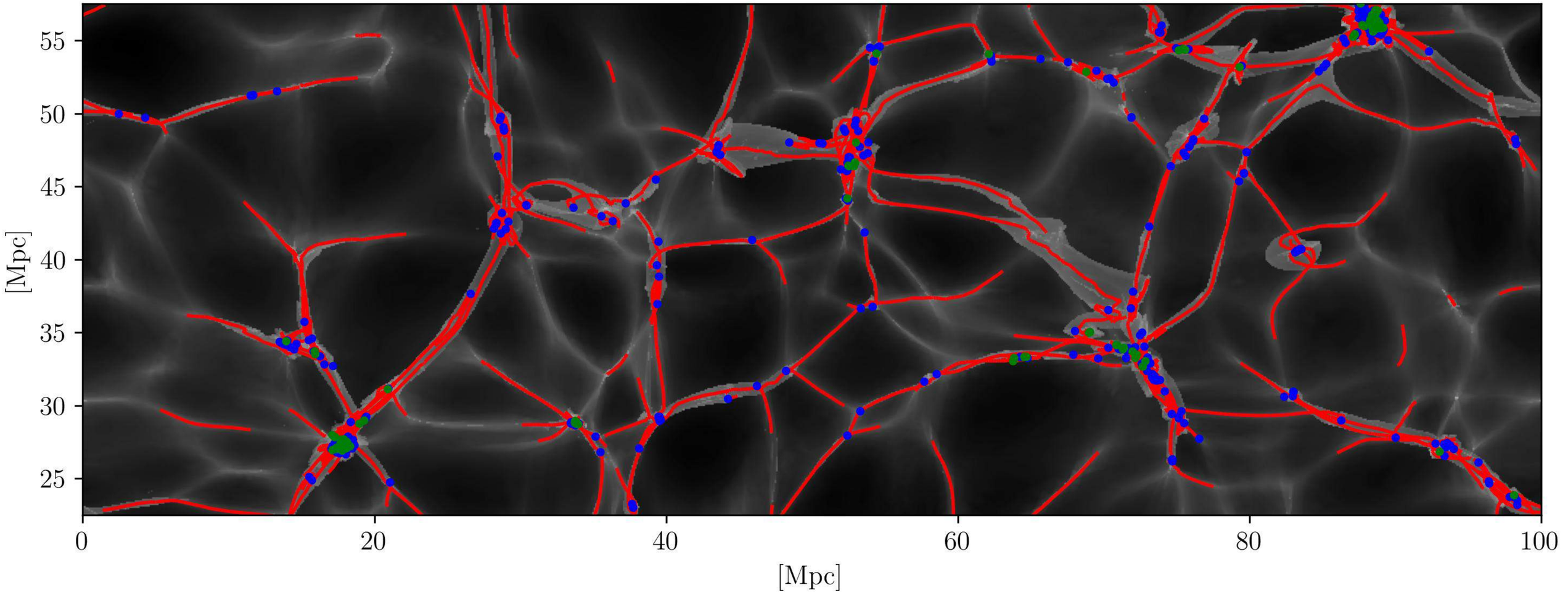

Caustic in 3D

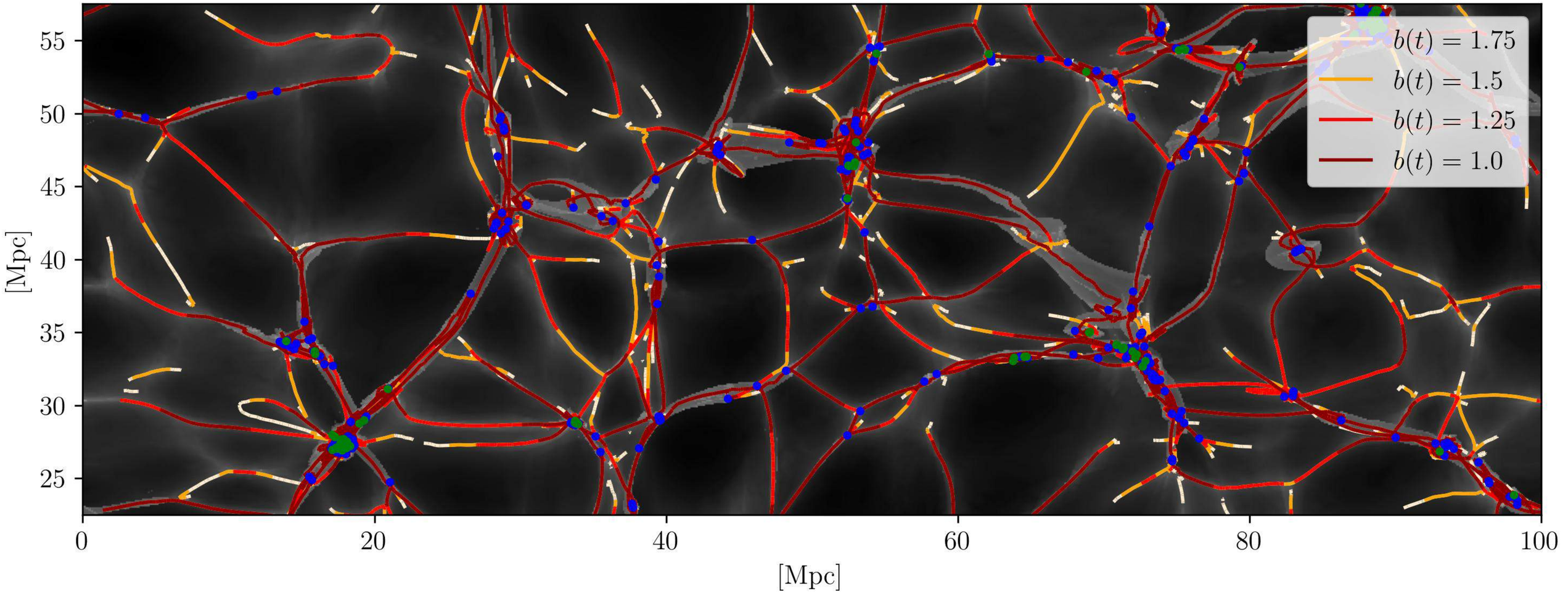

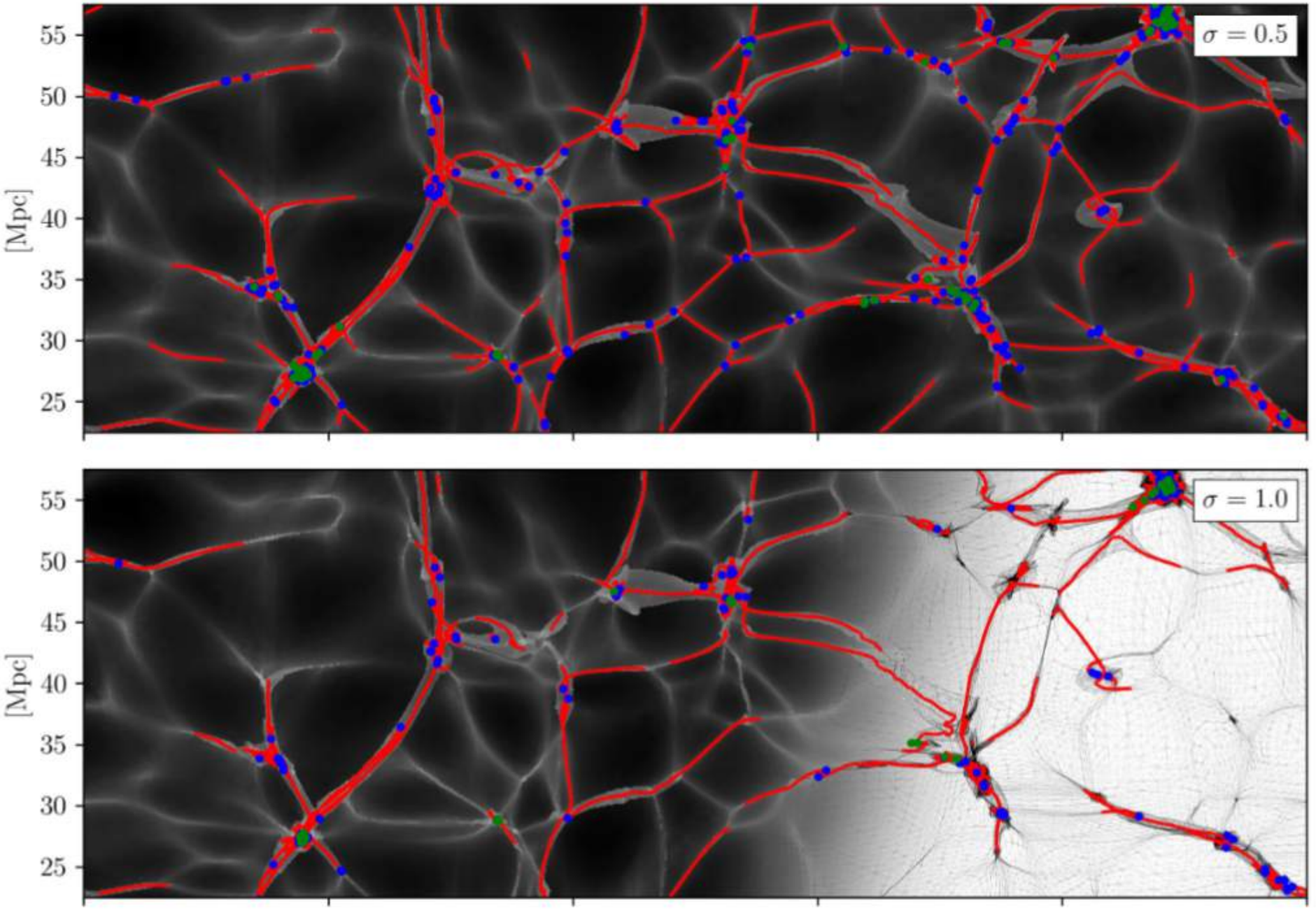
$\sigma = 0.5$
$\sigma = 1.0$
[Mpc]
55
50
45
40
35
30
25

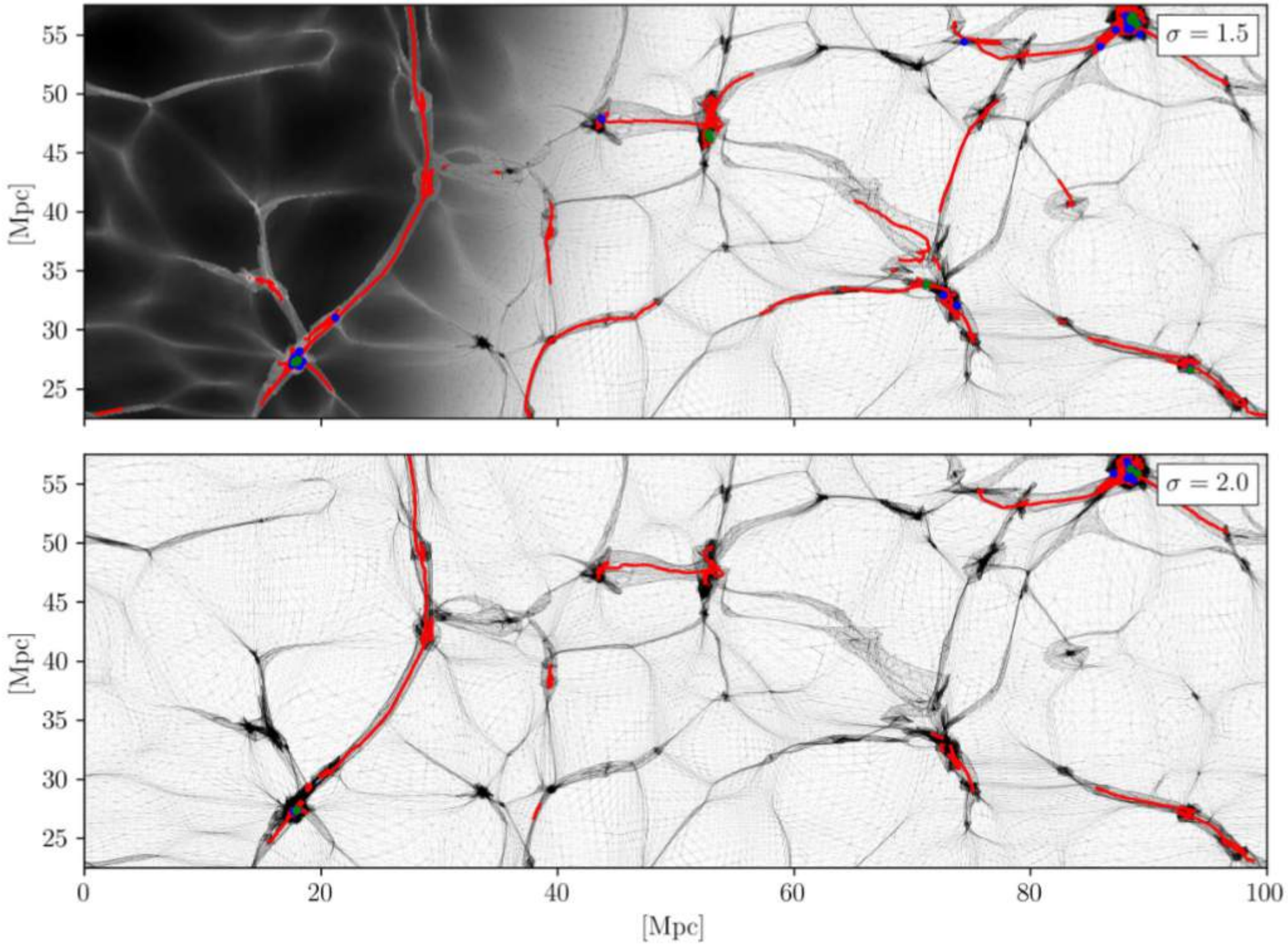
$\sigma = 1.5$
$\sigma = 2.0$
[Mpc]
[Mpc]
55
50
45
40
35
30
25
0
20
40
60
80
100

Caustics in 3D

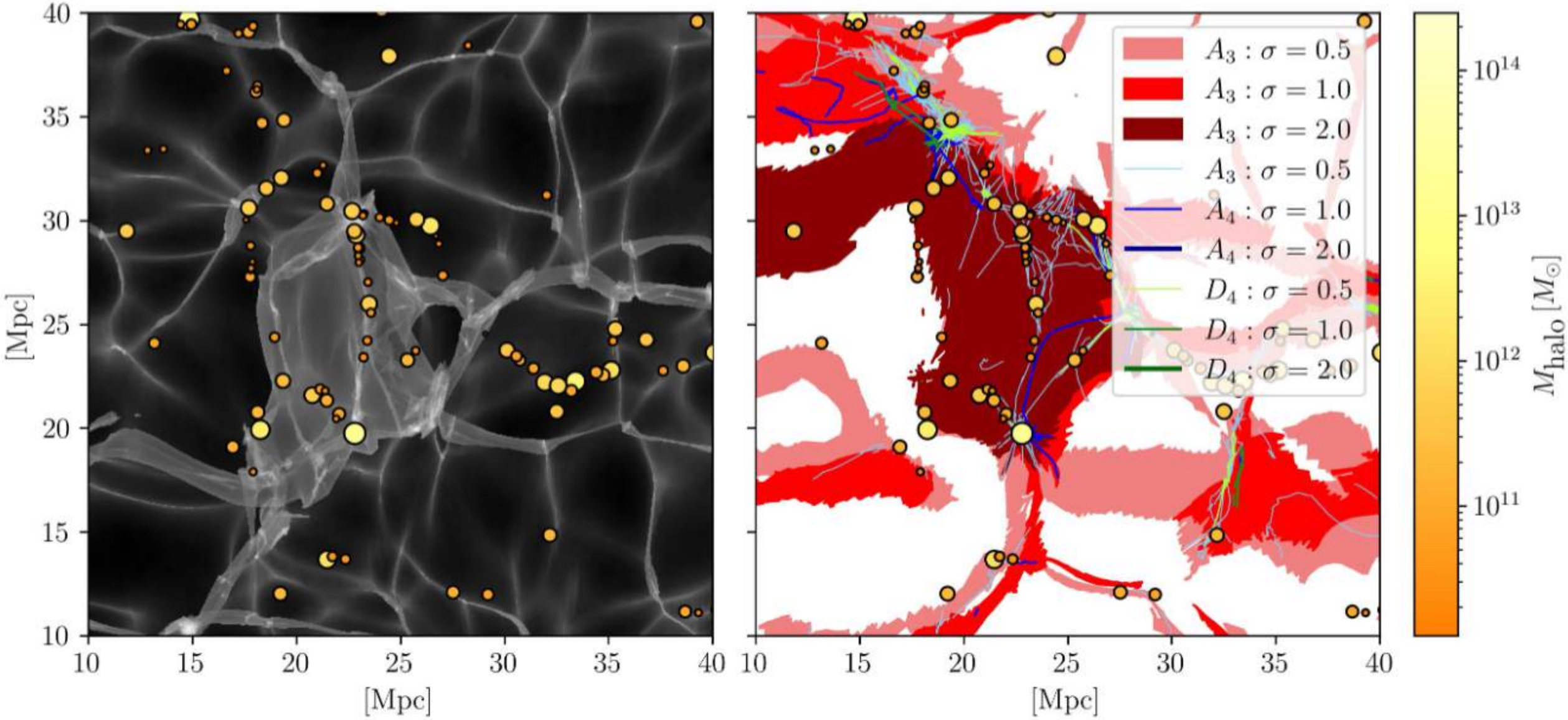

Caustics in 3D

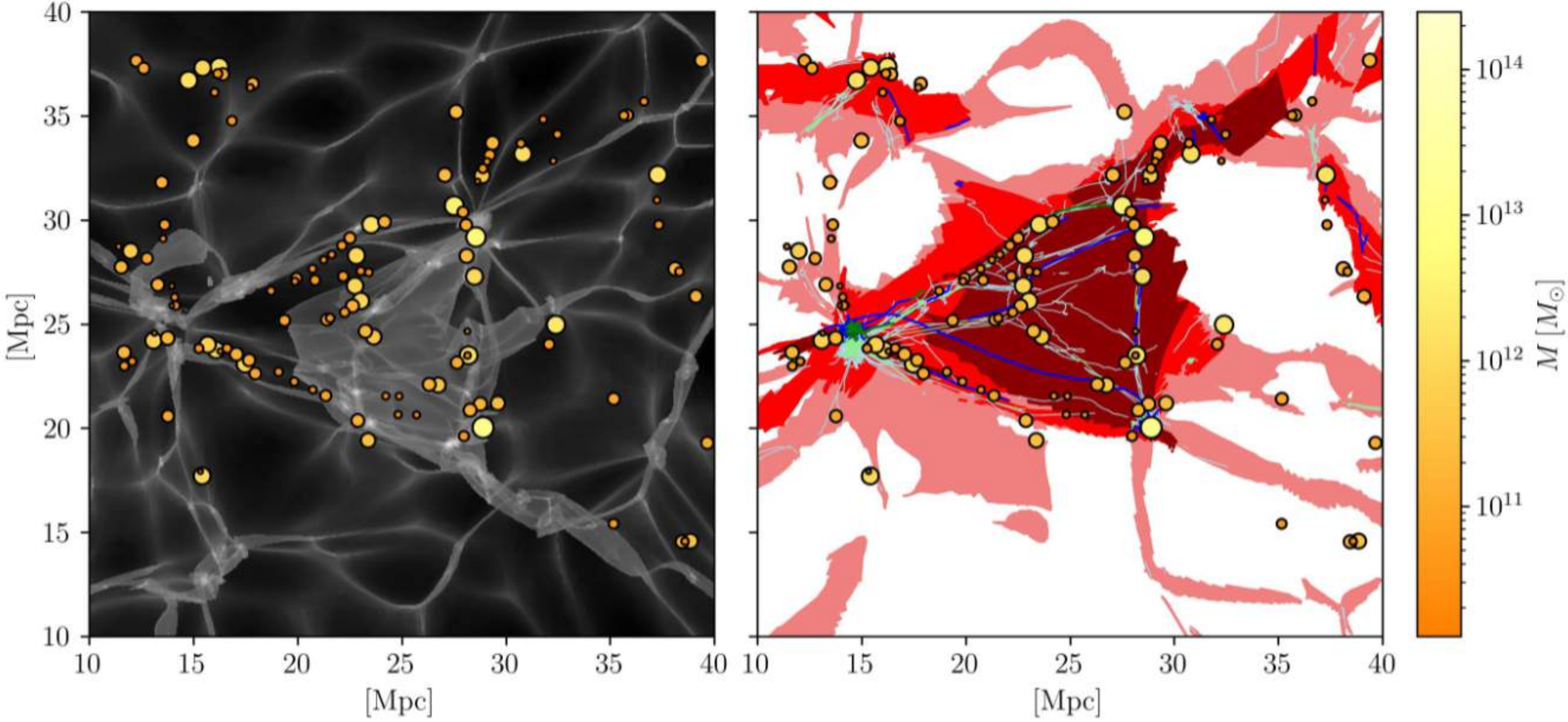

Caustics in 3D

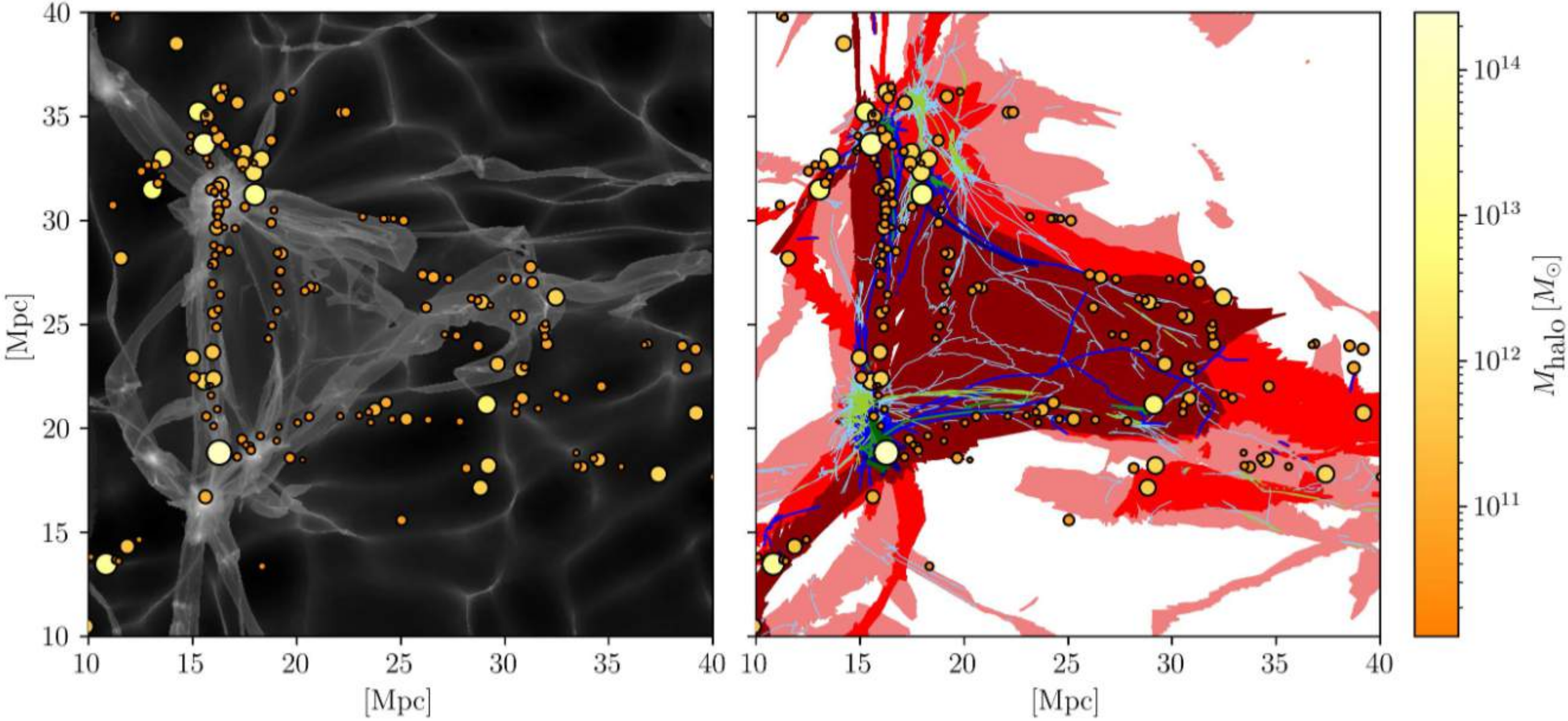

Constrained initial conditions

Dressing the caustic skeleton

Assessing the mass distribution in and around the caustic spine of the cosmic web:

- What are the properties of walls/ filaments/clusters?
- What is their mass distribution?
- How do they form and relate to the initial conditions?
- Detailed merging history and hierarchical evolution of the filamentary network?

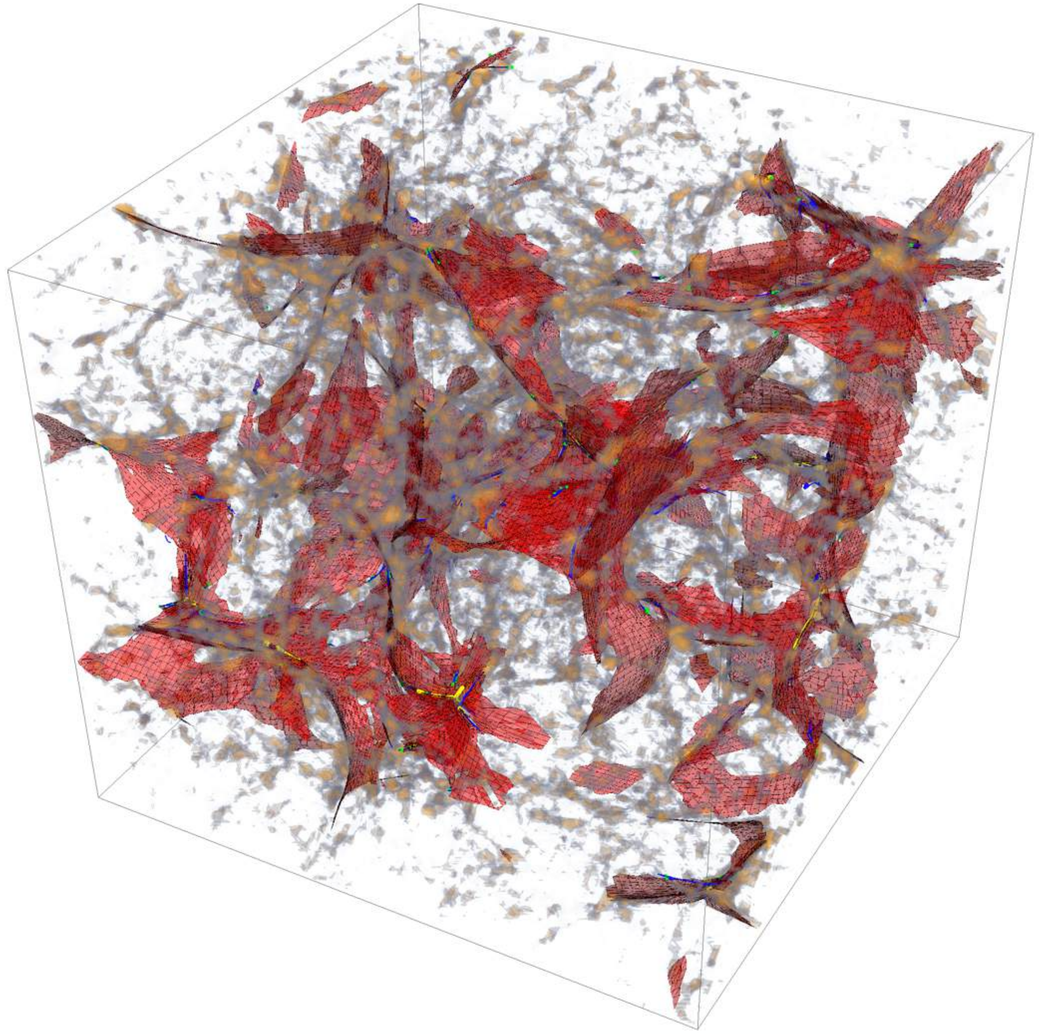

Gaussian random field

The cosmological initial conditions are often modelled by a Gaussian random field, which is an stochastic process:

$$P[f \in \mathcal{S}] = \mathcal{N} \int \mathbf{1}_{\mathcal{S}}(f) e^{-S[f]} \mathcal{D}f$$

with the ‘action’

$$S[f] \equiv \frac{1}{2} \iint [f(\boldsymbol{q}_1) - \bar{f}(\boldsymbol{q}_1)] K(\boldsymbol{q}_1, \boldsymbol{q}_2) [f(\boldsymbol{q}_2) - \bar{f}(\boldsymbol{q}_2)] \mathrm{d}\boldsymbol{q}_1 \mathrm{d}\boldsymbol{q}_2,$$

where the kernel is the inverse of the two-point correlation function

$$\int K(\boldsymbol{q}_1, \boldsymbol{q}) \xi(\boldsymbol{q}, \boldsymbol{q}_2) \mathrm{d}\boldsymbol{q} = \delta_D^{(2)}(\boldsymbol{q}_1 - \boldsymbol{q}_2)$$

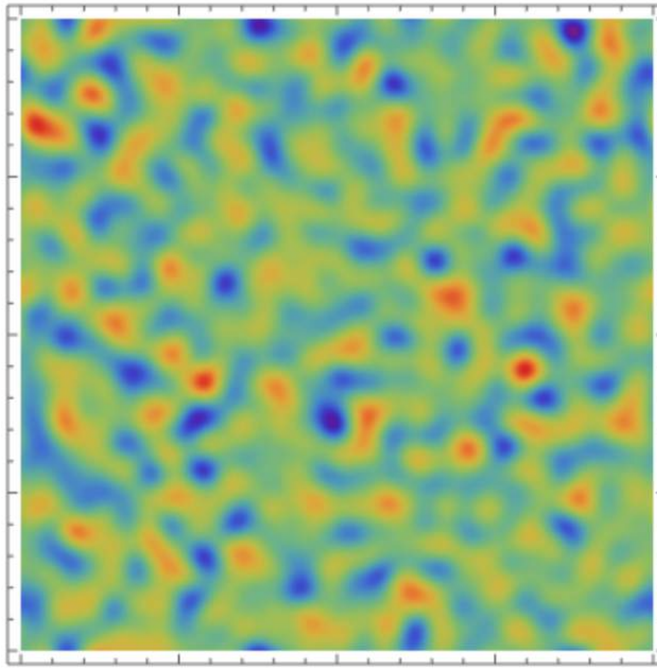

Linear constrained GRFs

We construct constrained simulations by adding constraints to the initial conditions

For linear constraints, the residue is independent of the value that the constraints assume:

$$\mathbf{x} = (\mathbf{x}_1, \mathbf{x}_2) \quad \mu = (\mu_1, \mu_2) \quad \Sigma = \begin{pmatrix} \Sigma_{11} & \Sigma_{12} \\ \Sigma_{21} & \Sigma_{22} \end{pmatrix}$$

when imposing $\mathbf{x}_2 = \mathbf{a}$ the constrained distribution is Gaussian with

$$\bar{\mu} = \mu_1 + \Sigma_{12}\Sigma_{22}^{-1}(\mathbf{a} - \mu_2) \qquad \bar{\Sigma} = \Sigma_{11} - \Sigma_{12}\Sigma_{22}^{-1}\Sigma_{21}$$

note that $\bar{\Sigma}$ is independent of $\mathbf{a}$

Constrained GRF theory

- Goal: Generate Gaussian random fields subject to constraints.
- Linear constraints: Hoffman-Ribak algorithm:

Bertschinger 1987
Hoffman, Ribak 1991
van de Weygaert & Bertschinger 1996

  - The statistical properties of the residue of a cGRF with respect to the mean field is independent of the values of the constraints

  - Generate GRF ➔ Measure constraint values ➔ Evaluate corresponding mean field ➔ Evaluate residue ➔ Add residue to mean field with target constraint values

- Drawback: Algorithm only works for **linear** constraints on a Gaussian field

Log-normal: Ravi Sheth 1997

Constrained GRF theory

Given the constraints: $\Gamma = \{C_i[f; \boldsymbol{q}_i] = c_i, \;\; i = 1, \ldots, M\}\,,$

Bertschinger 1987
Hoffman, Ribak 1991
Bertschinger and Weygaert 1996

we obtain the mean field: $\bar{f}_{\boldsymbol{c}}(\boldsymbol{q}) = \langle f(\boldsymbol{q})|\Gamma\rangle$

$$= \bar{f}(\boldsymbol{q}) + \sum_{i,j=1}^{M} \xi_i(\boldsymbol{q})\xi_{ij}^{-1}(c_j - \bar{C}_j)$$

and the variance of the residue: $\langle \delta f(\boldsymbol{q})^2|\Gamma\rangle = \sigma_0^2 - \sum_{i,j=1}^{M} \xi_i(\boldsymbol{q})\xi_{ij}^{-1}\xi_j(\boldsymbol{q})$

To generate realizations, we generate an unconstrained GRF, find the c_i's, find the residue and add the residue to the mean field of the target constraint values

Log-normal: Ravi Sheth 1997

Non-linear constraints

- The eigenvalue and eigenvector fields are not Gaussian, and the caustic conditions are non-linear. For this reason, we develop non-linear constraint Gaussian random field theory

$$\mathcal{M}_\mathcal{C} = \{\boldsymbol{c} \,|\, \mathcal{C}_i(\boldsymbol{c}) = 0 \text{ for all } i = 1, \dots, N\}.$$

- On this constraint manifold, we find the induced probability density

$$p(\boldsymbol{c} \,|\, \boldsymbol{c} \in \mathcal{M}_\mathcal{C}) = \frac{p(\boldsymbol{c})}{\int_{\mathcal{M}_\mathcal{C}} p(\boldsymbol{c}) \, \mathrm{d}\boldsymbol{c}} \, .$$

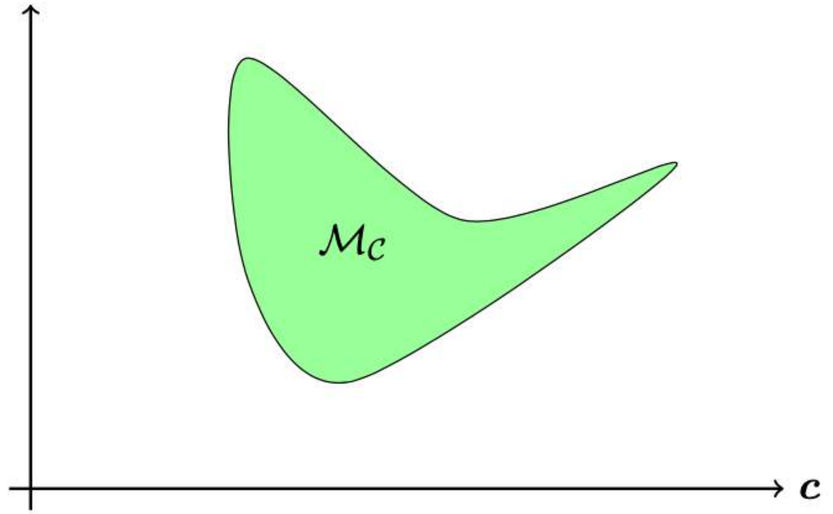

Feldbrugge and Weygaert (2022)

Non-linear constraints

- Using the properties of the constraint manifold we can leverage the Hoffman-Ribak principle for non-linear constraints:
  - The mean field: $\bar{f}_{\mathcal{C}}(\boldsymbol{q}) = \bar{f}_{\bar{\boldsymbol{c}}}(\boldsymbol{q})\,, \quad \bar{\boldsymbol{c}} \equiv \langle \boldsymbol{c} \,|\, \Gamma \rangle = \int_{\boldsymbol{c} \in \mathcal{M}_{\mathcal{C}}} \boldsymbol{c}\, p(\boldsymbol{c} \,|\, \boldsymbol{c} \in \mathcal{M}_{\mathcal{C}}) \mathrm{d}\boldsymbol{c}\,,$
  - The variance:

$$\left\langle \delta f(\boldsymbol{q})^2 \,|\, \Gamma \right\rangle = \sigma_0^2 - \sum_{i,j=1}^{M} \xi_i(\boldsymbol{q}) \zeta_{ij}^{-1} \xi_j(\boldsymbol{q})\,, \quad \zeta_{ij}^{-1} = \xi_{ij}^{-1} - \sum_{k,l=1}^{M} \xi_{ik}^{-1} \mathrm{cov}(c_k, c_l \,|\, \boldsymbol{c} \in \mathcal{M}_{\mathcal{C}}) \xi_{lj}^{-1}$$

- To generate realizations, we first sample the constraint manifold. Given the constraint values, we use the Hoffman-Ribak algorithm

Feldbrugge and Weygaert (2022)

What makes a filament (2D)?

JF and van de Weygaert 2024

Cusp filament (2D)

Candidate condition:

$$\lambda_1 = 1/b_+(t_c) \quad \mathbf{v}_1 \cdot \nabla \lambda_1 = 0$$

$$\mathbf{n} = \nabla(\mathbf{v}_1 \cdot \nabla \lambda_1)$$

Unsatisfactory as:

1. Points in Eulerian space **biased towards clusters**

2. Zel'dovich approximation **invalid in clusters**

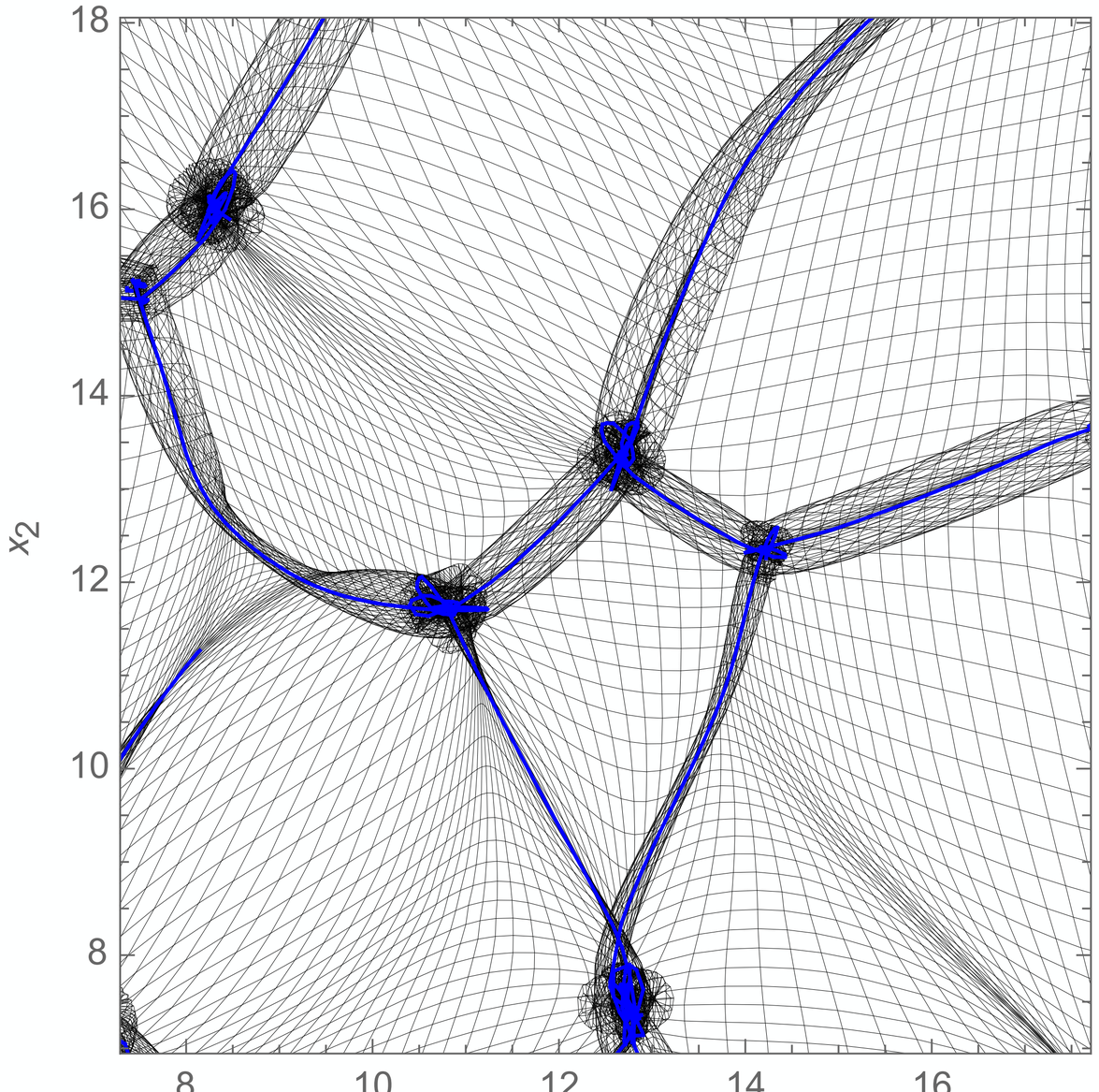

Cusp filament (2D)

Require that the cusp line is **maximally expanding along the direction of the filament**

$$\lambda_1 = 1/b_+(t_c) \qquad \lambda_2 < 0$$
$$\mathbf{v}_1 \cdot \nabla\lambda_1 = 0 \qquad \mathbf{v}_2 \cdot \nabla\lambda_2 = 0$$
$$\mathbf{n} = \nabla(\mathbf{v}_1 \cdot \nabla\lambda_1) \qquad \mathbf{v}_2[\mathscr{H}\lambda_2]\mathbf{v}_2 > 0$$

Note the **symmetry** between the first and second eigenvalue fields!

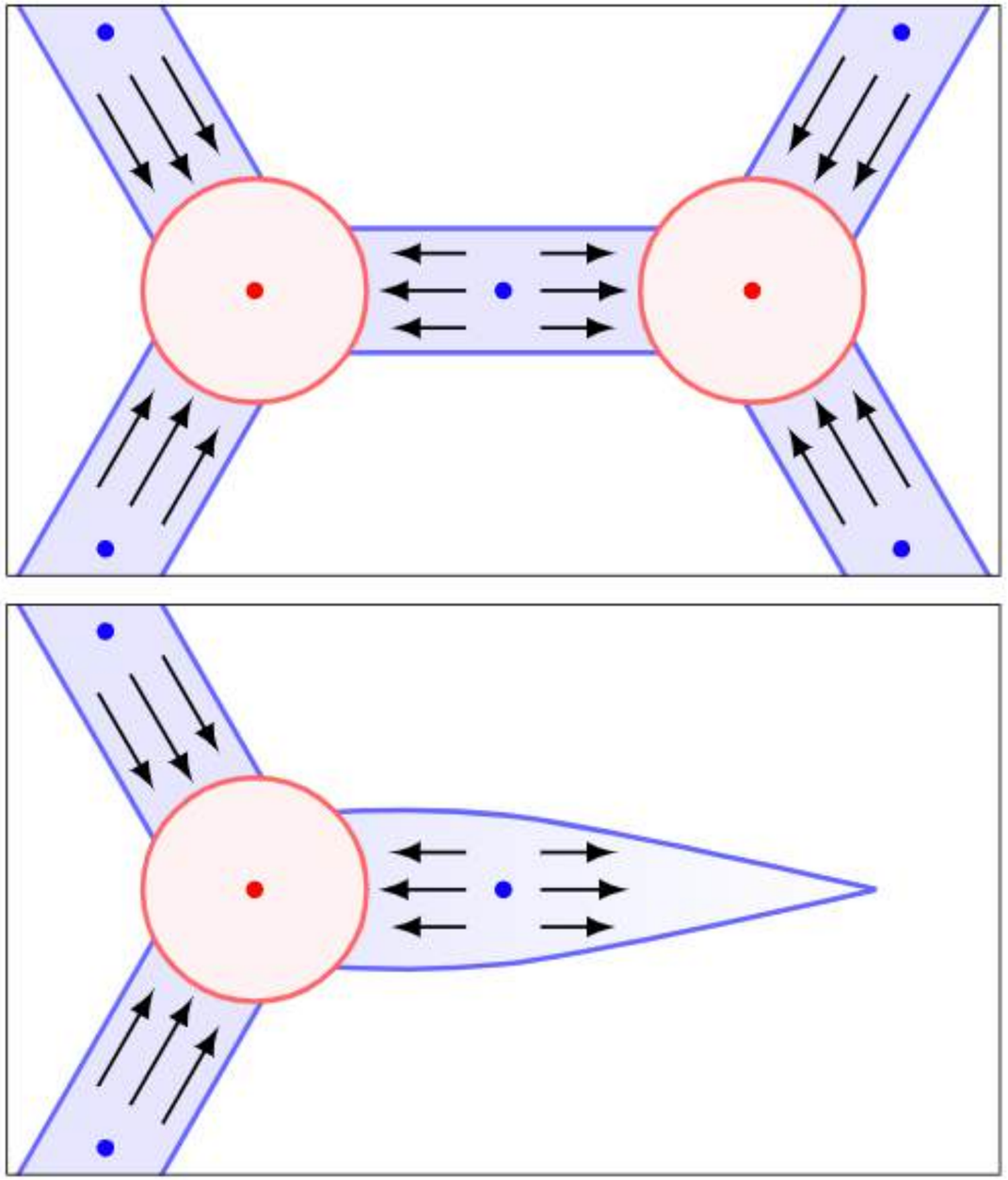

Cusp filament (2D)

Require that the cusp line is **maximally expanding along the direction of the filament**

$$\lambda_1 = 1/b_+(t_c) \qquad \lambda_2 < 0$$
$$\mathbf{v}_1 \cdot \nabla \lambda_1 = 0 \qquad \mathbf{v}_2 \cdot \nabla \lambda_2 = 0$$
$$\mathbf{n} = \nabla(\mathbf{v}_1 \cdot \nabla \lambda_1) \qquad \mathbf{v}_2[\mathscr{H}\lambda_2]\mathbf{v}_2 > 0$$

Note the **symmetry** between the first and second eigenvalue fields!

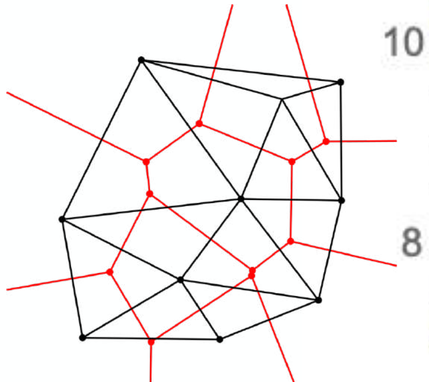

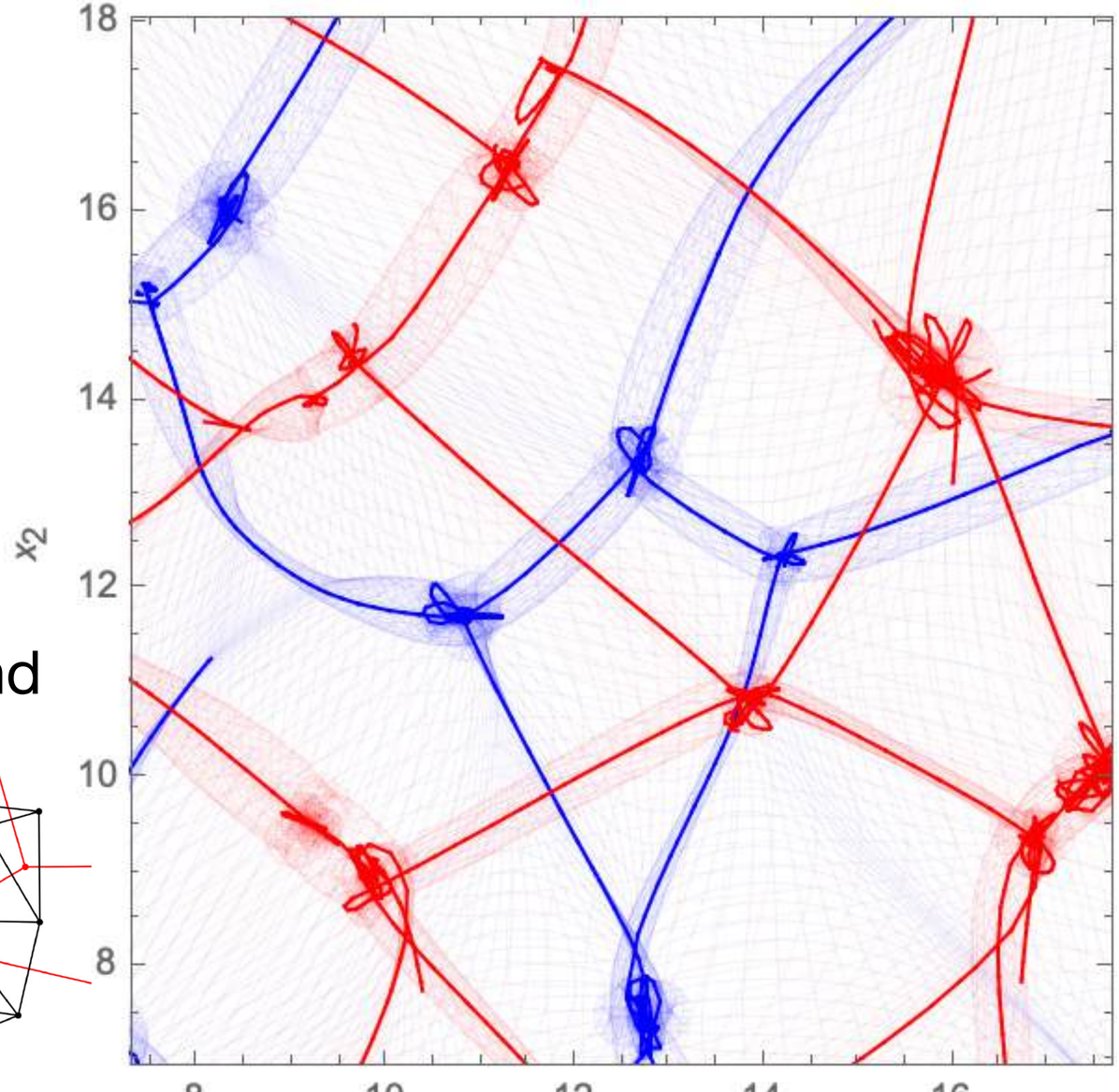

Cusp filament (2D)

After sampling the non-Gaussian distribution of the derivative of the primordial destitution in a point with an HMC algorithm,

$$\lambda_1 = 1/b_+(t_c) \qquad \lambda_2 < 0$$
$$\mathbf{v}_1 \cdot \nabla\lambda_1 = 0 \qquad \mathbf{v}_2 \cdot \nabla\lambda_2 = 0$$
$$\mathbf{n} = \nabla(\mathbf{v}_1 \cdot \nabla\lambda_1) \qquad \mathbf{v}_2[\mathscr{H}\lambda_2]\mathbf{v}_2 > 0$$

$$p(Y) \propto e^{-U(Y)}$$

we generate constrained initial conditions with the Hoffman-Ribak algorithm

Work with **Maé Rodriguez.**

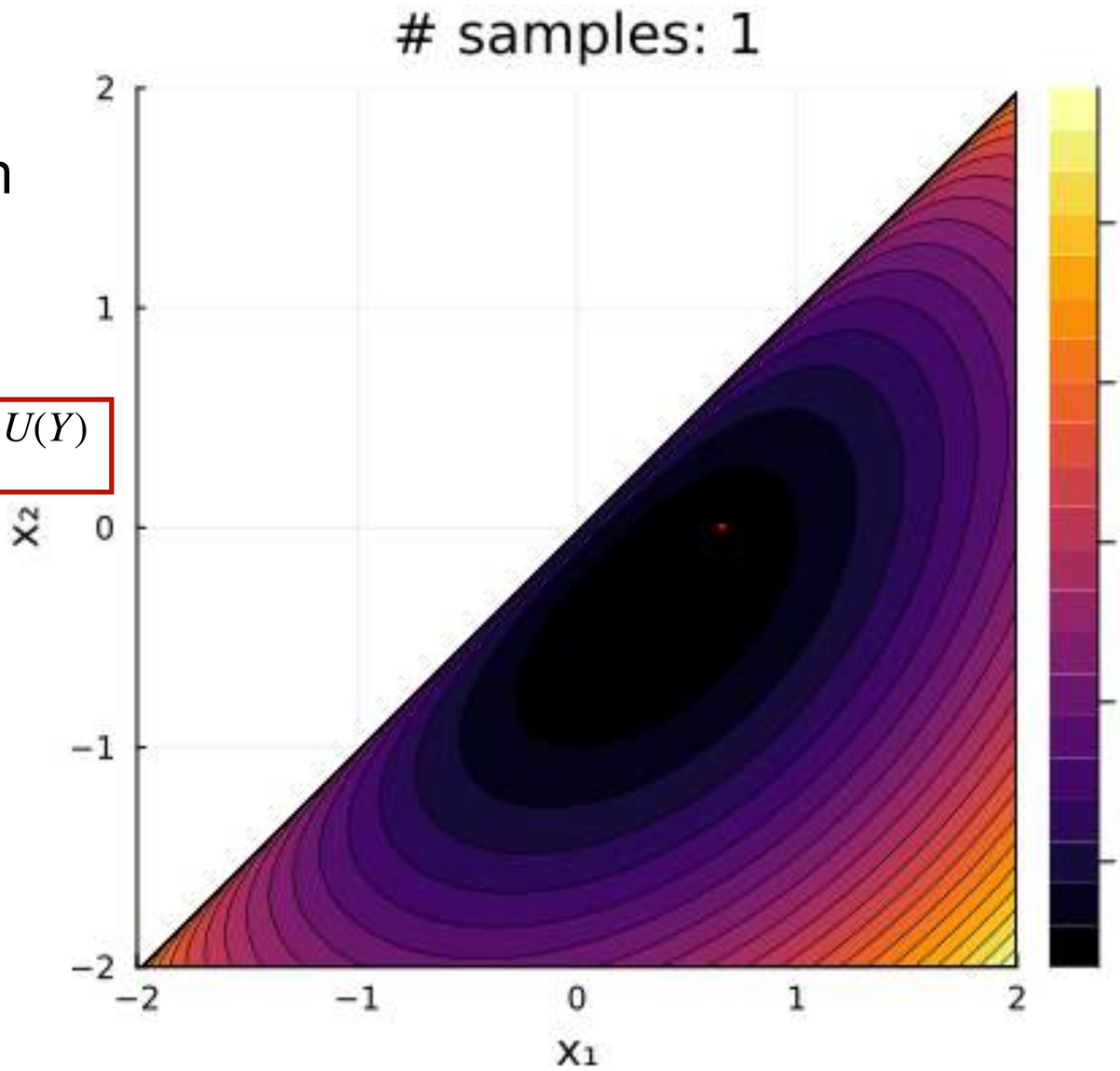

Cusp filament realizations (2D)

Specifying:

- **formation time**,
- **length scale**,
- and **orientation**

Dark matter
512 x 512 N-body
simulations

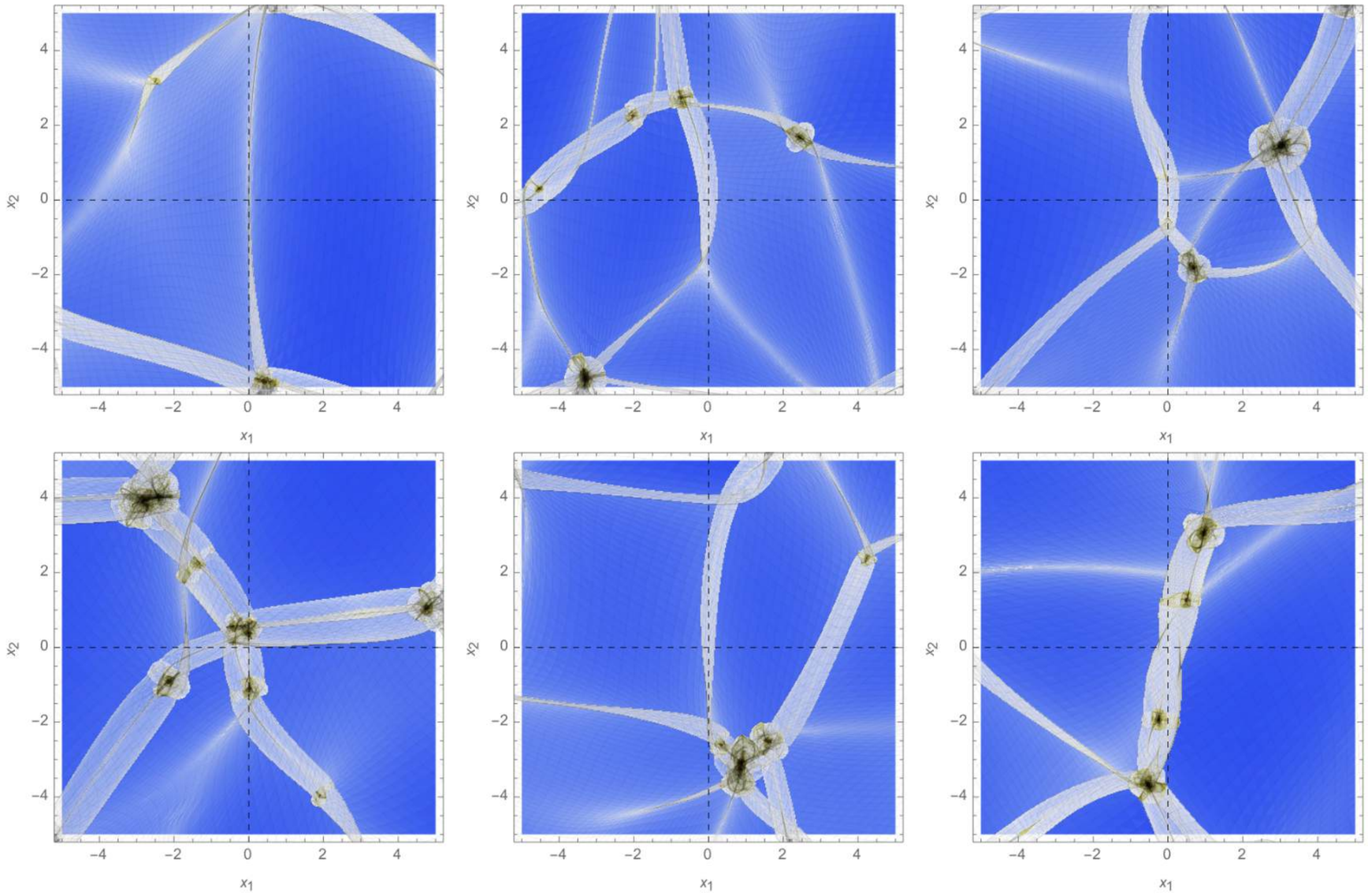

Median field (2D)

Formation time

Cusp filaments

We run 1000 dark matter 512 x 512 N-body simulations, evaluate the density field and compute the median for every pixel

Lengt scale

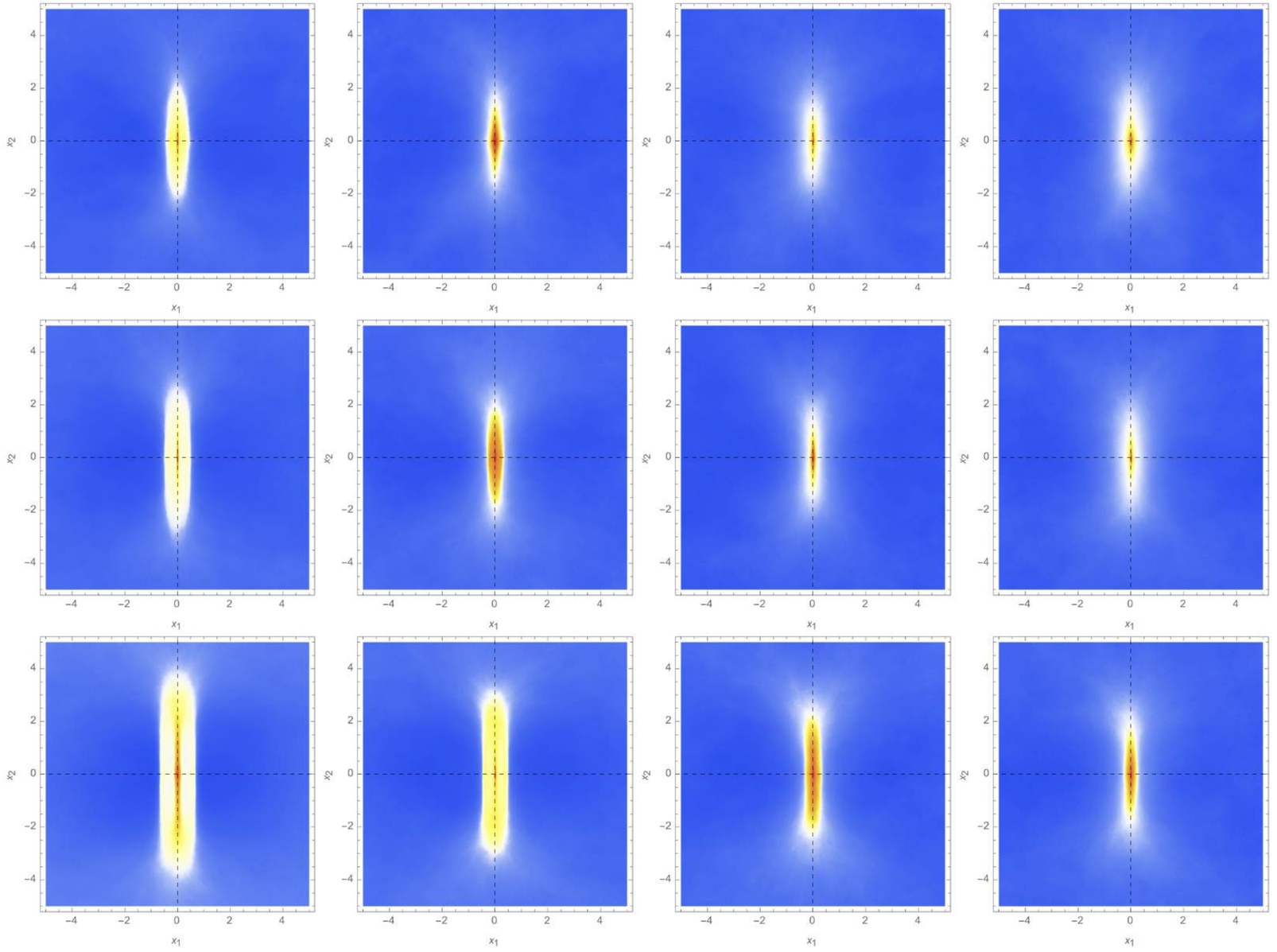

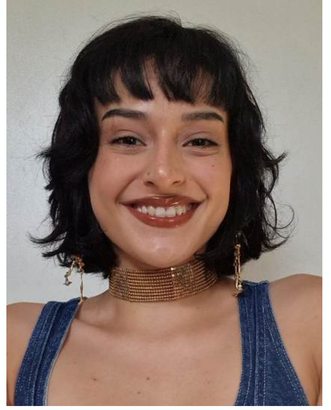

Maé Rodriguez

Benjamin Hertzsch

What makes a wall/filament (3D)?

Cosmic web (3D)

Cusp Wall

$$\lambda_1 = 1/b_+(t_c)$$

$$v_1 \cdot \nabla \lambda_1 = 0$$

and

$$0 > \lambda_2 > \lambda_3$$

$$v_2 \cdot \nabla(\lambda_2 + \lambda_3) = 0$$

$$v_3 \cdot \nabla(\lambda_2 + \lambda_3) = 0$$

$\mathscr{H}(\lambda_2 + \lambda_3)$ **positive definite**

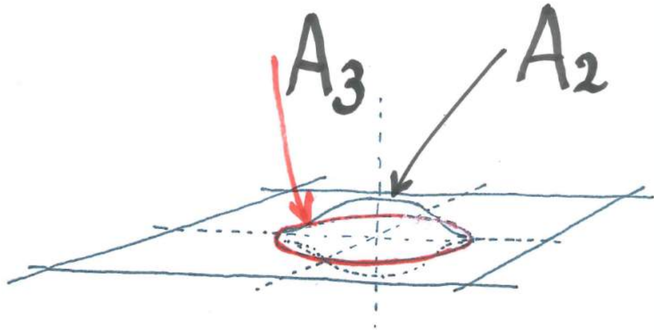

Swallowtail Filament

$$\lambda_1 = 1/b_+(t_c)$$

$$v_1 \cdot \nabla \lambda_1 = 0$$

$$v_1 \cdot \nabla(v_1 \cdot \nabla \lambda_1) = 0$$

and

$$\frac{\lambda_2(\boldsymbol{v}_3 \cdot \nabla(\boldsymbol{v}_1 \cdot \nabla\lambda_1))^2 + \lambda_3(\boldsymbol{v}_2 \cdot \nabla(\boldsymbol{v}_1 \cdot \nabla\lambda_1))^2}{(\boldsymbol{v}_2 \cdot \nabla(\boldsymbol{v}_1 \cdot \nabla\lambda_1))^2 + (\boldsymbol{v}_3 \cdot \nabla(\boldsymbol{v}_1 \cdot \nabla\lambda_1))^2} < 0$$

$$0 = ((\boldsymbol{v}_3 \cdot \boldsymbol{n}_c)\boldsymbol{v}_2 - (\boldsymbol{v}_2 \cdot \boldsymbol{n}_c)\boldsymbol{v}_3) \cdot \nabla \left[\lambda_2(\boldsymbol{v}_3 \cdot \boldsymbol{n}_c)^2 + \lambda_3(\boldsymbol{v}_2 \cdot \boldsymbol{n}_c)^2\right]$$

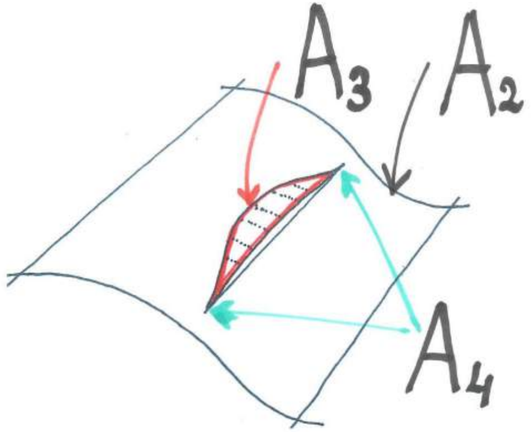

Umbilic Filament

$$\lambda_1 = \lambda_2 = 1/b_+(t_c)$$

and

$$\lambda_3 < 0$$

$$v_3 \cdot \nabla \lambda_3 = 0$$

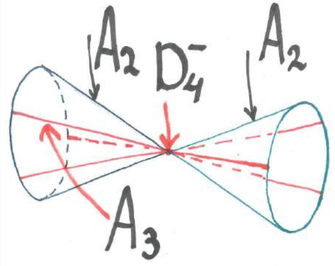

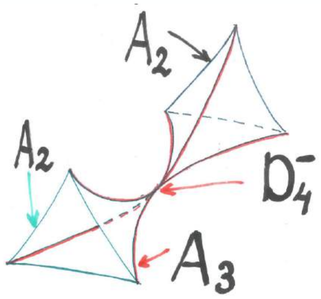

Cusp wall

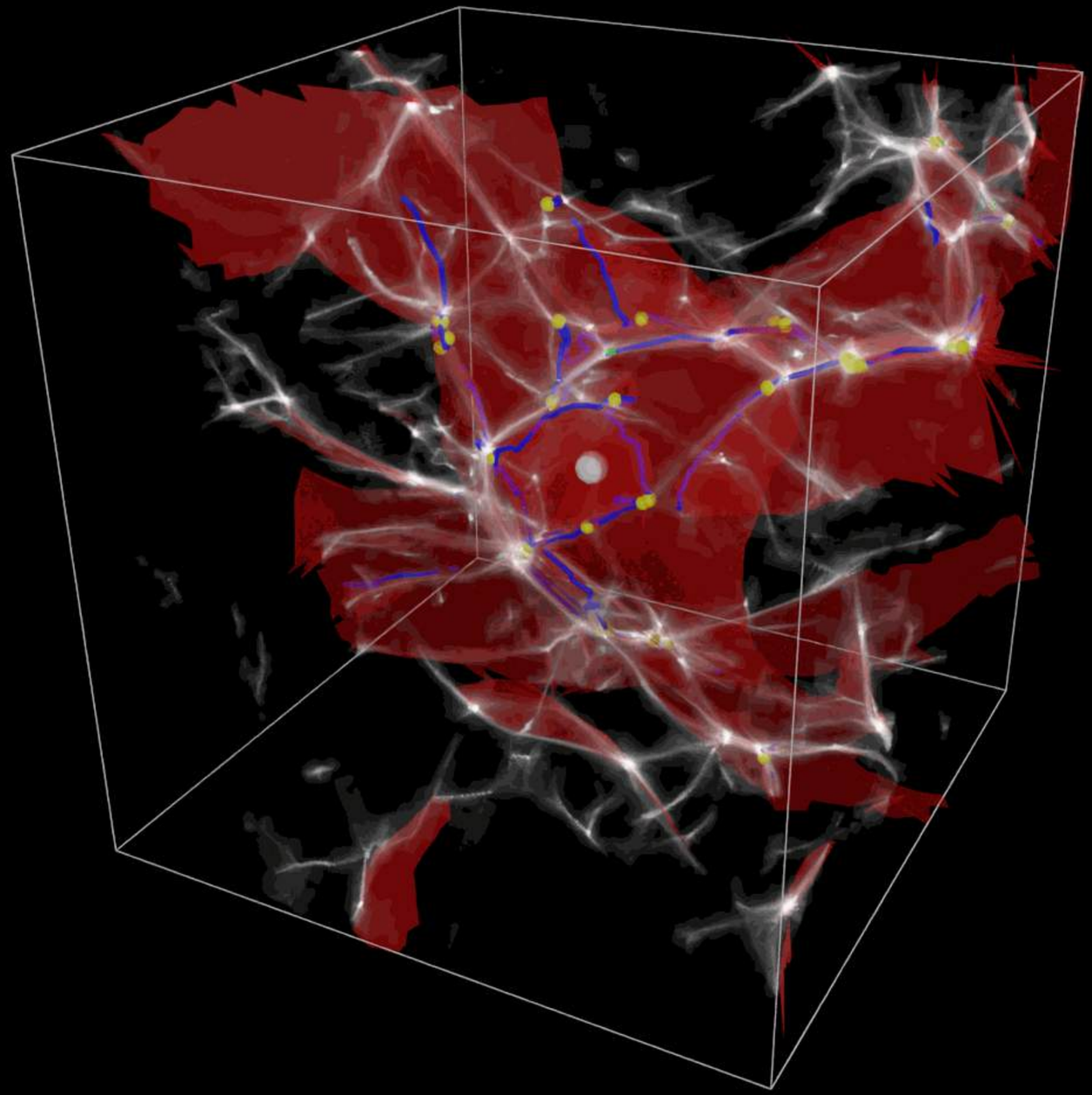

Swallowtail filament

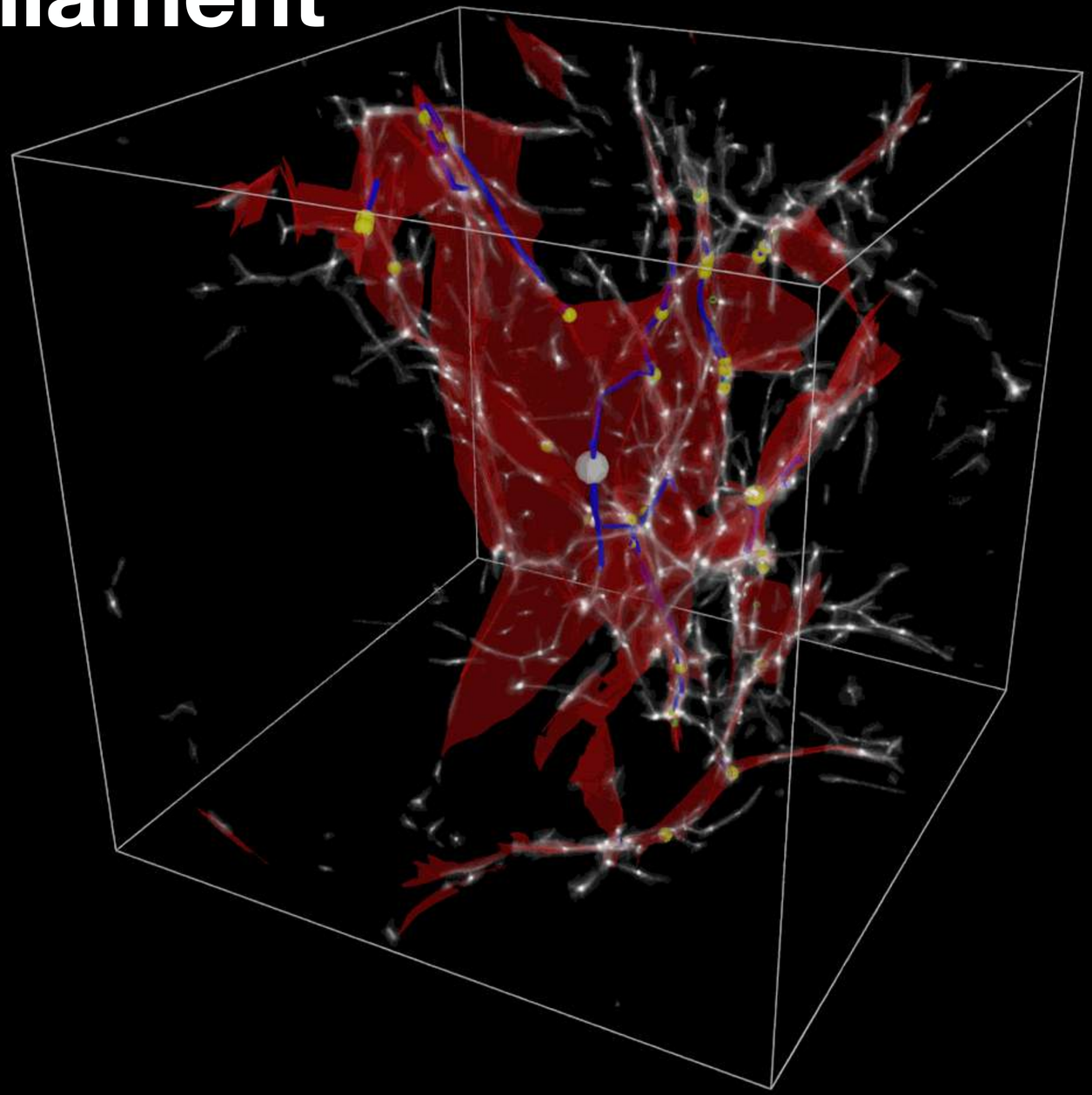

Umbilic filament

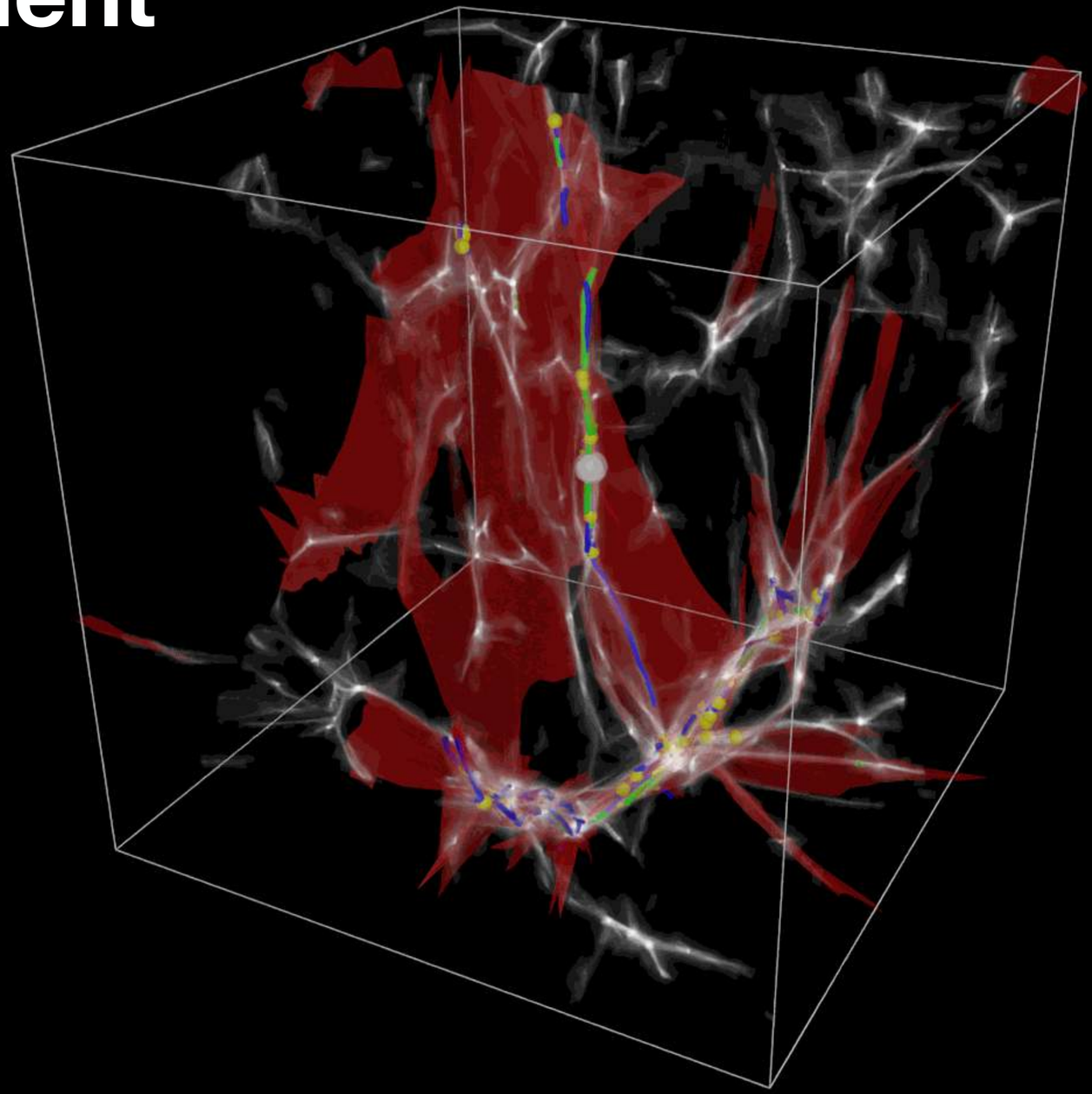

How are galaxies influenced by the cosmic web?

By generating customized initial conditions, using non-linear constrained Gaussian random field theory, we can systematically study the different elements of the cosmic web

$$A_3^i(t) = \{\mathbf{q} \in L \mid \mathbf{q} \in A_2^i(t), \mathbf{v}_i \cdot \nabla \mu_{it} = 0\}$$

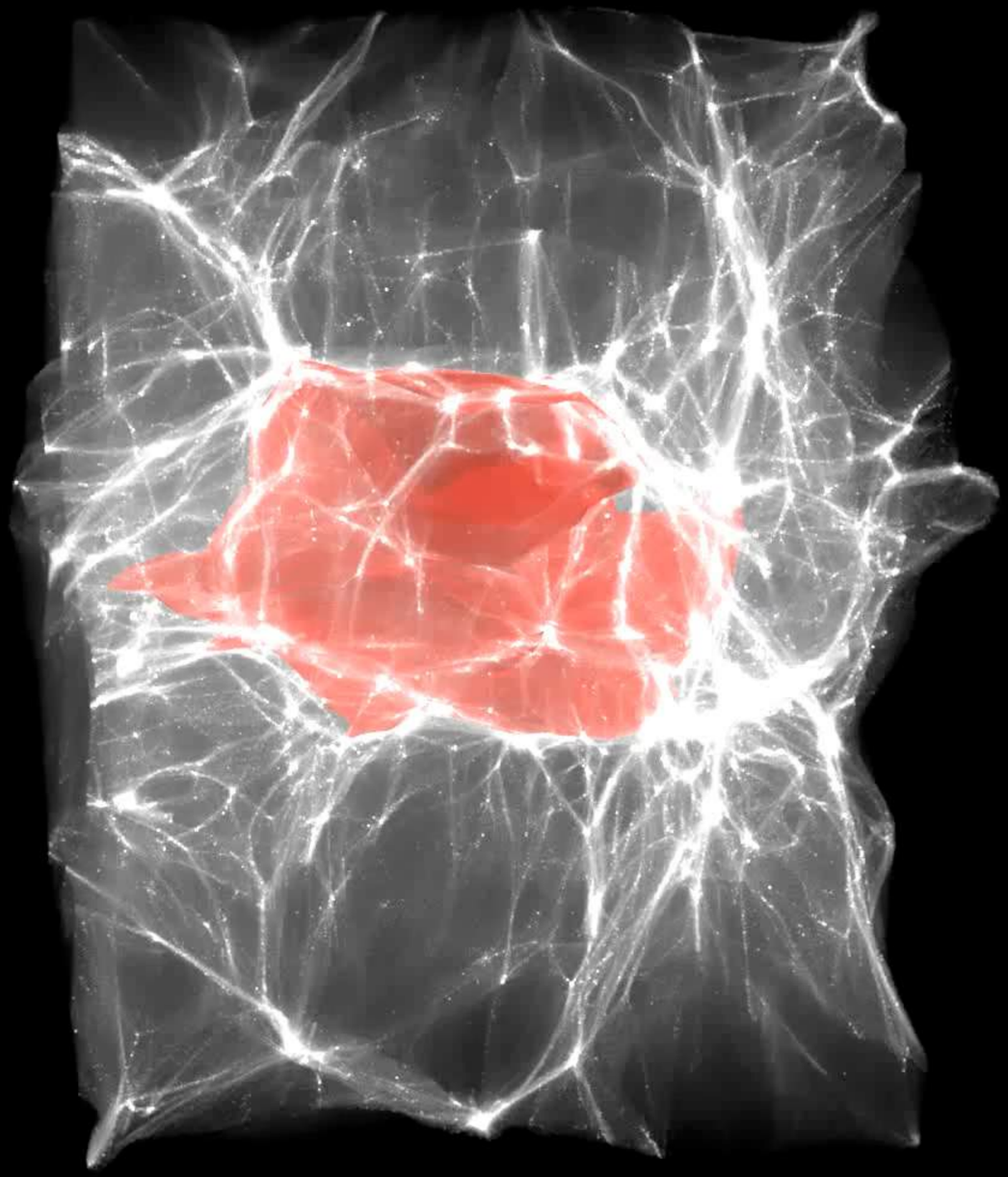

How are galaxies influenced by the cosmic web

By generating customized initial conditions, using non-linear constrained Gaussian random field theory, we can systematically study the different elements of the cosmic web

$$D_4^{ij}(t) = \{\mathbf{q} \in L \mid 1 + \mu_{it}(\mathbf{q}) = 1 + \mu_{jt}(\mathbf{q}) = 0\}$$

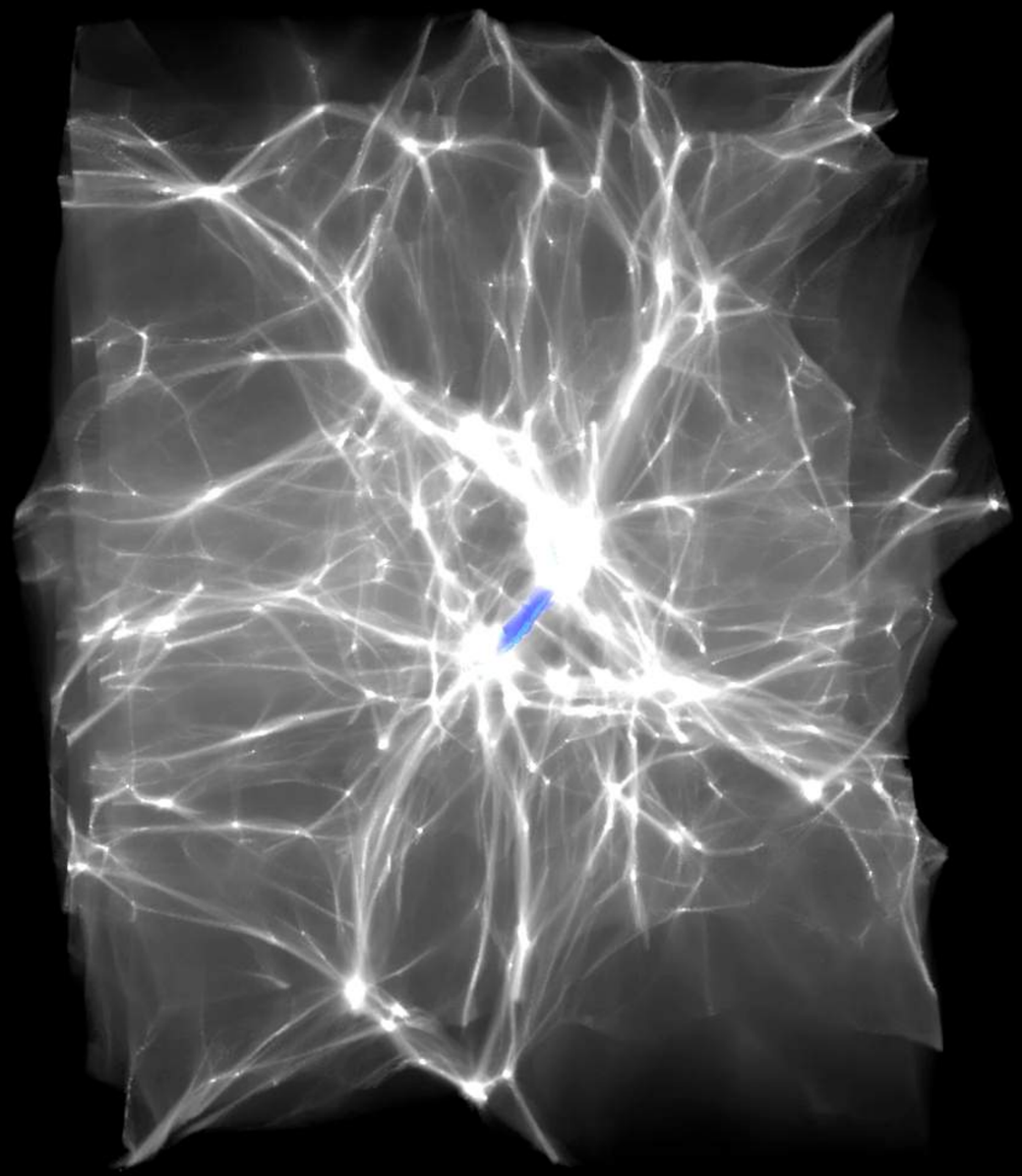

Constrained Gaussian Random field theory

By generating customized initial conditions, using non-linear constrained Gaussian random field theory, we can systematically study the different elements of the cosmic web

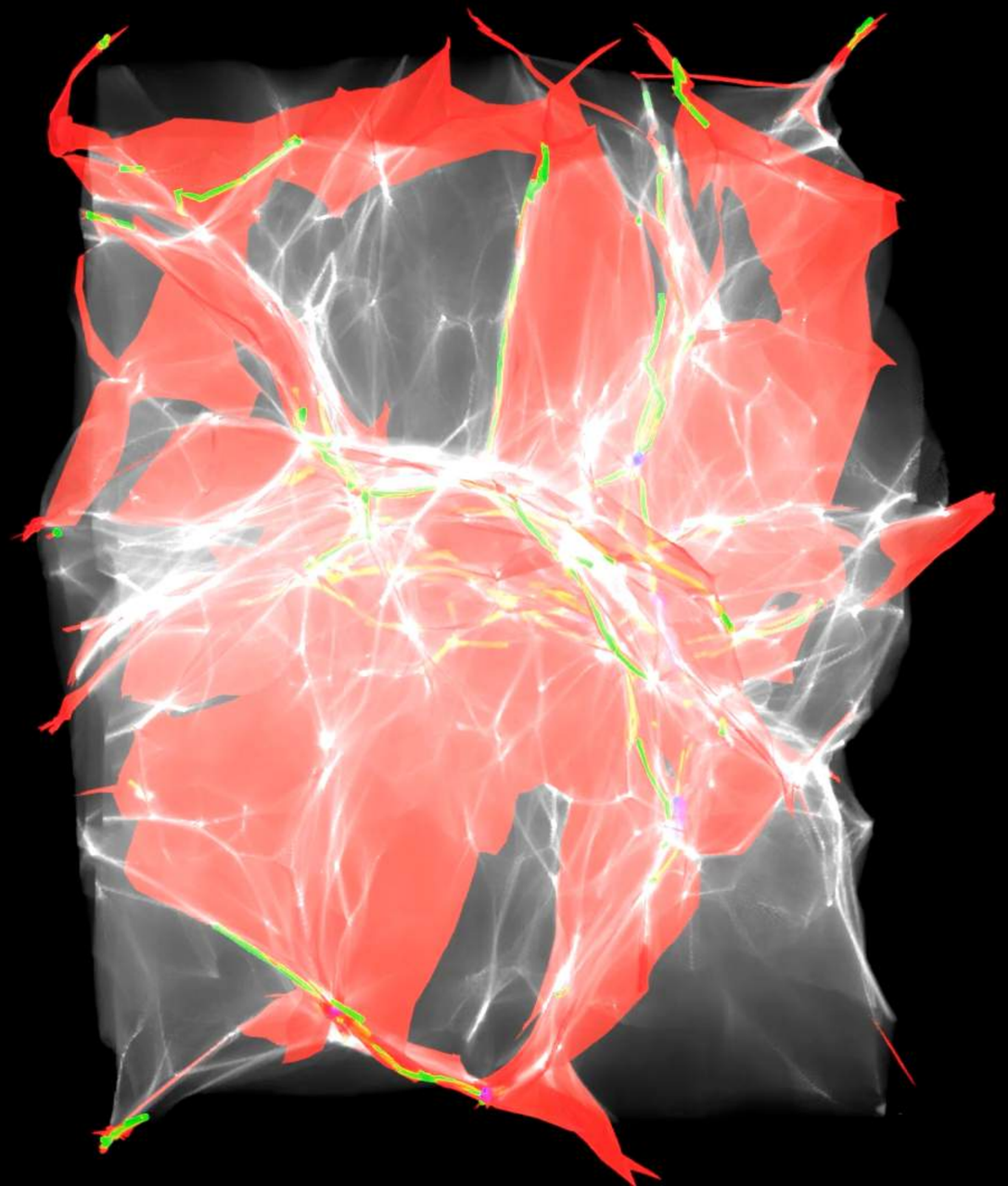

Constrained Gaussian Random field theory

Rotating an umbilic filament along the y-axes

Pablo López

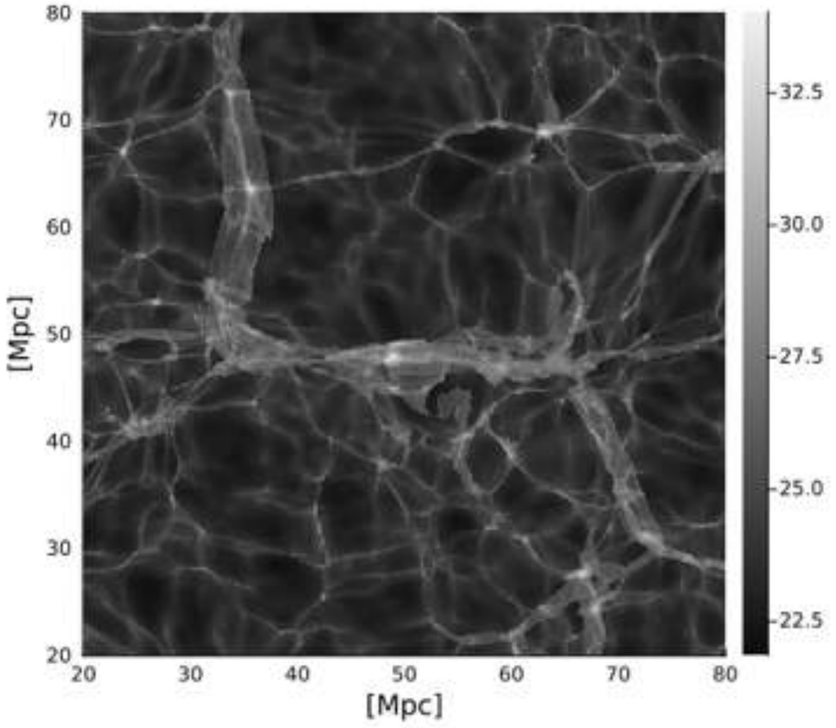

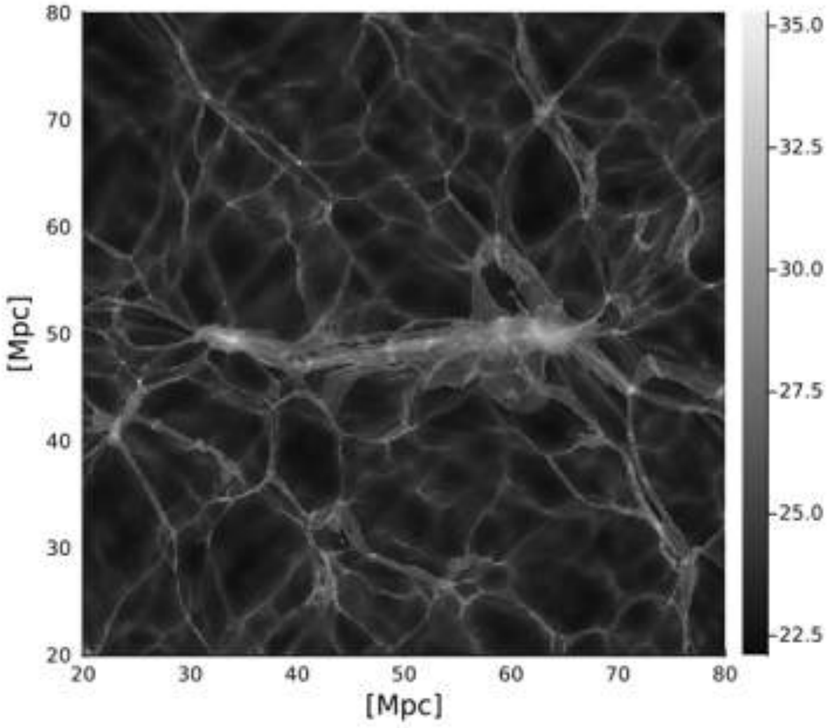

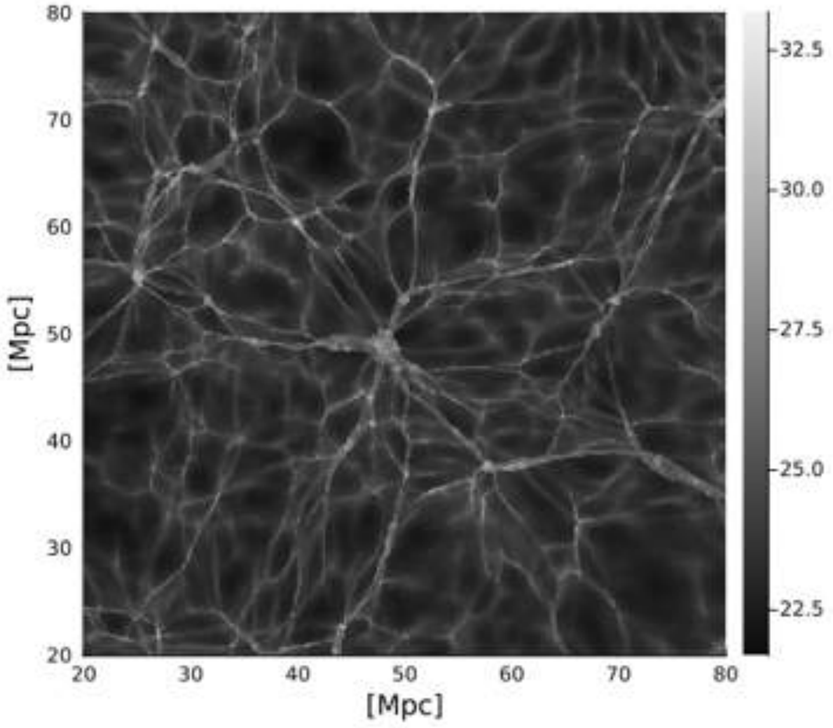

Constrained Gaussian Random field theory

Rotating an umbilic filament along the y-axes

Pablo López

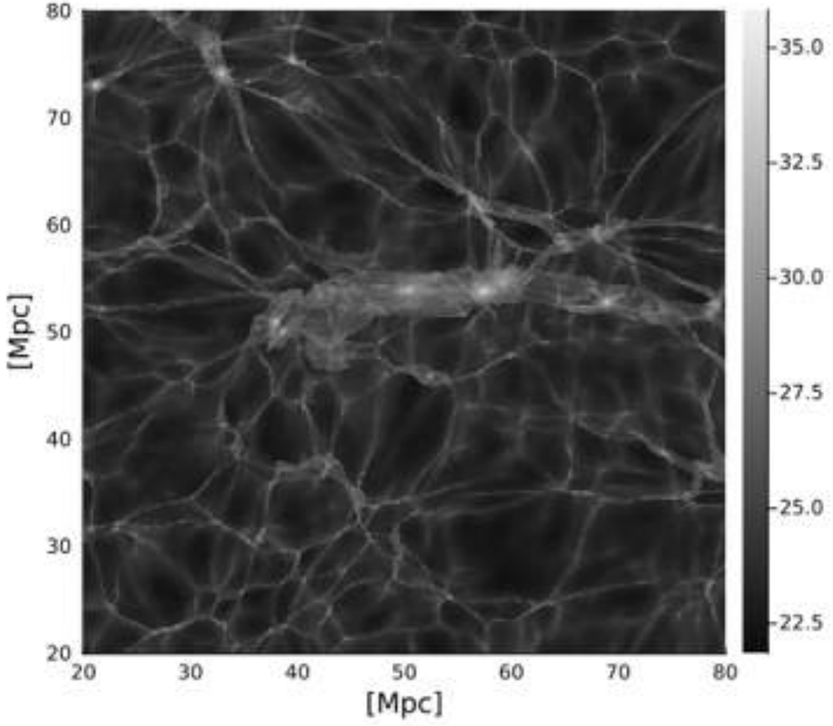

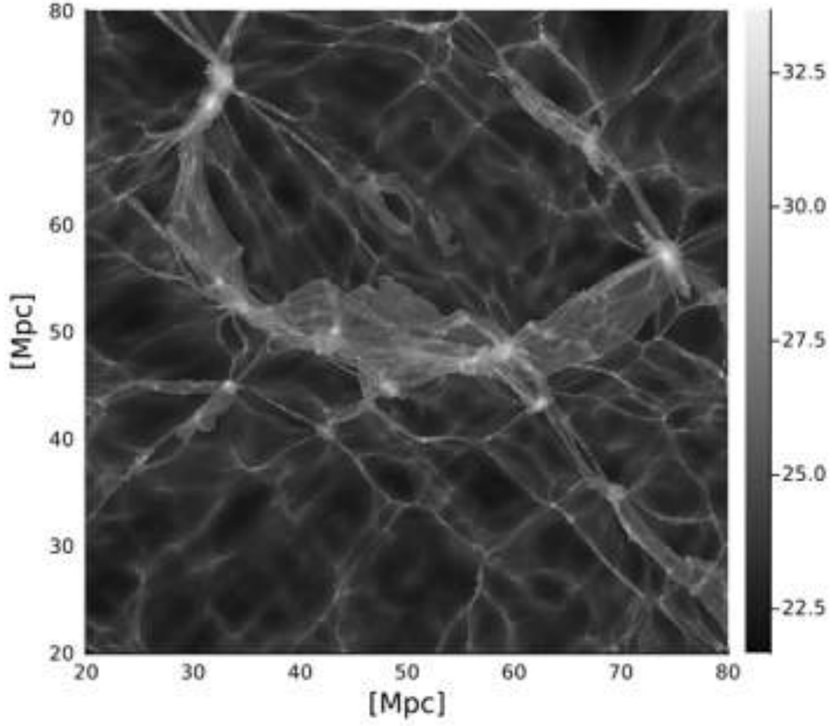

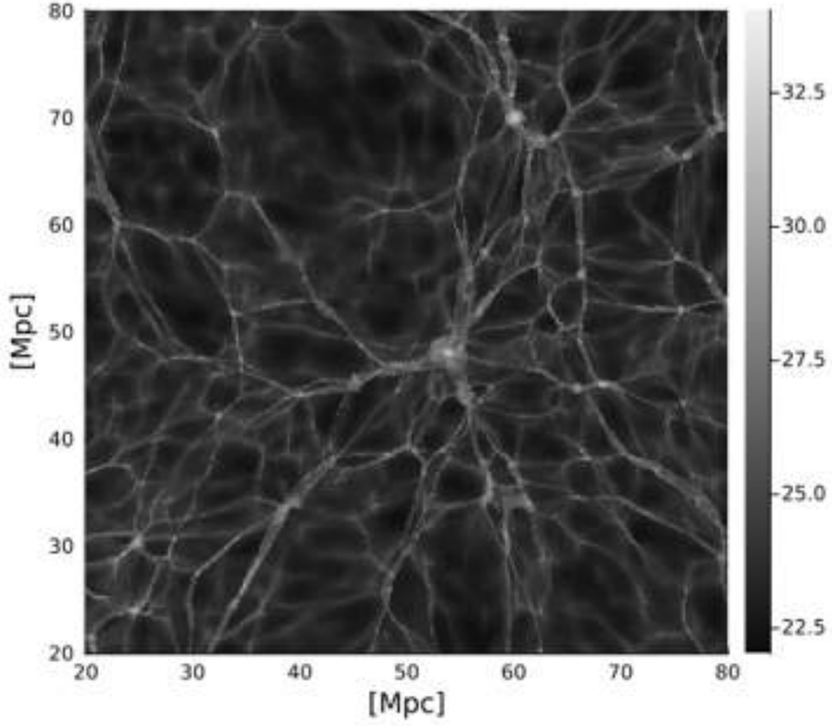

Feldbrugge (2024)

Phase-Space DTFE

Phase-Space Delaunay Tessellation Field Estimator
[github.com/jfeldbrugge/PS-DTFE]

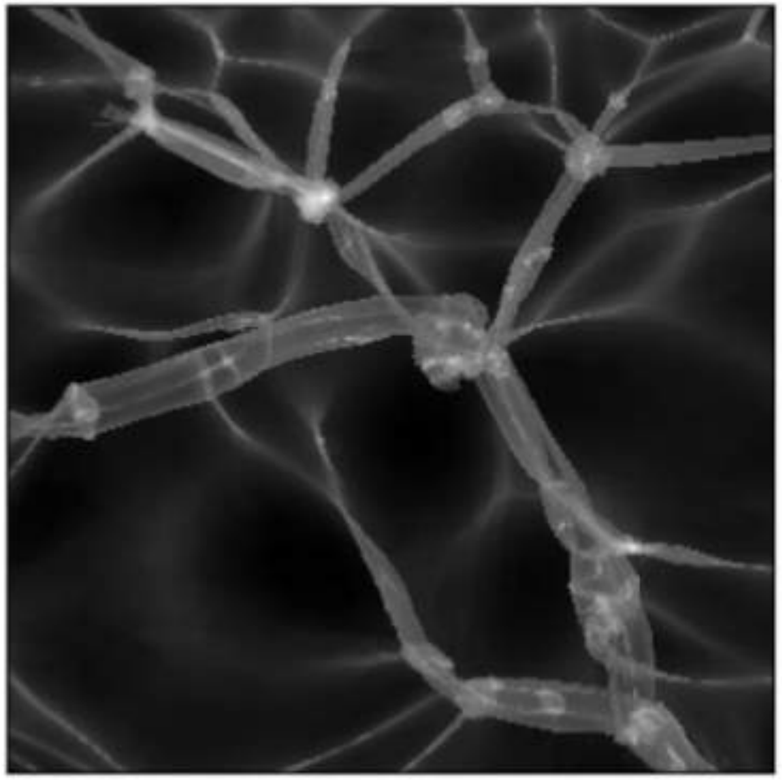

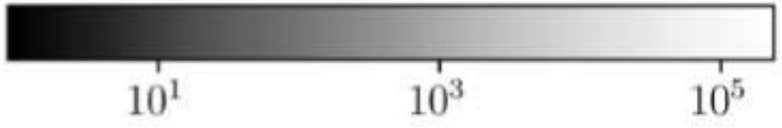

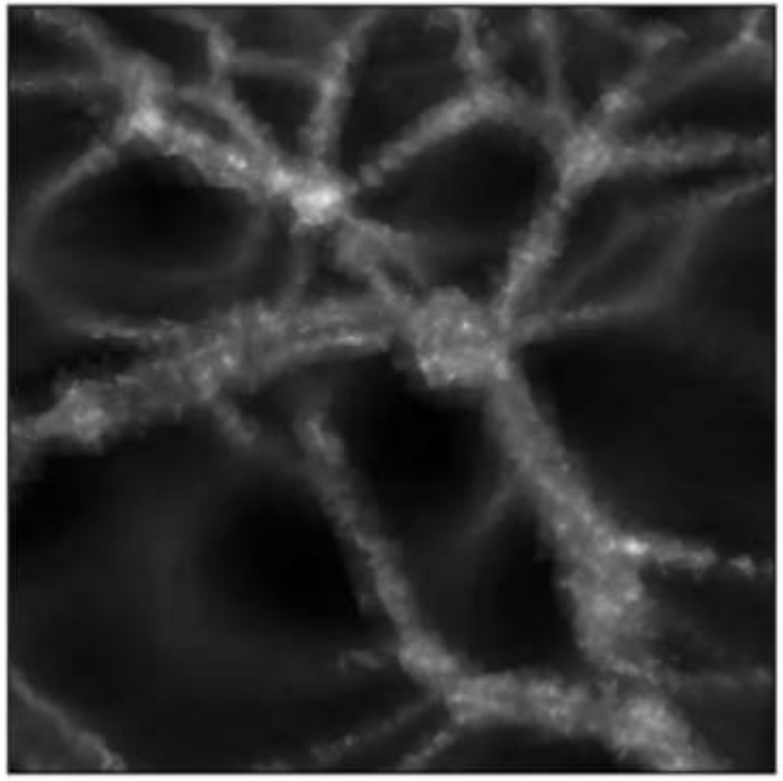

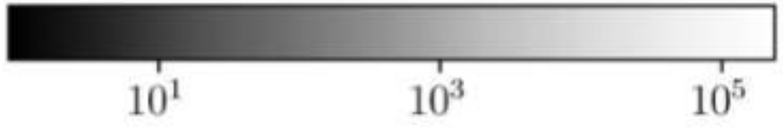

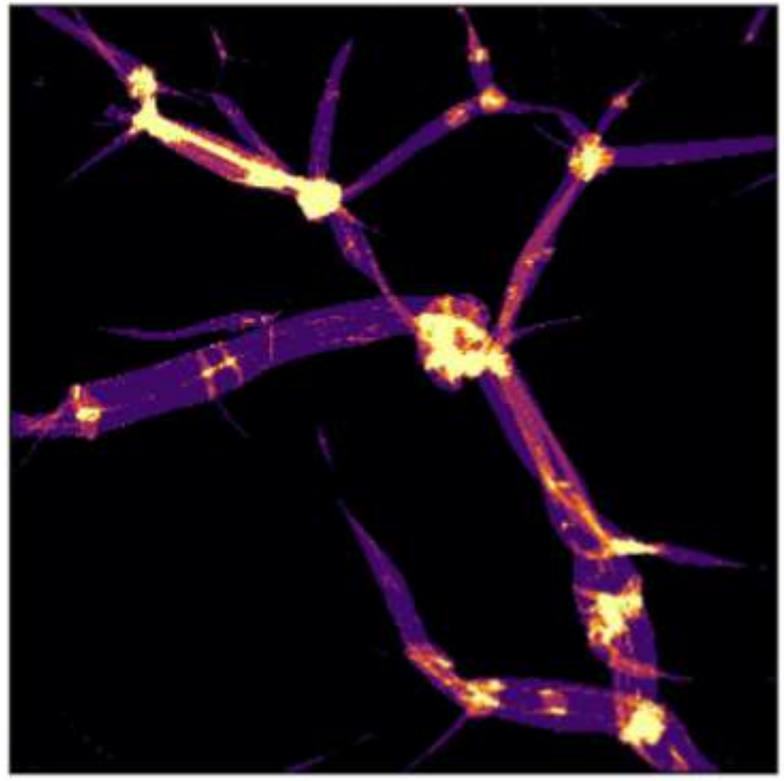

Conclusion

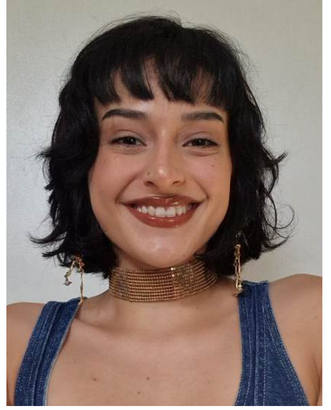

Maé Rodriguez

Benjamin Hertzsch

- The **geometry of the cosmic web** originates from foldings in phase space
- The **caustic skeleton** of the cosmic web depends on the **eigenvalue** *and* **eigenvector fields** and classifies the elements of the cosmic web by their unique **formation histories**
- We generate constrained **initial conditions** tied to the **dynamics of structure formation**
- I am hopeful that this will **improve our understanding** of **galaxies in the cosmic web.** Bridging the gap between astronomy and cosmology

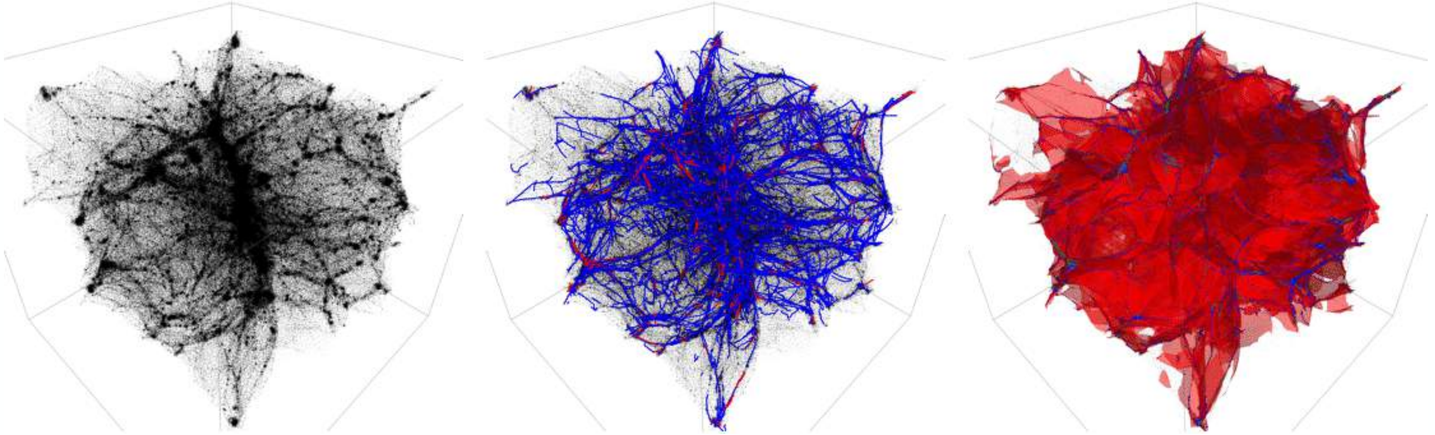

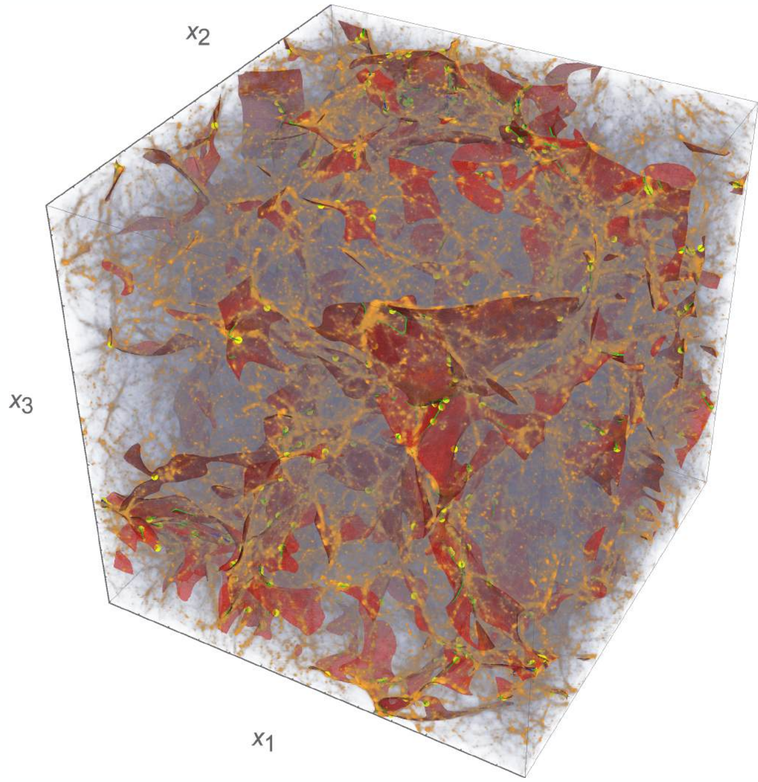

Thank you for your attention!